

**Technical University Delft**  
**Tall storeys: active control of wind impact on high-rise buildings**  
**Hans Breen**



**Graduation project**  
**Tall storeys: active control of wind impact on high-rise buildings**

**Technical University Delft**  
**Faculty of Civil Engineering and Geosciences**  
**Specialization: Structural Engineering**  
**Section: Structural Mechanics**

**Thesis committee:**

**Prof. ir. A.C.W.M. Vrouwenvelder, Structural Mechanics**  
**Dr. ir. P.C.J. Hoogenboom, Structural Mechanics**  
**Ir. W.A.A.M. Bierbooms, Wind Energy**  
**Ir. J.G. Kraus, DHV**

**Student:**

**Ing. Hans Breen**

**April 20, 2007**



## Table of contents

1.	Introduction.....	1
2.	Idealization of the building.....	3
2.1.	Bending stiffness and mass of the structure.....	3
2.2.	Element stiffness matrix: field element .....	4
2.3.	Element stiffness matrix: bottom element .....	5
2.4.	Mass matrix .....	6
2.5.	Damping matrix.....	6
3.	Numerical simulation in Simulink.....	9
3.1.1.	Validation of the static behaviour.....	10
3.1.2.	Validation of the dynamic behaviour: damping and eigenfrequency..	11
4.	Wind.....	15
4.1.	Wind load on the structure .....	15
4.2.	Mean part of the wind speed.....	16
4.3.	Fluctuating part of the wind speed.....	17
4.3.1.	Correlation between the wind speed at different locations .....	19
5.	Control algorithm.....	23
5.1.	Linear negative feedback: displacement and velocity control.....	23
5.1.1.	Energy consideration .....	24
5.2.	Feedback loop in Simulink .....	25
5.3.	Displacement of the mass .....	27
5.4.	Displacement control strategy .....	30
5.5.	Energy consumption .....	32
6.	Implementing an active control system in the Juffertoren .....	35
6.1.	Acceptable comfort level.....	35
6.2.	Parameter study .....	37
6.2.1.	Varying the control gains and the mass of the actuator.....	38
6.2.2.	Varying the mass, stiffness and damping of the structure .....	46
6.2.3.	Time delay .....	48
6.2.4.	Disturbances of the active control force.....	49
6.3.	Check of the accelerations at lower stories .....	49
6.4.	Configuration of the system .....	50
7.	Frequency-domain response analysis .....	53
7.1.	Single degree of freedom system.....	53
7.2.	Multi degree of freedom system.....	54
7.3.	Spectrum of the accelerations .....	57
8.	Conclusions and recommendations .....	61
8.1.	Conclusions .....	61
8.2.	Recommendations.....	61

## Appendices

Appendix I Drawing of the building

Appendix II Matlab code: mechanical characteristics of the structure

Appendix III Derivation of the element stiffness matrix

Appendix IV Matlab code: Stiffness-, mass- and damping matrix and eigenfrequencies

Appendix V Matlab code: correlation wind

Appendix VI Unsuccessful control algorithms

Appendix VII Deriving the spectrum from a linear relation

Appendix VIII Matlab code: Transfer function, spectrum forces, spectrum of the acceleration



## Preface

This thesis documents the graduation project which I undertook in order to complete my Master study in Civil Engineering at the Delft University of Technology. I've been working on this project for more than seven months now. It began with an investigation into active control in civil engineering and after six weeks I focused on the Juffertoren in Rotterdam. In the beginning it was quite difficult to know where to start and what to do, but, looking back on the total project I am content with the result.

This study wouldn't have been successfully completed without the help of my graduation committee and therefore I wish to thank them. Thanks to Prof. Ir. A.C.W.M. Vrouwenvelder, for his great expertise which he made available to me so that I could solve the more difficult problems. And Dr. Ir. P.C.J. Hoogenboom who had always time for consultancy. I am also indebted to Ir. W.A.A.M. Bierbooms for his expertise on wind loads and his critical view on the report. A special thanks to Ir. J.G. Kraus of DHV, for making available the information on the Juffertoren and other practical information.

Finally, I wish to express my gratitude to my family and friends for their unceasing support and encouragement.

Hans Breen  
April '07



## Summary

In this Masters project, the possibilities of implementing an active control system suitable for high-rise buildings which are affected by the impact of the wind were investigated. Applying a variable force on the structure, depending on the dynamic state of the building, aims at limiting unwanted accelerations caused by wind impact. For example a specific project was chosen. The mechanical properties of the building have been determined and modelled with the help of a computer program. The wind load was determined and implemented in the computer model. Following that, an active control system was implemented. Different simulations were made of the dynamic behaviour in the time domain. This resulted in a properly working system with a reduction of the accelerations of 50% at the top of the building. The sensitivity of the system was analysed with a parameter study. A frequency-domain analysis was performed in order to give further insight into the accelerations at different frequencies.



## List of symbols

$A$	area	$[\text{m}^2]$
$A_s$	effective area against shear deformation	$[\text{m}^2]$
$a_0$	constant determining the proportionality of the mass to the damping	$[\text{s}^{-1}]$
$a_1$	constant determining the proportionality of the stiffness to the damping	$[-]$
$a_i$	acceleration of node $i$	$[\text{m}/\text{s}^2]$
$a_m$	acceleration of the mass of the active control system	$[\text{m}/\text{s}^2]$
$\hat{a}_i$	amplitude of the acceleration of node $i$	$[\text{m}/\text{s}^2]$
$b$	width of the building	$[\text{m}]$
$\mathbf{C}$	damping matrix	$[\text{kg}/\text{s}]$
$C_h$	shape factor	$[-]$
$C_r$	rotational stiffness of the foundation	$[\text{Nm}]$
$\mathbf{C}^e$	modal damping matrix	$[\text{kg}/\text{s}]$
$C_y$	coherence constant in $y$ -direction	$[-]$
$C_z$	coherence constant in $z$ -direction	$[-]$
$coh_{v_i, v_k}$	coherence between the wind speed in point $i, k$	$[-]$
$d_w$	displacement height	$[\text{m}]$
$E$	Young's modulus	$[\text{N}/\text{m}^2]$
$\mathbf{E}$	eigenmatrix containing the eigenvectors	$[-]$
$\mathbf{E}_f$	location vector of the control force	$[-]$
$E$	subtracted energy	$[\text{J}]$
$e$	rotation in a node	$[\text{rad}]$
$\mathbf{F}$	vector wind forces on the nodes	$[\text{N}]$
$F_i$	force on node $i$	$[\text{N}]$
$F_c$	control force	$[\text{N}]$
$F_{ik}$	force on node $i$ on discrete time point $k$	$[\text{N}]$
$f$	frequency	$[\text{rad}/\text{s}]$
$f_i$	frequency of mode $i$	$[\text{rad}/\text{s}]$
$G$	shear stiffness	$[\text{N}/\text{m}^2]$
$g_1$	control gain for the relative displacement of the mass	$[\text{N}/\text{m}]$
$g_2$	control gain for the velocity of the top of the building	$[\text{Ns}/\text{m}]$
$g_3$	control gain for the relative velocity of the mass	$[\text{Ns}/\text{m}]$
$h$	length of the building	$[\text{m}]$
$I$	moment of inertia	$[\text{m}^4]$
$\mathbf{I}$	identity matrix	$[-]$
$i$	node number	$[-]$
$I$	turbulence intensity factor	$[-]$
$L$	height of the building	$[\text{m}]$

$L_{gust}$	characteristic length of a wind gust	[m]
$l$	length of 1 element	[m]
$\mathbf{K}$	stiffness matrix	[N/m]
$\mathbf{K}^*$	modal stiffness matrix	[N/m]
$\mathbf{M}$	mass matrix	[kg]
$\mathbf{M}^*$	modal mass matrix	[kg]
$M$	moment	[Nm]
$N$	number of draws	[-]
$k$	bending stiffness	[N/m]
$k_a$	acceleration control gain	[kg]
$k_c$	dimensionless factor	[-]
$k_d$	displacement control gain	[kg/s <sup>2</sup> ]
$k_v$	velocity control gain	[kg/s]
$m_i$	lumped mass in node $i$	[kg]
$m$	mass of 1 storey	[kg]
$m_{eq}$	mass of equivalent 1 degree of freedom system	[kg]
$m_m$	weight of the mass of the active control system	[kg]
$n$	node number	[-]
$n.a.$	distance between the neutral axis and a parallel reference line	[m]
$P$	required mechanical power	[kW]
$q$	force per length	[N/m]
$S_{xx}$	auto spectrum of signal $x$	[dim( $x$ ) <sup>2</sup> ]
$S_{xy}$	cross-spectrum in point $x$ and $y$	[dim( $x$ )dim( $y$ )]
$T_1$	period	[s]
$t$	time	[s]
$\mathbf{u}$	vector with the displacements of the nodes	[m]
$\hat{\mathbf{u}}_i$	eigenvector of mode $i$	[-]
$\hat{\mathbf{u}}_i$	eigenvector of mode $i$	[-]
$u_{b,top}$	displacement at the top of the structure due to bending	[m]
$u_i$	displacement of node $i$	[m]
$u_m$	displacement of the mass of the active control system	[m]
$u_{r,m}$	relative displacement of the mass	[m]
$u_{r,top}$	rotation at the top of the structure	[rad]
$u_{s,top}$	displacement at the top of the structure due to shear	[m]
$u_{top}$	displacement at the top	[m]
$u_*$	Friction velocity	[m/s]
$\hat{u}_i$	amplitude of the displacement of node $i$	[m]
$v_i$	velocity of node $i$	[m/s]
$v_m$	velocity of the mass of the active control system	[m/s]
$\hat{v}_i$	amplitude of the velocity of node $i$	[m/s]

$\bar{v}$	hourly averaged wind speed	[m/s]
$\tilde{v}$	fluctuating part of the wind speed	[m/s]
$W$	work done by the mass	[kWh]
$x$	dimensionless frequency	[-]
$y$	coordinate in width direction of the building	[m]
$z$	height above the surface of the earth	[m]
$z_0$	roughness length	[m]
$\zeta_i$	damping ratio of the $i$ -th mode	[-]
$\kappa$	Von Karman constant	[-]
$\mu_x$	mean value for signal $x$	[dim( $x$ )]
$\nu$	poisson ratio	[-]
$\rho$	density of air	[kg/m <sup>3</sup> ]
$\rho_c$	specific gravity of reinforced concrete	[kg/m <sup>3</sup> ]
$\sigma_x$	standard deviation of signal $x$	[dim( $x$ )]
$\varphi_k$	random phase shift	[rad]
$\mathbf{\Omega}$	diagonal matrix with the eigenfrequencies	[rad/s]
$\omega_e$	damped natural frequency of the uncontrolled system	[rad/s]
$\omega_i$	eigenfrequency of the $i$ -th mode	[rad/s]



# 1. Introduction

With a growing population and an increasing demand for accommodation, high-rise buildings are becoming more and more popular. According to the Dutch- and also most European standards, there must be enough daylight in the buildings, which means that the width has to be limited. As result of this, the high-rise buildings will become slender, which makes them vulnerable for dynamic loadings. Besides this, construction materials and construction methods have been improving constantly, which results in fewer and stiffer connections. Where the structure gets a lot of its damping from its connections and cracks by friction, a consequence of this is that the damping of modern structures has decreased compared to older structures. Therefore dynamic behaviour occurring in the ultimate or serviceability limit state is becoming more and more important.

In the Wijnhaven district of Rotterdam, a new tower called the Juffertoren will be built. The first design of the Juffertoren includes 48 stories of living space with apartments, salvage and entry and on top of the building a technical space. The cross-section from the first floor to the 37<sup>th</sup> floor has dimensions of 15,44 m x 26,34 m. Above the 37<sup>th</sup> floor, the cross-section will be broadened. The total height of the building is 145 m, with a slenderness of 9,5. Due to this slenderness the building is sensitive to dynamic loading. Design calculations made by the company DHV have shown that the wind load will cause an acceleration level which will be detrimental to the comfort level of the residents. Therefore the owner has decided to adapt the design to a lower and less slender structure.

In this thesis, an investigation will be performed into the possibility of limiting the dynamic accelerations with the help of active control. An active control system is a system that can determine the state of a system and decide on a set of actions that will change the present state to a more desirable one. In the case of controlling the dynamic behaviour of a building, this can be done by applying a force to the building. According to the second law of Newton, this force can be achieved by accelerating a heavy mass where the force is desired. The mass will be driven by an engine and guided by a rail.

This study will be focused on active control and not particularly on the Juffertoren. So it is permitted to make some simplifications to the design. I decided to adapt some dimensions of the tower so that complicated influences on the dynamic behaviour of the building do not need to be considered in interpreting the results. For instance the larger dimensions of the top floors of the building will not be included in this study. The building will be modelled as a 144 meters high building with 48 stories, all having the same dimensions as can be seen in Appendix I.



## 2. Idealization of the building

The complete building will be modelled with 48 elements. The elements are connected at the nodes. Each node has one degree of freedom which is the horizontal displacement in the weak direction of the structure.

To determine whether the building has to be modelled as a shear, a bending or a combination of a shear and bending beam, a representative cross-section will be introduced. See Figure 2.1a). The maximum displacement at the top due to shear and bending will be determined and compared. Figure 2.1 b) and c) show respectively the displacement due to shear and bending of two floors of the building.

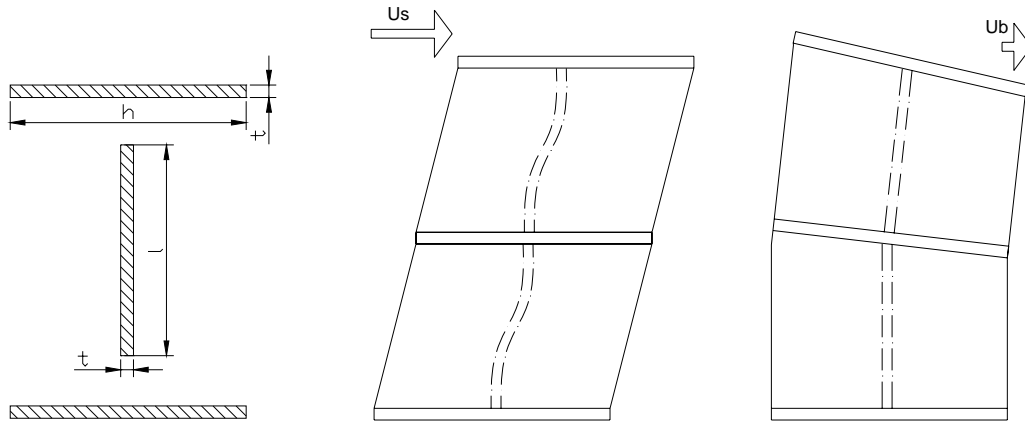


Figure 2.1 a) representative cross-section; b) shear deformation; c) bending deformation

The moment of inertia of the cross-section is approximately:

$$I = 2 * \frac{1}{12} th^3 \quad (2.1)$$

The effective area against shear deformation is roughly:

$$A_s = 2 * \frac{5}{6} th \quad (2.2)$$

We assume  $\nu = 0$  therefore  $G = \frac{E}{2}$ .

The displacement at the top of the building due to bending divided by the displacement at the top of the building due to shear is then given by:

$$\frac{u_{b:top}}{u_{s:top}} = \frac{\frac{qL^4}{8EI}}{\frac{qL^2}{EA_s}} = \frac{\frac{L^2}{8I}}{\frac{1}{A_s}} = \frac{A_s L^2}{8I} \approx \frac{5thL^2}{4th^3} = \frac{5}{4} \left( \frac{L}{h} \right)^2 \quad (2.3)$$

With  $L = 144$  m and  $h = 15$  m it becomes clear that bending dominates the behaviour. Therefore the building can be modelled as a bending beam and the shear deformation may be neglected.

### 2.1. Bending stiffness and mass of the structure

Before the stiffness matrix and the mass matrix can be calculated, the bending stiffness and the mass of the building have to be known. The location of the neutral axis of the cross-section of the building can be determined from:

$$n.a. = \frac{\sum sA}{\sum A} \quad (2.4)$$

where:

- $n.a.$  distance between the neutral axis and a parallel reference line;
- $s$  the perpendicular distance between the reference line and the centre of gravity of the considered wall;
- $A$  area of the considered wall.

The calculation of the location of the neutral axis is performed in Matlab as can be seen in Appendix I. The outcome is that the neutral-axis is located at 21 mm from the centreline. To make it easy it is assumed that the neutral-axis coincides with the centreline.

The second moment of inertia can be calculated as:

$$I = \sum s^2 A + \sum \frac{bh^3}{12} \quad (2.5)$$

The calculation has been worked out in Matlab as can be seen in Appendix I. With the application of concrete B65 Young's modulus is assumed at  $E = 30000 N/mm^2 = 3 \cdot 10^{10} N/m^2$  which leads to a bending stiffness of:

$$EI = 2,00 \cdot 10^{13} \text{ Nm}^2 \quad (2.6)$$

The mass of the walls of one storey can be calculated from:

$$m = \rho_c hA$$

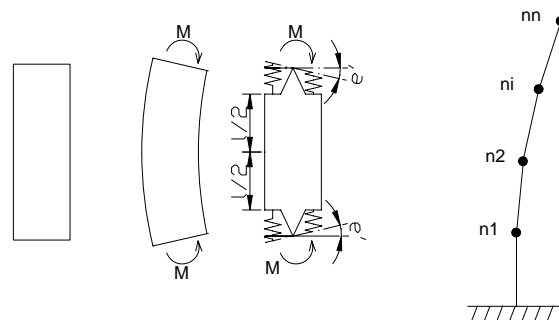
where:

- $\rho_c$  specific gravity of reinforced concrete,  $\rho_c = 2500 \text{ kg/m}^3$ ;
- $h$  height of the walls,  $h = 2,75 \text{ m}$

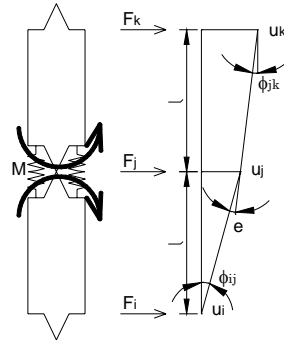
To find the mass of one storey, a floor has to be added to this mass. See Appendix I. The loading on the floors of  $250 \text{ N/m}^2$  has been added to this mass, which leads to a mass of:  $m = 6,32 \cdot 10^5 \text{ kg/storey}$ .

## 2.2. Element stiffness matrix: field element

The model is build up of 48 undeformable elements with deformable nodes. See Figure 2.2. The flexibility of the elements will be concentrated in the springs at the nodes.



**Figure 2.2** The building will be modelled as a bending beam with lumped deformations  
The aim is to find a relation between the nodal displacements and the nodal forces.


**Figure 2.3 Bending element**

This relation is derived in Appendix I which provides the stiffness matrix of a bending element:

$$\begin{Bmatrix} F_i \\ F_j \\ F_k \end{Bmatrix} = \frac{EI}{l^3} \begin{bmatrix} 1 & -2 & 1 \\ -2 & 4 & -2 \\ 1 & -2 & 1 \end{bmatrix} \begin{Bmatrix} u_i \\ u_j \\ u_k \end{Bmatrix} \quad (2.7)$$

### 2.3. Element stiffness matrix: bottom element

The connection between the ground and the building is not a fully clamped connection, because the piles will act like springs. The foundation will work as a rotational spring. The stiffness of this rotational spring will be determined so that the displacement at the top due to rotation of the foundation is equal to 20% of the displacement due to bending, when the building is loaded by an equally distributed load. This assumption is based on experience<sup>1</sup>.

$$u_{b:top} = \frac{qL^4}{8EI} \quad (2.8)$$

$$u_{r:top} = \frac{ML}{C_r} = \frac{1}{2} \frac{qL^3}{C_r} \quad (2.9)$$

The rotation stiffness can be determined by:

$$u_{r:top} = 0,2u_{b:top} \rightarrow \frac{qL^3}{2C_r} = \frac{qL^4}{40EI} \rightarrow C_r = \frac{20EI}{L} \quad (2.10)$$

The derivation of the elements stiffness matrix of the bottom element can be found in Appendix I which gives:

$$\begin{Bmatrix} F_i \\ F_j \end{Bmatrix} = \frac{1}{l^2} \frac{1}{\frac{l}{2EI} + \frac{1}{C_r}} \begin{bmatrix} 1 & -1 \\ -1 & 1 \end{bmatrix} \begin{Bmatrix} u_i \\ u_j \end{Bmatrix} \quad (2.11)$$

The stiffness matrix of the bending beam can be assembled with the stiffness matrix of the elements. Figure 2.4 shows how this has to be done with a system containing 4 degrees of freedom. With the use of Matlab, it is easy to assemble a much larger system, as has been done in Appendix I. Here the two bottom lines and two farthest right rows are assembled according to eqn. (2.11).

<sup>1</sup> Private investigations with Mathew Vola, Constructor of DHV

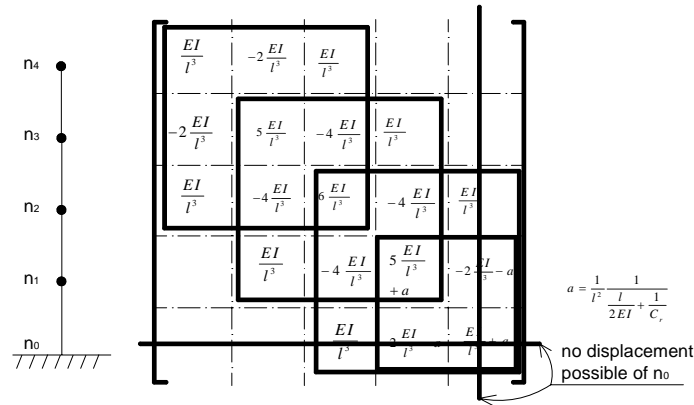


Figure 2.4 Assembling the system stiffness matrix

## 2.4. Mass matrix

The mass of the structure will be lumped in the nodes. The elements which represent the masses will appear on the diagonal of the mass matrix, as has been done in Appendix I.

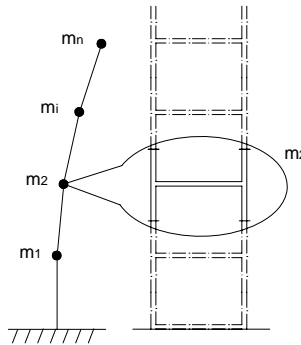


Figure 2.5 Lumping the mass in the nodes

## 2.5. Damping matrix

It is practically impossible to determine the damping matrix of a structure by calculating the damping of the different elements of the structure. There are too many uncertainties about the connections and the material properties. A well-known method for determining the damping matrix is the proportional damping method, also known as the Rayleigh damping method [2],[3]. With proportional damping we assume that the damping matrix is proportional to the mass and stiffness matrix.

$$\mathbf{C} = a_0 \mathbf{M} + a_1 \mathbf{K} \quad (2.12)$$

The constants can easily be determined by:

$$a_0 = \frac{2\omega_1\omega_2(\zeta_1\omega_2 - \zeta_2\omega_1)}{\omega_2^2 - \omega_1^2} \quad (2.13)$$

$$a_1 = \frac{2(\zeta_2\omega_2 - \zeta_1\omega_1)}{\omega_2^2 - \omega_1^2}$$

This can be proven by making use of modal analysis. The matrix  $\mathbf{E}$  is introduced which is the eigenmatrix.

$$\mathbf{E} = \sum_{i=1}^n \hat{\mathbf{u}}_i \quad (2.14)$$

Now the modal mass matrix and modal stiffness matrix are introduced, which are by definition diagonal because of the orthogonal equations.

$$\begin{aligned}\mathbf{M}^* &= \mathbf{E}^T \mathbf{M} \mathbf{E} \\ \mathbf{K}^* &= \mathbf{E}^T \mathbf{K} \mathbf{E}\end{aligned}\quad (2.15)$$

Introducing a modal damping matrix, which because of (2.12) also appears to be diagonal will give the following result:

$$\mathbf{C}^* = \mathbf{E}^T \mathbf{C} \mathbf{E} = a_0 \mathbf{M}^* + a_1 \mathbf{K}^* = a_0 \mathbf{E}^T \mathbf{M} \mathbf{E} + a_1 \mathbf{E}^T \mathbf{K} \mathbf{E} \quad (2.16)$$

Now we assume a modal damping ratio which means that every mode  $i$  has its own damping ratio  $\zeta_i$ . (Note that this equation is totally decoupled)

$$[2\zeta_i \omega_i] = \mathbf{M}^{*-1} \mathbf{C}^* \quad (2.17)$$

Making use of eqn. (2.15) and eqn. (2.16) this results in:

$$[2\zeta_i \omega_i] = \mathbf{M}^{*-1} [a_0 \mathbf{E}^T \mathbf{M} \mathbf{E} + a_1 \mathbf{K}^*] = a_0 \mathbf{I} + a_1 \mathbf{M}^{*-1} \mathbf{K}^* = a_0 \mathbf{I} + a_1 \mathbf{\Omega}^2 \quad (2.18)$$

Where  $\mathbf{\Omega}$  represents the diagonal matrix with the eigenfrequencies of the undamped system on the diagonal, hence:

$$\zeta_i = \frac{a_0}{2\omega_i} + \frac{a_1}{2} \omega_i \quad (2.19)$$

Which proves eqn. (2.13). The constants  $a_0$  and  $a_1$  can now be determined from:

$$\frac{1}{2} \begin{bmatrix} 1/\omega_i & \omega_i \\ 1/\omega_j & \omega_j \end{bmatrix} \begin{bmatrix} a_0 \\ a_1 \end{bmatrix} = \begin{bmatrix} \zeta_i \\ \zeta_j \end{bmatrix} \rightarrow \begin{bmatrix} a_0 \\ a_1 \end{bmatrix} = 2 \begin{bmatrix} 1/\omega_i & \omega_i \\ 1/\omega_j & \omega_j \end{bmatrix}^{-1} \begin{bmatrix} \zeta_i \\ \zeta_j \end{bmatrix} \quad (2.20)$$

The first and second eigenfrequency can be found in the analysis made in Matlab: see Appendix I. So taking  $i=1$  and  $j=2$  in eqn.(2.20), the only unknowns left for determining  $a_0$  and  $a_1$  are  $\zeta_1$  and  $\zeta_2$ . When  $\zeta_1$  and  $\zeta_2$  are known, the total damping matrix - see eqn. (2.12) - can be determined.

On the basis of experience it will be assumed that the damping ratios of the first and second eigenmode of a modern concrete building are  $\zeta_1 = \zeta_2 = 1\%$ . The total damping matrix is determined in Appendix I.



### 3. Numerical simulation in Simulink

Simulink is a component of Matlab, which provides an environment where a physical system and controller can be modelled as a block diagram.

The equation of motion of the building loaded by wind can be written as:

$$\mathbf{M}\ddot{\mathbf{u}} + \mathbf{C}\dot{\mathbf{u}} + \mathbf{K}\mathbf{u} = \mathbf{F} \quad (3.1)$$

The number of degrees of freedom is 48, so  $\mathbf{M}$ ,  $\mathbf{C}$  and  $\mathbf{K}$  are (48x48) matrices and  $\mathbf{u}$  and  $\mathbf{F}$  are (48x1) vectors. Farther on in eqn. (4.4) - where eqn. (3.1) is discretised -  $\mathbf{F}$  is defined as a matrix. Simulink cannot handle a second order differential equation. So the equation has to be rewritten in the state space formulation. This can be done by introducing a vector:

$$\mathbf{X} = \begin{bmatrix} \mathbf{u} \\ \dot{\mathbf{u}} \end{bmatrix} \quad (3.2)$$

Substitution of eqn. (3.2) in eqn.(3.1) gives:

$$\begin{bmatrix} \mathbf{I} & \mathbf{0} \\ \mathbf{0} & \mathbf{M} \end{bmatrix} \begin{bmatrix} \dot{\mathbf{X}} \\ \mathbf{X} \end{bmatrix} + \begin{bmatrix} \mathbf{0} & -\mathbf{I} \\ \mathbf{K} & \mathbf{C} \end{bmatrix} \begin{bmatrix} \mathbf{X} \\ \mathbf{X} \end{bmatrix} = \begin{bmatrix} \mathbf{0} \\ \mathbf{F} \end{bmatrix} \quad (3.3)$$

Multiplying on the left side of the second row of eqn.(3.3) with  $\mathbf{M}^{-1}$  gives:

$$\begin{bmatrix} \dot{\mathbf{X}} \\ \mathbf{X} \end{bmatrix} = \begin{bmatrix} \mathbf{0} & \mathbf{I} \\ -\mathbf{M}^{-1}\mathbf{K} & -\mathbf{M}^{-1}\mathbf{C} \end{bmatrix} \begin{bmatrix} \mathbf{X} \\ \mathbf{X} \end{bmatrix} + \begin{bmatrix} \mathbf{I} & \mathbf{0} \\ \mathbf{0} & \mathbf{M}^{-1} \end{bmatrix} \begin{bmatrix} \mathbf{0} \\ \mathbf{F} \end{bmatrix} \quad (3.4)$$

In Simulink the state space equation is formulated as:

$$\begin{aligned} \dot{\mathbf{x}} &= \mathbf{Ax} + \mathbf{Bu} \\ \mathbf{y} &= \mathbf{Cx} + \mathbf{Du} \end{aligned} \quad (3.5)$$

Where  $\mathbf{u}$  is the input and  $\mathbf{y}$  is the output. The output we are interested in is the displacement  $\mathbf{u}$  and the velocity  $\dot{\mathbf{u}}$  so  $\mathbf{y}$  will be defined as:

$$\mathbf{y} = \mathbf{X} \quad (3.6)$$

Rewriting eqn.(3.4) and eqn.(3.6) gives:

$$\begin{bmatrix} \dot{\mathbf{X}} \\ \mathbf{X} \end{bmatrix} = \begin{bmatrix} \mathbf{0} & \mathbf{I} \\ -\mathbf{M}^{-1}\mathbf{K} & -\mathbf{M}^{-1}\mathbf{C} \end{bmatrix} \begin{bmatrix} \mathbf{X} \\ \mathbf{X} \end{bmatrix} + \begin{bmatrix} \mathbf{0} \\ \mathbf{M}^{-1} \end{bmatrix} \begin{bmatrix} \mathbf{0} \\ \mathbf{F} \end{bmatrix} \quad (3.7)$$

$$\mathbf{y} = \begin{bmatrix} \mathbf{I} & \mathbf{0} \\ \mathbf{0} & \mathbf{I} \end{bmatrix} \begin{bmatrix} \mathbf{X} \\ \mathbf{X} \end{bmatrix} + \begin{bmatrix} \mathbf{0} \\ \mathbf{0} \end{bmatrix} \begin{bmatrix} \mathbf{0} \\ \mathbf{F} \end{bmatrix} \quad (3.8)$$

This can be introduced in Simulink by defining the following matrices:

$$\begin{aligned}
 \mathbf{A} &= \begin{bmatrix} \mathbf{0} & \mathbf{I} \\ -\mathbf{M}^{-1}\mathbf{K} & -\mathbf{M}^{-1}\mathbf{C} \end{bmatrix} \quad (96 \times 96) \\
 \mathbf{B} &= \begin{bmatrix} \mathbf{0} \\ \mathbf{M}^{-1} \end{bmatrix} \quad (96 \times 48) \\
 \mathbf{C} &= \begin{bmatrix} \mathbf{I} & \mathbf{0} \\ \mathbf{0} & \mathbf{I} \end{bmatrix} \quad (96 \times 96) \\
 \mathbf{D} &= \begin{bmatrix} \mathbf{0} \\ \mathbf{0} \end{bmatrix} \quad (96 \times 48) \\
 \mathbf{u} &= [\mathbf{F}] \quad (48 \times t_i) \quad (t_i = \text{number of timesteps})
 \end{aligned} \tag{3.9}$$

Note that the matrix  $\mathbf{C}$  and the vector  $\mathbf{u}$  in Simulink are not the same as respectively the damping matrix  $\mathbf{C}$  and the displacement vector  $\mathbf{u}$ . The Simulink model can be seen in Figure 3.1 and will be explained here. When Simulink is running, the state will be recalculated for every time step. The first block from the left contains the nodal forces as defined by eqn. (4.4). The output of this block is 48 elements for every time step. The second block transforms the elements of the first block into a vector. The third block contains the matrices defined in eqn. (3.9). The input of this block are the nodal forces and the output of this block are the displacements and velocities of the 48 degrees of freedom. Furthermore, 2 blocks can be seen which are selecting only the displacement and velocity of the top of the building as output from the total vector with all degrees of freedom. At far left, 3 output blocks can be seen. These blocks store the output in combination with the time and Matlab can make plots of these. Then there is one block which differentiates the velocity in time with as result the acceleration of the top.

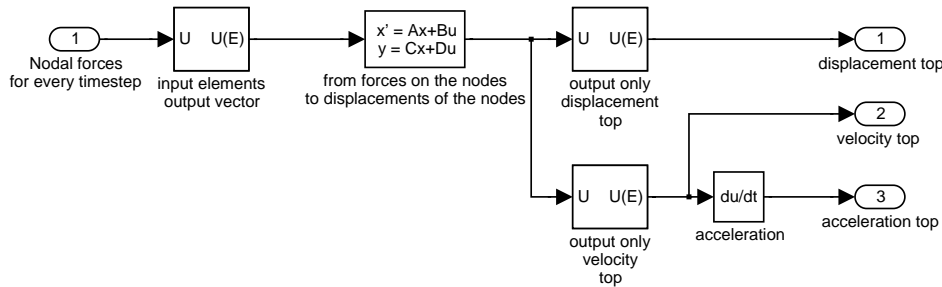


Figure 3.1 Uncontrolled model of the MDF system in Simulink

### 3.1.1. Validation of the static behaviour

The mass matrix is very simple with only elements on the diagonal and it is not necessary to validate it.

The stiffness matrix can easily be validated by application of a static evenly distributed load. Taking  $q = 62,1$  kN/m the total static displacement of the top of the building must be:

$$u_{static,top} = 1,2 \frac{qL^4}{8EI} = 0,200 \text{ m (20\% extra due to deformation of the foundation, see section 2.3).}$$

Now the stiffness matrix can easily be checked in Matlab with:

$$\mathbf{u} = \mathbf{K}^{-1}\mathbf{F} \tag{3.10}$$

with:

$\mathbf{K}$  Is the stiffness matrix derived in Appendix I according to section 2.2 and 2.3

**F** (48x1) vector with forces on the nodes, each force equals the height of one storey times the distributed load  $F_i = 3 * 62,1 = 186,3$  kN .

Executing eqn. (3.10) in Matlab results in a static deflection at the top of  $u_{top} = 0,205$  m , as can be seen in Figure 3.2, so the stiffness matrix is well defined.

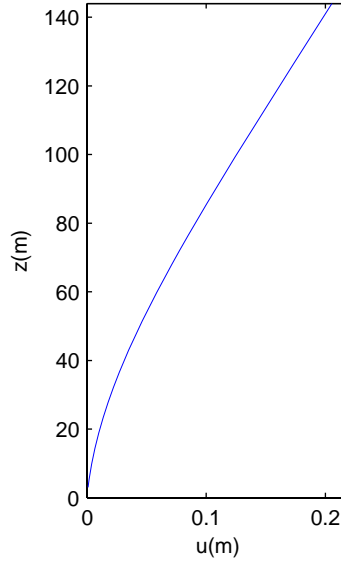


Figure 3.2 Static deflection to check the stiffness matrix

### 3.1.2. Validation of the dynamic behaviour: damping and eigenfrequency

The damping matrix and dynamic behaviour can be checked by applying a step function to the system in Simulink. By taking the same force as has been done for the static control, a vibration of the displacement of the top around  $u_{top} = 0,205$  m can be expected: see Figure 3.2. The natural frequencies can be determined from the homogeneous equation:

$$\mathbf{M}\ddot{\mathbf{u}} + \mathbf{C}\dot{\mathbf{u}} + \mathbf{K}\mathbf{u} = \mathbf{0} \quad (3.11)$$

With eqn. (2.15) and eqn.(2.16) this can be rewritten as:

$$\mathbf{E}^T \mathbf{M} \mathbf{E} \ddot{\mathbf{u}} + \mathbf{E}^T \mathbf{C} \mathbf{E} \dot{\mathbf{u}} + \mathbf{E}^T \mathbf{K} \mathbf{E} \mathbf{u} = \mathbf{M}^* \ddot{\mathbf{u}} + \mathbf{C}^* \dot{\mathbf{u}} + \mathbf{K}^* \mathbf{u} = \mathbf{0} \quad (3.12)$$

This is a fully decoupled differential equation. By multiplying this equation on the left with  $(\mathbf{M}^*)^{-1}$  and with the help of the relation  $(\mathbf{M}^*)^{-1} \mathbf{K}^* = \mathbf{\Omega}^2$  we find:

$$\ddot{\mathbf{u}} + (\mathbf{M}^*)^{-1} \mathbf{C}^* \dot{\mathbf{u}} + \mathbf{\Omega}^2 \mathbf{u} = \mathbf{0} \quad (3.13)$$

Where  $\mathbf{\Omega}$  is a diagonal matrix with on the diagonal  $\omega_i$  ( $i=1,2,\dots,48$ ). With eqn.(2.17), this decoupled system can be written as follows:

$$\ddot{u}_i + 2\zeta_i \omega_i \dot{u}_i + \omega_i^2 u_i = 0 \quad (i=1,2,\dots,48) \quad (3.14)$$

The homogeneous solution then is [2]:

$$u_i(t) = A_i e^{(-\zeta_i \omega_i t)} \sin(\omega_i t \sqrt{1 - \zeta_i^2} + \varphi_i) \quad (i=1,2,\dots,48) \quad (3.15)$$

This leads to the natural vibration:

$$u_1(t) = A_1 e^{(-\zeta_1 \omega_1 t)} \sin(\omega_1 t \sqrt{1 - \zeta_1^2} + \varphi_1) \quad (3.16)$$

With  $(\mathbf{M}^*)^{-1} \mathbf{K}^* = \mathbf{\Omega}^2$ , Matlab can determine  $\omega_i$ , as has been done in Appendix I. With  $\zeta_1 = 0,01$  and  $\omega_1 = 1,48$  rad/s the eigenfrequency of the damped system can be determined:

$$\omega_e = \omega_1 \sqrt{1 - \zeta_1^2} = 1,48 \sqrt{1 - 0,01^2} = 1,48 \text{ rad/s} \quad (3.17)$$

The dynamic displacement of the structure will exist for 95% of the vibration of the first mode [4]. So the contribution of the higher modes to the displacements is small. Therefore by knowing the damping ratio of the first eigenmode (see 2.5) and the natural frequency, the behaviour of the multi degree of freedom (MDF) system can be approached by the behaviour of an single degree of freedom (SDF) system see Figure 3.3.

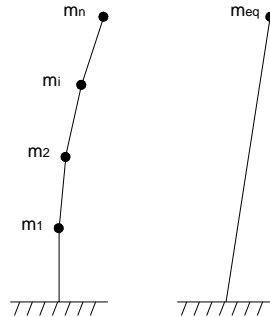


Figure 3.3 MDF and SDF system with equivalent mass

Schematizing the structure as an SDF system with the displacement at the top as the degree of freedom gives [2]:

$$u(t) = \frac{F}{k} \left( 1 - e^{-\zeta \sqrt{\frac{k}{m_{eq}}} t} * \sin(\omega_e t) \right) \quad (3.18)$$

with:

$$\omega_e = 1,48 \text{ rad/s}$$

$$k = \frac{8EI}{1,2L^4} = 3,11 * 10^5 \text{ N/m}^2$$

$$\zeta = 0,01$$

$$F = ku_{top} = 62200 \text{ N}$$

$$m_{eq} = \frac{k}{\omega_1^2} = \frac{8EI}{1,2L^4 \omega_1^2} = 1,42 * 10^5 \text{ kg}$$

The response of the SDF system eqn. (3.18) and the MDF system from Simulink, to a step load can be seen in Figure 3.4. The responses are almost the same; the difference can be accounted for by the higher modes of the MDF system which are not included in the SDF system. The vibrations converge to a displacement of  $u_{top} = 0,200$  m and the period equals:

$$T_1 = \frac{2\pi}{\omega_1} = \frac{2\pi}{1,48} = 4,25 \text{ s} \quad (3.19)$$

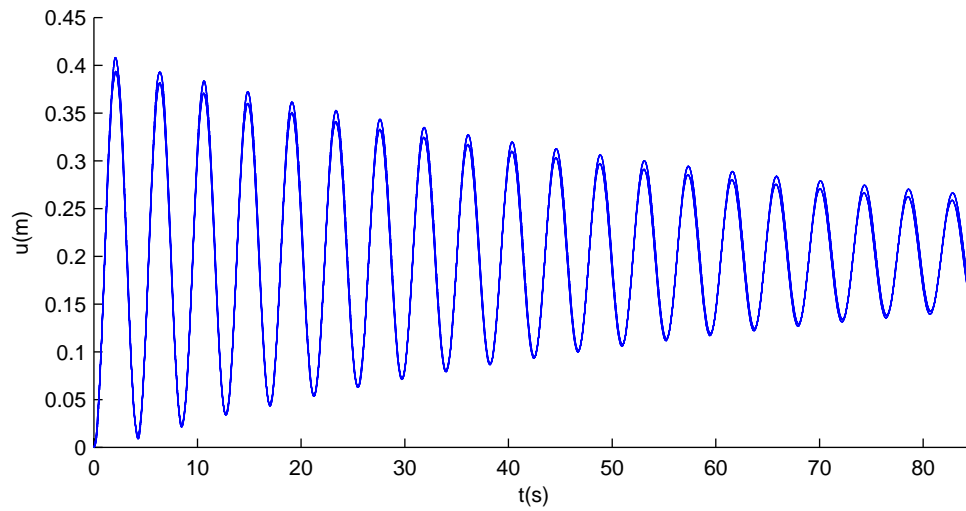


**Figure 3.4** Response to a step load of analytical SDF system and MDF system with Simulink simulation.



## 4. Wind

The building will be located in an urban area II according to NEN 6702 [5]. The wind consists of an hourly-averaged part  $\bar{v}(z)$  and a fluctuating part  $\tilde{v}(y, z, t)$ .

### 4.1. Wind load on the structure

The wind load will be lumped as forces on the nodes as can be seen in Figure 4.1. The force on a node is equal to:

$$F_i(t) = AC_h q_w \quad (4.1)$$

with:

$$q_w = \frac{1}{2} \rho (\bar{v} + \tilde{v})^2 \quad (4.2)$$

$i$	Node number
$A$	The area loaded by wind; $A = 3 * 26,34 = 79 \text{ m}^2$
$\rho$	Density of air; $\rho = 1,25 \text{ kg/m}^3$
$C_h$	Shape factor; $C_h = 0,8 + 0,4 = 1,2$ (NEN 6702 figure A.4)

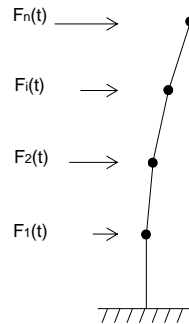


Figure 4.1 Forces on the nodes as a function of time

The forces on the nodes can be presented as a vector where each element represents a nodal force. By discretization in time, these nodal forces can be calculated for every time step, which makes a matrix of the nodal forces as shown in eqn. (4.3). The nodes are numbered  $1, i, \dots, n$  and the time steps are numbered  $1, k, \dots, m$ .

$$\mathbf{F}(t) = \begin{bmatrix} F_1(t) \\ F_i(t) \\ \cdot \\ F_n(t) \end{bmatrix} \xrightarrow{\text{discretization in time}} = \begin{bmatrix} F_{11} & F_{1k} & \cdot & F_{1m} \\ F_{i1} & F_{ik} & \cdot & \cdot \\ \cdot & \cdot & \cdot & \cdot \\ F_{n1} & \cdot & \cdot & F_{nm} \end{bmatrix} \quad (4.3)$$

The nodal force matrix can be calculated by making use of eqn. (4.1) and eqn. (4.2) where  $\bar{v}$  is only fluctuating in place and  $\tilde{v}$  is fluctuating in place and in time, which gives:

$$\mathbf{F} = \begin{bmatrix} F_{11} & F_{1k} & \cdot & F_{1m} \\ F_{i1} & F_{ik} & \cdot & \cdot \\ \cdot & \cdot & \cdot & \cdot \\ F_{n1} & \cdot & \cdot & F_{nm} \end{bmatrix} = \frac{1}{2} AC_h \rho \begin{bmatrix} (\bar{v}_1 + \tilde{v}_{11})^2 & (\bar{v}_1 + \tilde{v}_{1k})^2 & \cdot & (\bar{v}_1 + \tilde{v}_{1m})^2 \\ (\bar{v}_i + \tilde{v}_{i1})^2 & (\bar{v}_i + \tilde{v}_{ik})^2 & \cdot & \cdot \\ \cdot & \cdot & \cdot & \cdot \\ (\bar{v}_n + \tilde{v}_{n1})^2 & \cdot & \cdot & (\bar{v}_n + \tilde{v}_{nm})^2 \end{bmatrix} \quad (4.4)$$

NEN 6702 assumes that the wind load on a structure for  $z < 9m$  is equal to the wind load for  $z = 9m$ . For the sake of simplicity for the Matlab files it is assumed that for the constant part it holds that  $\bar{v}(z \leq 9 \text{ m}) = \bar{v}(z = 9 \text{ m})$  and for the fluctuating part it holds that  $\tilde{v}(y, z \leq 9 \text{ m}, t) = \tilde{v}(y, z = 9 \text{ m}, t)$ .

## 4.2. Mean part of the wind speed

The hourly-averaged wind speed varies with the height above ground level and can be described by [5]:

$$\bar{v}(z) = \frac{u_*}{\kappa} \ln \left( \frac{z - d_w}{z_0} \right) \quad (4.5)$$

where:

$u_*$	Friction velocity [m/s]
$\kappa$	Von Karman constant [1]; = 0,4
$z$	height above the surface of the earth [m]
$d_w$	displacement height [m]
$z_0$	roughness length [m]

The values can be found in the last but one column of Table 1.

	<i>Open flat terrain</i>			<i>Urban</i>		
	I	II	III	I	II	III
$u_*$	2,25	2,30	2,25	3,08	<b>2,82</b>	2,60
$z_0$	0,1	0,2	0,3	0,7	<b>0,7</b>	0,7
$d_w$	0	0	0	3,5	<b>3,5</b>	3,5
$k_c$	1,0	1,0	1,0	0,9	<b>0,9</b>	0,9

**Table 1** Parameters for hourly averaged wind speed, NEN 6702 page 128

Substituting in eqn. (4.5) results in a wind speed profile as can be seen in Figure 4.2.

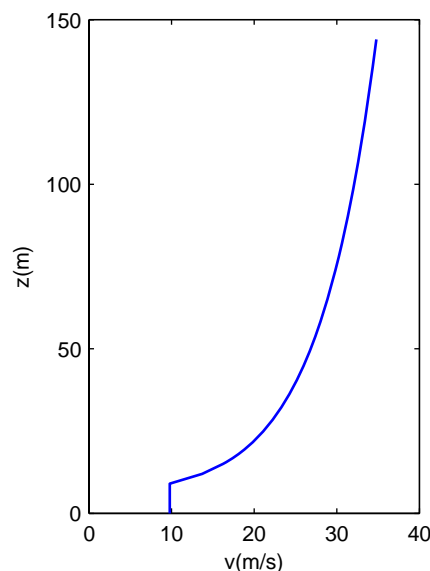


**Figure 4.2** Extreme hourly-averaged wind speed profile once in 12,5 years, once in 50 years under unfavourable direction

### 4.3. Fluctuating part of the wind speed

The fluctuating part of the wind speed  $\tilde{v}$  will be modelled with the Davenport spectrum [1]. The variance spectrum of the wind can be written as a function of the Davenport spectrum by:

$$S_{vv}(f) = \frac{F_D \sigma_v^2}{f} \quad (4.6)$$

with:

$$F_D = \frac{2}{3} \frac{x^2}{(1+x^2)^{4/3}} \quad \text{Davenport variance spectrum;}$$

$\sigma_v$  standard deviation of the wind speed;

$$x = \frac{fL_{gust}}{v(10)} \quad \text{dimensionless frequency;}$$

This gives the variance spectrum of the wind speed as a function of  $f$  :

$$S_{vv}(f) = \frac{2}{3} \frac{\left(\frac{fL_{gust}}{v(10)}\right)^2}{\left(1 + \left(\frac{fL_{gust}}{v(10)}\right)^2\right)^{4/3}} \frac{\sigma_v^2}{f} \quad (4.7)$$

with:

$f$  frequency;

$v(10)$  mean wind speed at 10 m height = 10 m/s see Figure 4.2 ;

$L_{gust}$  characteristic length of a wind gust.

If the spectrum is written as a function of the circle-frequency  $\omega$  the spectrum

$S_{vv}(\omega)$  is defined such that  $\sigma_v^2 = \int_0^{\infty} S_{vv}(\omega) d\omega$ . Where the spectrum is written as a

function of  $f$ , the spectrum  $S_{vv}(f)$  is defined such that  $\sigma_v^2 = \int_0^{\infty} S_{vv}(f) df$ . The relation

between those spectra can be given by:

$$S_{vv}(\omega) d\omega = S_{vv}(f) df \rightarrow S_{vv}(\omega) = S_{vv}\left(f = \frac{\omega}{2\pi}\right) \frac{df}{d\omega} = S_{vv}\left(f = \frac{\omega}{2\pi}\right) \frac{1}{2\pi} \quad (4.8)$$

With the help of eqn. (4.8), the variance spectrum of eqn. (4.7) can be written as a function of  $\omega$  :

$$S_{vv}(\omega) = \frac{1}{2\pi} \frac{2}{3} \frac{\left(\frac{\omega L}{2\pi v(10)}\right)^2}{\left(1 + \left(\frac{\omega L}{2\pi v(10)}\right)^2\right)^{4/3}} \frac{2\pi \sigma_v^2}{\omega} = \frac{\left(\frac{L}{v(10)}\right)^2}{\left(1 + \left(\frac{\omega L}{2\pi v(10)}\right)^2\right)^{4/3}} \frac{\omega \sigma_v^2}{6\pi^2} \quad (4.9)$$

The standard deviation of the wind can be calculated with:

$$\sigma_v = \bar{v}l \quad (4.10)$$

With:

$$I(z) = \frac{k_c}{\ln\left(\frac{z-d_w}{z_0}\right)} \quad \text{Turbulence intensity factor:}$$

$k_c = 0,9$  is a factor see Table 1

Taking for  $\bar{v}$  eqn. (4.5), this results in:

$$\sigma_v = \frac{ku_s}{\kappa} = \frac{0,9 * 2,82}{0,4} = 6,35 \text{ m/s} \quad (4.11)$$

The variance spectrum of the wind speed as a function of  $\omega$  is plotted in Figure 4.3.

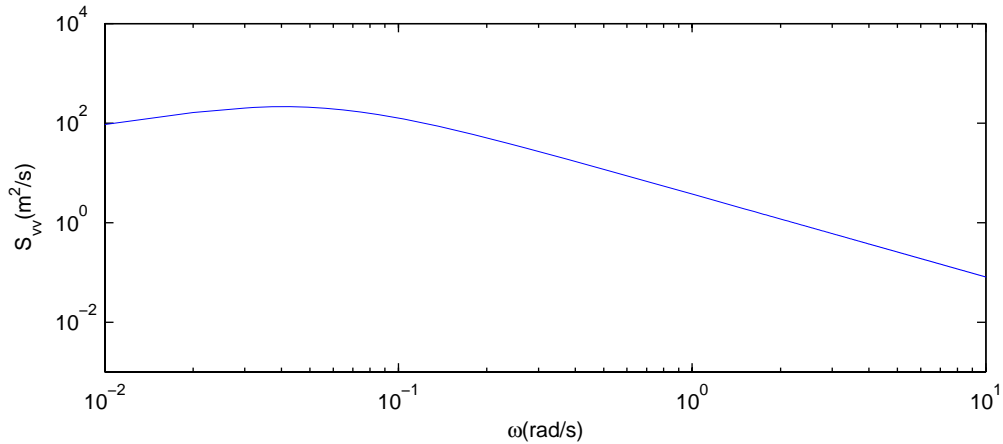


Figure 4.3 Spectrum of the wind speed

A realisation of the wind in the time domain can now be calculated by dividing the  $\omega$  domain into a finite number of points  $\omega_k$  equally distanced at  $\Delta\omega$ . The fluctuating part of the wind speed is now described by:

$$\tilde{v} = \sum_{k=1}^N a_k \sin(\omega_k t + \varphi_k) \quad (4.12)$$

with:

$$a_k = \sqrt{2S_{vv}\Delta\omega_k}$$

$\varphi_k$  Random number between 0 and  $2\pi$

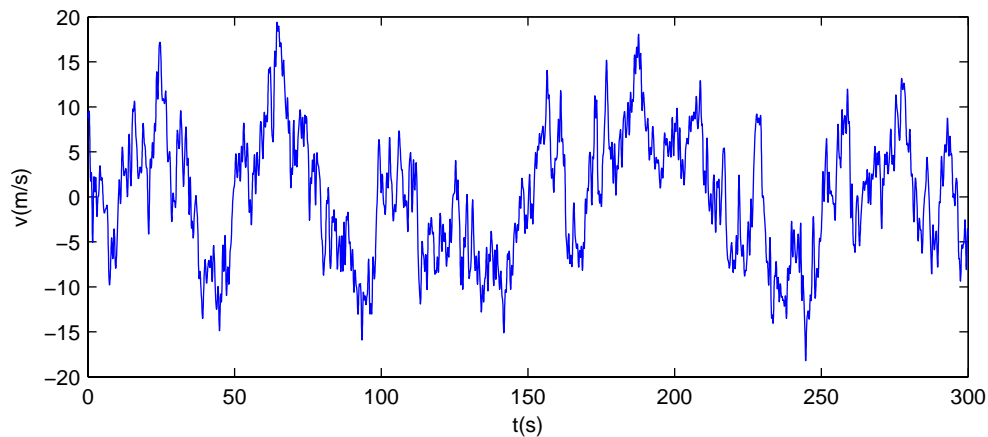


Figure 4.4 A realization of the fluctuating wind speed

### 4.3.1. Correlation between the wind speed at different locations

The fluctuating part of the wind speed is not only varying in time but also in place. The wind speed at the locations on the facade of the building is naturally not the same at each moment. When there is a peak of the wind speed at the top of the building there may not be a peak at the bottom of the building too. This is due to the dimensions of a wind gust.

When we assume that the wind speed at every node is the same we speak about total correlation, but this is much too conservative: see Figure 4.5. When the wind speed at the different nodes are totally independent of each other this is called uncorrelated in z-direction. Placing 46 uncorrelated signals on the building with a mean of  $0\text{ m/s}$  will result in a mean wind speed on the building of about  $0\text{ m/s}$ . The result of this is that the dynamic load will also be about zero. The reality is somewhere in between totally correlated and uncorrelated.

The correlation between the wind speeds at different points can be described with cross-spectra:

$$|S_{v_1v_2}(f)|^2 = S_{v_1v_1}(f)S_{v_2v_2}(f)coh_{v_1v_2}^2(f) \quad (4.13)$$

with:

$S_{v_1v_2}(f)$	the cross-spectrum of the wind speeds in points 1 and 2
$S_{v_iv_i}(f)$	auto-spectrum of the wind in point $i$
$coh_{v_1v_2}(f)$	coherence between the wind speeds in point 1 and 2

and:

$$coh_{v_1v_2}(f) = \exp\left(-\frac{f\sqrt{C_z^2(z_1 - z_2)^2 + C_y^2(y_1 - y_2)^2}}{\bar{v}(10)}\right) \quad (4.14)$$

with:

$y, z$	lateral and vertical coordinate, respectively;
$C_z, C_y$	coherence constant in z- and y-direction, respectively see Table 2

	$C_z$	$C_y$
<i>lateral spectrum</i>	7	10

**Table 2 Coherence constants**

To take into account the correlation, use is made of a Matlab program [9]. This program calculates the wind speed for every predefined point with coordinates  $(y, z)$  as a discrete function of the time. Before running the file, the standard deviation, the mean wind speed and the coherence, see eqn.(4.14), have to be defined. The Matlab program can be seen in Appendix I.

The façade of the building has to be divided in equal areas with in the centre of each area a point for which the wind speed as a function of time will be calculated. By knowing the wind speed in a point, the wind load on the considered area can be calculated with eqn. (4.1). The wind loads on the different areas will be lumped in the 48 nodes.

Now the question is: for how many points does the wind speed need to be calculated, or in other words, how fine should the mesh be. If the wind speed is calculated for too few points or for an area that is too big, there will still be still too much correlation taken into account. For example, calculating the wind speed at  $(y; z) = (13\text{ m}; 48\text{ m})$  and at  $(y; z) = (13\text{ m}; 96\text{ m})$  and assuming that the wind at the lower half of the building equals the wind speed at  $(y; z) = (13\text{ m}; 48\text{ m})$  and the wind

speed at the upper half of the building equals the wind speed at  $(y; z) = (13 \text{ m}; 96 \text{ m})$  is inaccurate. The reason for this is because, now, fluctuations within the lower- and upper half are not taken into account. To take into account these fluctuations the mutual distance between the different points has to be small enough. Or in other words the areas have to be refined by increasing the number of points.

How many points/areas have to be evaluated can be found by simulations. Too few points give too little variation and this gives too heavy accelerations. Increasing the number of points will smooth out the peak values, which means less variation and a less heavy dynamic behaviour. By taking more and more points, the loading will converge to the “real” loading on the building.

A totally correlated signal gives a peak value for the acceleration of the top of the building of about  $0,35 \text{ m/s}^2$  as can be seen in Figure 4.5. To make clear what totally correlated means, the force on the top and the bottom of the building has been represented in Figure 4.5a). The graphs of the force are parallel to each other, because the fluctuating part of the wind speed at the top is equal to the fluctuating wind speed at the bottom. In Figure 4.6 the results can be seen of the calculation of the wind speed at 46 points. Note that the wind load on the first and second node equals the wind load on the third node as prescribed in NEN 6702, which delivers the force on 48 nodes instead of 46. Figure 4.6a) shows that the graphs of the force at the top and the bottom are not parallel to each other. This is because the fluctuating part of the wind speed at the top and the bottom of the building are not totally correlated. It must be noticed that all the simulations give upper bounds of the acceleration of the top of the building, so they are all safe. The wind speed and the accompanying accelerations of the top of the building have been calculated for 46, 460 and 910 points. See respectively Figure 4.6, Figure 4.7 and Figure 4.8. The graphs are plotted with an offset of 50 s, because it takes some time for damping out of the relative high influence of the initial conditions.

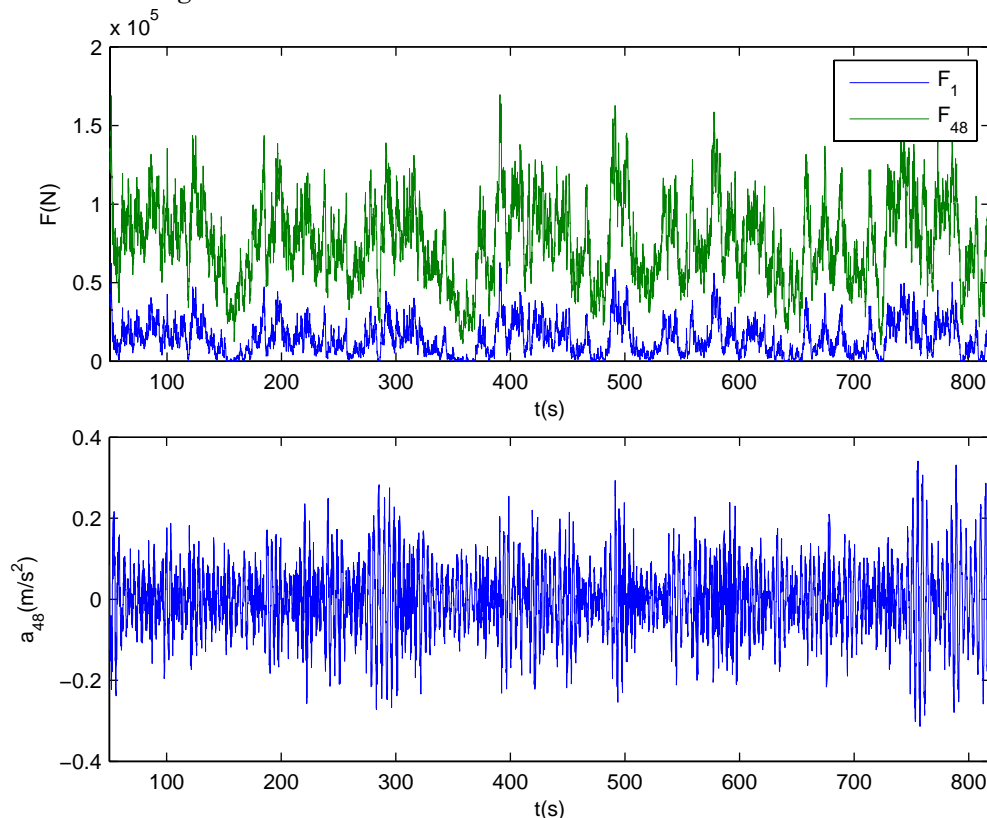


Figure 4.5 Totally correlated: a) forces on the nodes; b) acceleration of the top

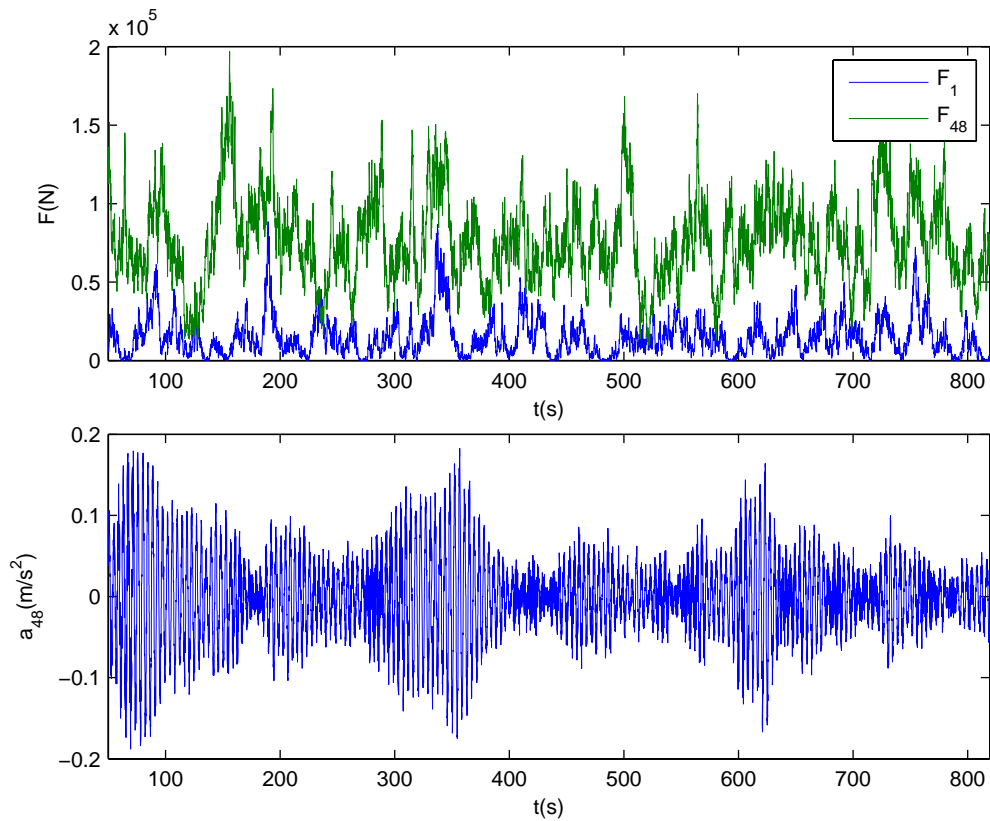


Figure 4.6 Wind speed calculated at 46 points: a) forces on the nodes; b) acceleration of the top

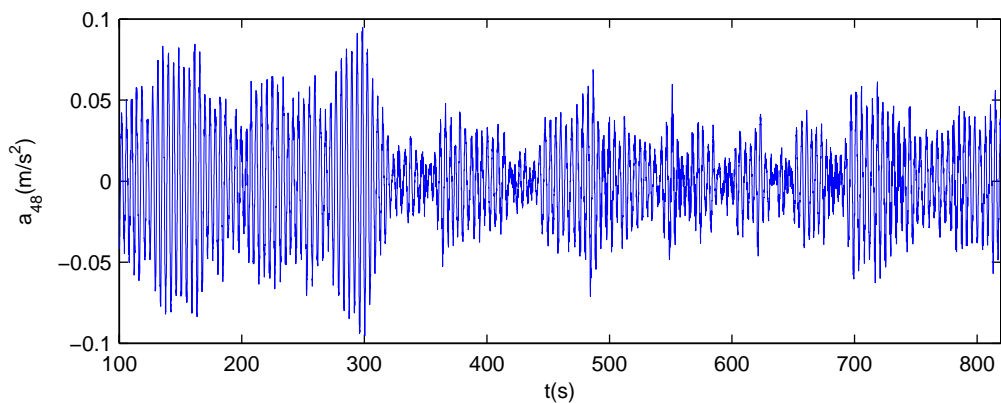
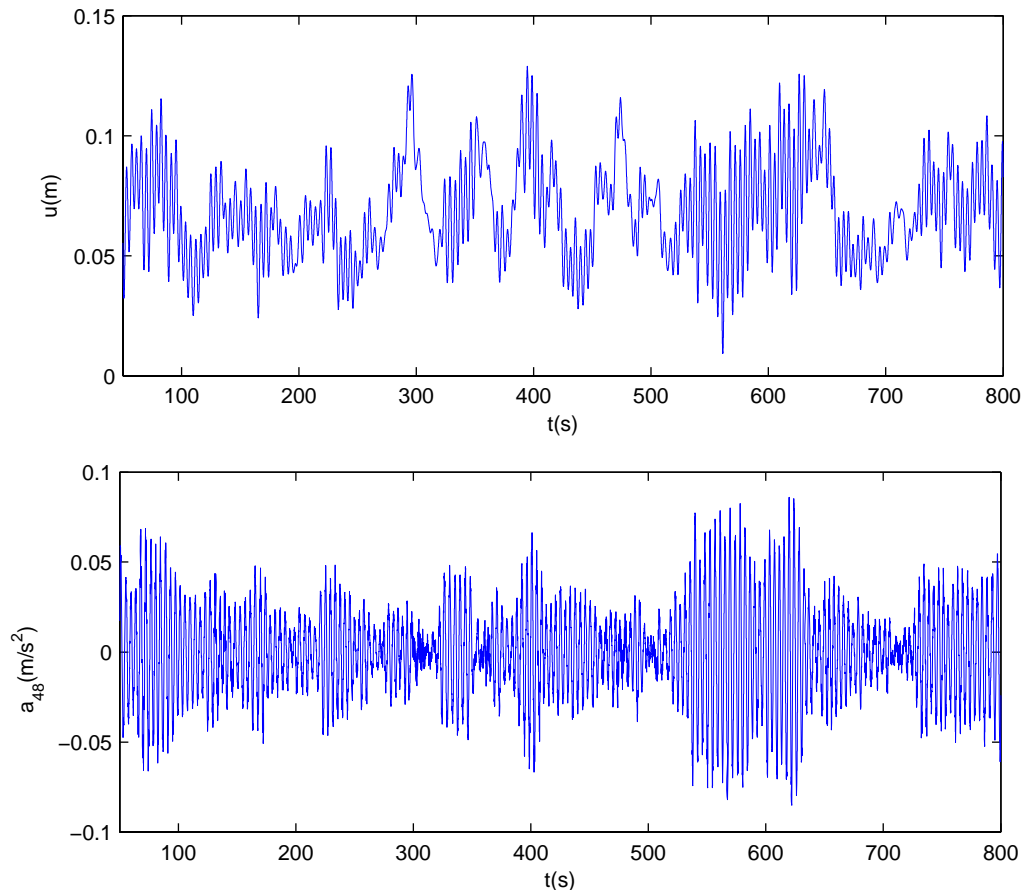


Figure 4.7 Wind speed calculated at 460 points, acceleration of the top



**Figure 4.8 Wind speed calculated at 910 points:  
a) displacement of the top; b) acceleration of the top.**

It is clear that calculating the wind speed in 460 points will give a quite large reduction of the acceleration compared to the simulation with the wind speed calculated at 46 points. From this it can be concluded that taking 46 points will give a too coarse mesh. Refining the mesh further to 910 points will give a little more reduction of the acceleration of the top of the building compared to the simulation with the wind speed calculated in 460 points. Refining the mesh further will give no considerable reduction of the acceleration of the top of the building. From here on, the acceleration according to Figure 4.8 will be called “the uncontrolled acceleration of the top of building”.

## 5. Control algorithm

### 5.1. Linear negative feedback: displacement and velocity control

The control force will be most effective when positioned at the top. The active control system can mechanically be schematised as a control force at the top of the building, Figure 5.1.

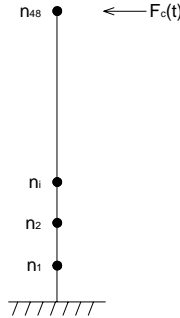


Figure 5.1 Schematisation of the active control force on the building

The equation of motion, eqn. (3.1) can now be rewritten as:

$$\mathbf{M}\ddot{\mathbf{u}} + \mathbf{C}\dot{\mathbf{u}} + \mathbf{K}\mathbf{u} = \mathbf{F} - \mathbf{E}_r F_c \quad (5.1)$$

Where  $F_c$  is the control force and  $\mathbf{E}_r$  is a 48x1 vector that defines the location of the control force with respect to the nodes:

$$\mathbf{E}_r = \begin{bmatrix} 0 \\ 0 \\ \cdot \\ 0 \\ 1 \end{bmatrix} \quad (5.2)$$

The magnitude of  $F_c(t)$  can be coupled to the velocity and displacement of the top of the building. This method is called linear negative feedback control. Coupling the active control force to the acceleration of the top of the building is not an option as will become clear in section 5.1.1. See also [6] and [7].

$$F_c(t) = \mathbf{k}_d \mathbf{u} + \mathbf{k}_v \dot{\mathbf{u}} = \begin{bmatrix} 0 & 0 & \cdot & 0 & k_d \end{bmatrix} \begin{bmatrix} u_1 \\ u_2 \\ \cdot \\ u_{48} \end{bmatrix} + \begin{bmatrix} 0 & 0 & \cdot & 0 & k_v \end{bmatrix} \begin{bmatrix} \dot{u}_1 \\ \dot{u}_2 \\ \cdot \\ \dot{u}_{48} \end{bmatrix} \quad (5.3)$$

Where  $k_d$  and  $k_v$  stand for, respectively displacement control and velocity control. Combining eqn. (5.1) and eqn. (5.3) gives:

$$\mathbf{M}\ddot{\mathbf{u}} + (\mathbf{C} + \mathbf{E}_r \mathbf{k}_v) \dot{\mathbf{u}} + (\mathbf{K} + \mathbf{E}_r \mathbf{k}_d) \mathbf{u} = \mathbf{F} \quad (5.4)$$

Where  $\mathbf{E}_r \mathbf{k}_v$  and  $\mathbf{E}_r \mathbf{k}_d$  gives a 48x48 matrix with only zeros except for the entry (48,48). So  $\mathbf{k}_v$  gives extra damping and  $\mathbf{k}_d$  gives extra stiffness to the 48<sup>th</sup> degree of freedom as can be seen in Figure 5.2. Displacement control gives a higher stiffness to the system, which results in a higher eigenfrequency, which makes the system less sensitive to the wind load. A higher stiffness will also give smaller displacements. Velocity control gives more damping to the system, which gives a faster convergence of the system to the desired value. It will be clear that coupling

the active force to the acceleration of the top of the building is the same as adding mass at the top of the building. This will give no changes in the dynamic behaviour of the structure. More about the effect of displacement control and velocity control can be found in [6].

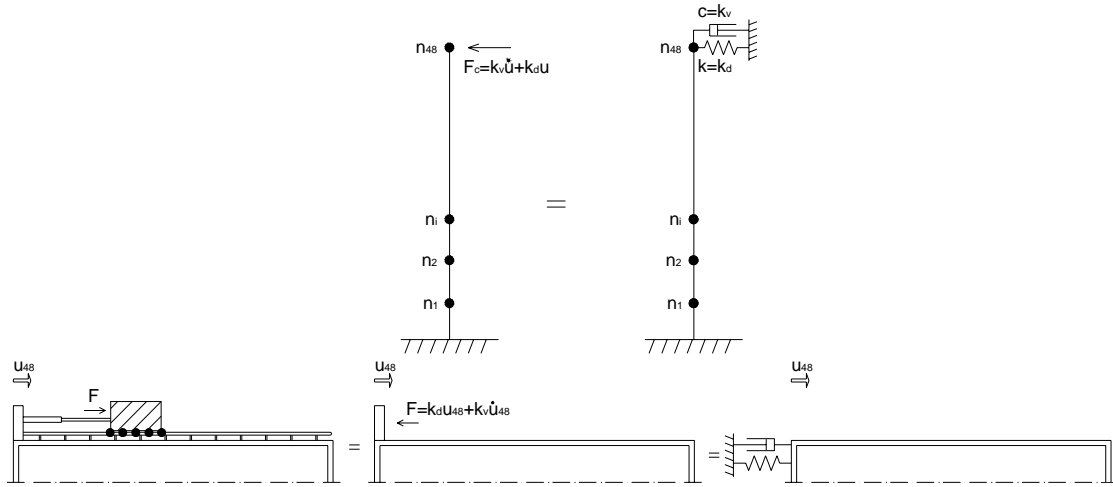


**Figure 5.2** The effect of adding an active control force to the structure: a) mechanical model of the total structure; b) roof of the building with mass and jack.

In the case of a building loaded by wind, displacement control will not work. Because the wind load consists of a constant part and a fluctuating part, the displacement also consists of a constant and a fluctuating part. See Figure 4.8 b). If the control force is now coupled to the displacement, it should be coupled only to the fluctuating part of the displacement. But in practice the magnitude of the fluctuating part and the constant part is not known. Coupling of the force to the constant and fluctuating part of the displacement would give a reduction of the displacement. But the aim is not reducing the displacement, but reducing the accelerations. Another problem would be that the control force will also have a constant part, which results in a constant acceleration of the mass of the active control system.

The only possibility left is coupling the force to the velocity of the top of the building.

### 5.1.1. Energy consideration

When the dynamic behaviour of the building is heavy, this means that there is a large amount of energy in the building in the form of distortion- and kinetic energy. The aim of the active control system is reducing these forms of energy by subtracting kinetic energy from the system with the accelerating mass. The subtracted energy equals:

$$E = \int F_c dx = \int F_c v_{48} dt \quad (5.5)$$

When the subtracted energy is get negative, this means that the active control adds energy to the moving structure, which will cause still heavier dynamic behaviour. Now it can be shown why coupling the active control force to the velocity of the top of the building is most effective. Assuming for the displacement of the top of the building:

$$u_{48} = \hat{u}_{48} \sin(\omega t) \quad (5.6)$$

Then the velocity equals:

$$v_{48} = \omega \hat{u}_{48} \cos(\omega t) \quad (5.7)$$

And the acceleration equals:

$$a_{48} = -\omega^2 \hat{u}_{48} \sin(\omega t) \quad (5.8)$$

With  $k_d$ ,  $k_v$  and  $k_a$  for respectively displacement-, velocity-, and acceleration control the energy subtracted from the moving structure will be:

$$E = \int (k_d u_{48} + k_v v_{48} + k_a a_{48}) v_{48} dt \quad (5.9)$$

Substituting eqn. (5.6), eqn. (5.7) and eqn. (5.8) gives:

$$\begin{aligned} E &= \int \left[ k_d \hat{u}_{48} \sin(\omega t) + k_v \omega \hat{u}_{48} \cos(\omega t) - k_a \omega^2 \hat{u}_{48} \sin(\omega t) \right] \omega \hat{u}_{48} \cos(\omega t) dt \\ &= \omega \hat{u}_{48}^2 \int \left[ (k_d - k_a \omega^2) \sin(\omega t) \cos(\omega t) + k_v \omega \cos^2(\omega t) \right] dt \end{aligned} \quad (5.10)$$

It is clear that only velocity control will always have a positive contribution to the subtracted energy by the active control system. Displacement and acceleration control will give a negative contribution to the subtraction of energy from the moving building, and therefore it will be less effective.

## 5.2. Feedback loop in Simulink

The uncontrolled model of the system of Figure 3.1 is extended with a feedback loop, see Figure 5.3.

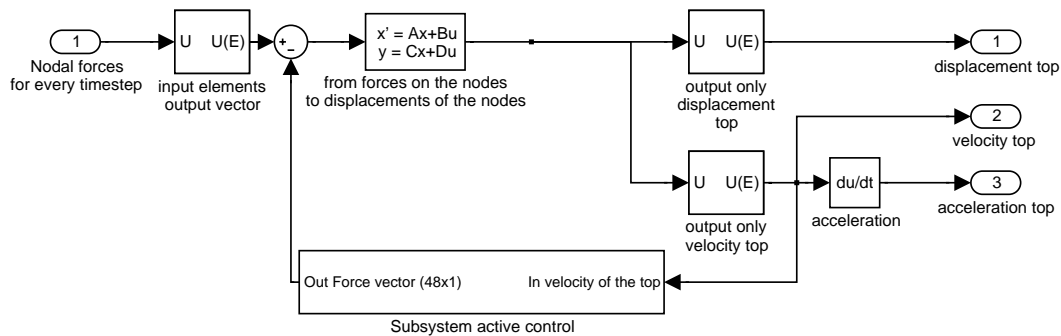


**Figure 5.3 Simulink model with feedback loop for active control**

The active control system is integrated in a subsystem which can be seen in Figure 5.4, with as input the velocity of the top and as output the active control force. The second block from the left will multiply the velocity with  $k_v$  which gives a force as output. In the next block to the right there is a transport delay which will be treated in section 6.2.3. The second last block on the right makes a (48x1) vector, with only zeros except for the last entry. This force vector is the output vector of the subsystem which will be added to the vector of the wind load. See Figure 5.3. By setting  $k_v = 3 \cdot 10^5$  kg and the transport delay equal to zero and running Simulink again with the input forces - as can be seen in Figure 4.8 a) - the results of Figure 5.6 will be obtained, which is a notable reduction compared with the acceleration of the top of the building of the uncontrolled system: see Figure 5.5.

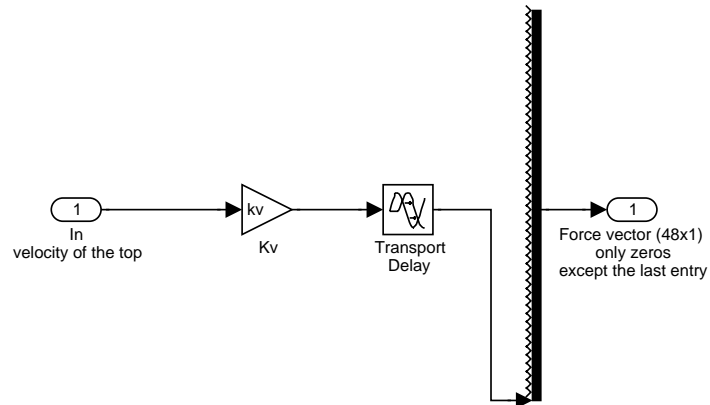


Figure 5.4 Simulink subsystem active control

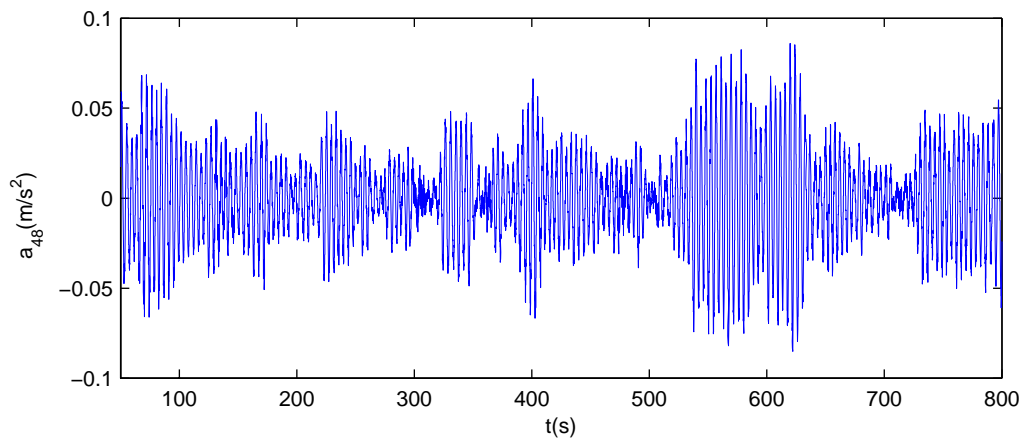


Figure 5.5 Acceleration of the top of the building of the uncontrolled system

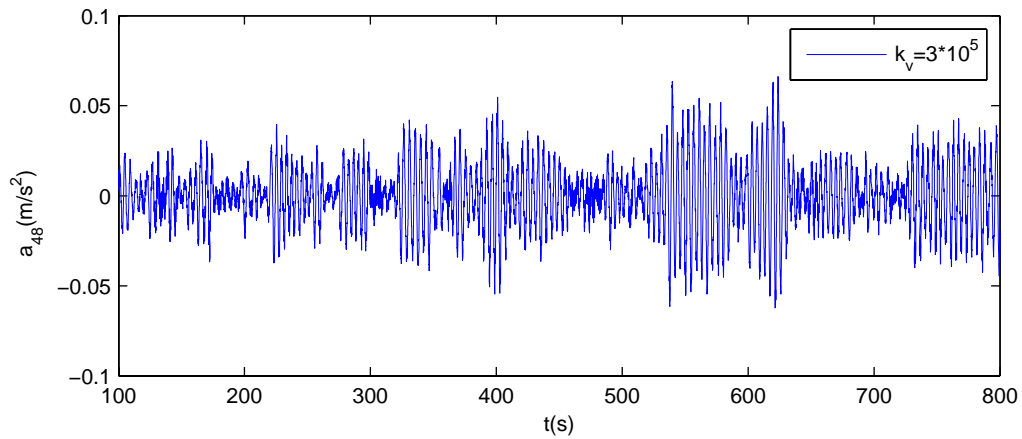


Figure 5.6 Acceleration of the top of the building of the controlled system

### 5.3. Displacement of the mass

In Figure 5.7 a part of the active control force is shown. This force will be generated by accelerating the mass of the active control system. The acceleration of the mass of the active control system can be written as:

$$a_m = \frac{F_c}{m} \quad (5.11)$$

Where:

$a_m$	acceleration of the mass [m/s <sup>2</sup> ];
$F_c$	active control force [N];
$m_m$	mass [kg].

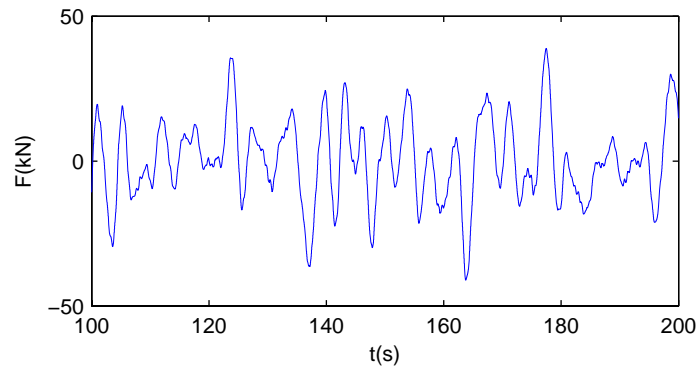


Figure 5.7 Active control force

The velocity of the mass can be found by integrating the acceleration of the mass in time. Integrating once more will give the displacement of the mass. By integrating twice, two integration constants can be found. In determining these there will be a problem which will be explained here. Assume that the acceleration equals a single sine function, then the velocity and displacement of the mass can be determined with:

$$a_m = \hat{a} \sin(\omega t) \quad (5.12)$$

$$v_m(t) = \int_0^t a_m dt = -\frac{\hat{a}}{\omega} \cos(\omega t) + c_1 \quad (5.13)$$

$$u_m(t) = \int_0^t v_m dt = -\frac{\hat{a}}{\omega^2} \sin(\omega t) + c_1 t + c_2 \quad (5.14)$$

By taking the initial velocity and the initial displacement equal to zero  $v_m(0) = u_m(0) = 0$ , the constants can be determined:

$$v_m(0) = -\frac{\hat{a}}{\omega} + c_1 = 0 \rightarrow c_1 = \frac{\hat{a}}{\omega} \quad (5.15)$$

$$u_m(0) = c_2 = 0 \quad (5.16)$$

With  $c_1 \neq 0$  the displacement, eqn. (5.14), will grow in time, which will result in unacceptable large displacements as can be seen in Figure 5.8.

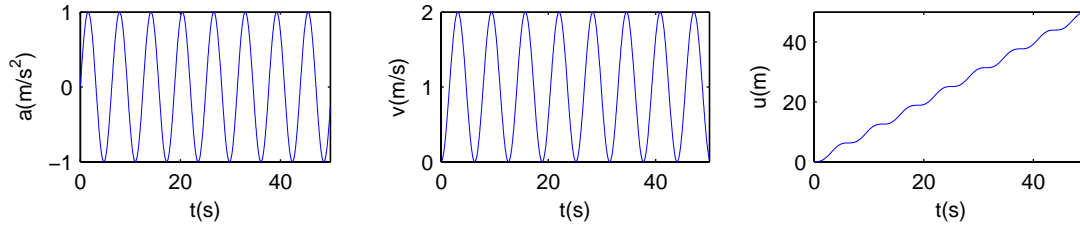


Figure 5.8 Integrating the acceleration two times

In this case - where the acceleration is one single sine function - it is easy to avoid this growth of the displacement by setting the initial velocity to  $v_m(0) = -1$  m/s. In reality, the wind load consist of large number of sines, so the acceleration of the mass is also built up of a large number of sines. See Figure 5.7. Now it is impossible to determine the initial velocity such that  $c_1 = 0$ . Even if it were possible there is another situation in which the displacement of the mass will have a constant growth. This is when the wind load is increasing at a certain time. As result of this, there will be a ramp in the displacement of the top of the building as can be seen in the top graph of Figure 5.9. By splitting up the displacement in a fluctuating part and a mean part, it can be made clear what the displacement of the mass of the active control system will be. Now only the mean part will be discussed because this part will cause a growing displacement of the mass.

The velocity of the top of the building  $v_{48}$  is the derivative of the displacement of the top of the building which will be a step function. The active control force is related to the velocity of the top of the building as  $F_c = k_v v_{48}$  so the acceleration of the mass equals  $a_m = k_v v_{48} / m_m$  which is also a step function. Integrating one time will give the velocity of the mass which is a ramp function. Integrating once more will give the displacement which will grow in time. This growth in time is shown in the bottom graph of Figure 5.9.

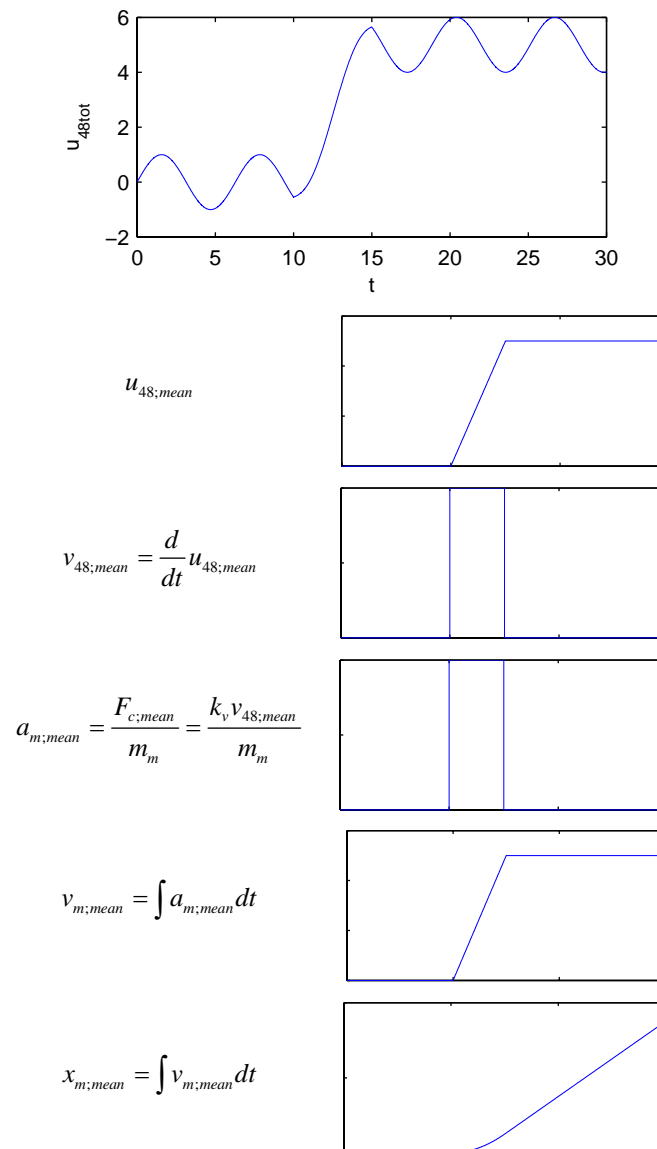


Figure 5.9 A ramp in the mean part of the displacement of the top will result in a growth of the displacement of the mass.

## 5.4. Displacement control strategy

In trying to limit the displacement of the mass, different control algorithms - which were all unsuccessful – were tested: see Appendix I. It became clear that limiting the displacement of the mass is an important part of the control algorithm of the active control system. Velocity control alone or velocity control with a gain depending on the velocity of the top and the displacement of the top (see Appendix I), will not give the desired behaviour. In controlling the displacement of the mass the active control force has to be coupled to the displacement of the mass. Also the velocity of the mass can be coupled to the active control force [7]:

$$F_c = g_1 u_{r,m} + g_2 v_{48} + g_3 \dot{u}_{r,m} \quad (5.17)$$

Here  $u_{r,m}$  is the relative displacement of the mass with respect to the top of the building and  $g_1$  to  $g_3$  are the control gains. The calculation of the absolute displacement of the mass equals, see Figure 5.10:

$$u_m = u_{48} + u_{r,m} \quad (5.18)$$

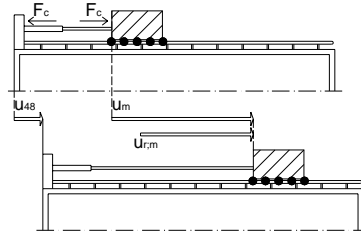


**Figure 5.10 Interaction force and absolute and relative displacement of the mass**

When  $u_{r,m}$  and  $\dot{u}_{r,m}$  have to be limited  $F_c$  has to decrease and when  $v_{48}$  has to be limited  $F_c$  has to be increased. Therefore  $g_1 \leq 0, g_2 \geq 0$  and  $g_3 \leq 0$ . See Figure 5.10. The equation of motion of the mass is:  $m\ddot{u}_m = F_c$ .

The equation of motion of the building eqn. (5.1) will be expanded by adding the equation of motion of the mass:

$$\begin{bmatrix} \mathbf{M} & 0 \\ 0 & m \end{bmatrix} \begin{bmatrix} \ddot{\mathbf{u}} \\ \ddot{u}_m \end{bmatrix} + \begin{bmatrix} \mathbf{C} & 0 \\ 0 & 0 \end{bmatrix} \begin{bmatrix} \dot{\mathbf{u}} \\ \dot{u}_m \end{bmatrix} + \begin{bmatrix} \mathbf{K} & 0 \\ 0 & 0 \end{bmatrix} \begin{bmatrix} \mathbf{u} \\ u_m \end{bmatrix} = \begin{bmatrix} \mathbf{F} \\ 0 \end{bmatrix} - \begin{bmatrix} \mathbf{E}_f \\ -1 \end{bmatrix} F_c \quad (5.19)$$

This will be written as:

$$\mathbf{M}_m \ddot{\mathbf{u}}_m + \mathbf{C}_m \dot{\mathbf{u}}_m + \mathbf{K}_m \mathbf{u}_m = \mathbf{F}_m - \mathbf{E}_{f,m} F_c \quad (5.20)$$

With this formulation, the state space formulation (see chapter 3) will be redefined and substituted in the Simulink model.

$$\begin{aligned} \mathbf{A} &= \begin{bmatrix} \mathbf{0} & \mathbf{I} \\ -\mathbf{M}_m^{-1} \mathbf{K}_m & -\mathbf{M}_m^{-1} \mathbf{C}_m \end{bmatrix} \quad (98 \times 98) \\ \mathbf{B} &= \begin{bmatrix} \mathbf{0} \\ \mathbf{M}_m^{-1} \end{bmatrix} \quad (98 \times 49) \\ \mathbf{C} &= \begin{bmatrix} \mathbf{I} & \mathbf{0} \\ \mathbf{0} & \mathbf{I} \end{bmatrix} \quad (98 \times 98) \\ \mathbf{D} &= \begin{bmatrix} \mathbf{0} \\ \mathbf{0} \end{bmatrix} \quad (98 \times 49) \\ \mathbf{u} &= \begin{bmatrix} \mathbf{F} \\ 0 \end{bmatrix} \quad (49 \times t_i) \quad (t_i = \text{number of time steps}) \end{aligned} \quad (5.21)$$

Besides the displacements and velocities of the nodes, the state space block of Simulink will now also give the absolute displacement and absolute velocity of the mass. With this model, integration of the velocity of the mass is not necessary for determining the displacement and velocity of the block. The active control force eqn. (5.17) has to be rewritten with respect to the absolute displacement and velocity of the mass:

$$F_c = g_1(u_m - u_{48}) + g_2 v_{48} + g_3(v_m - v_{48}) \quad (5.22)$$

The Simulink model including the displacement and velocity of the mass can be seen in Figure 5.11. The subsystem which calculates the active control force can be seen in Figure 5.12.

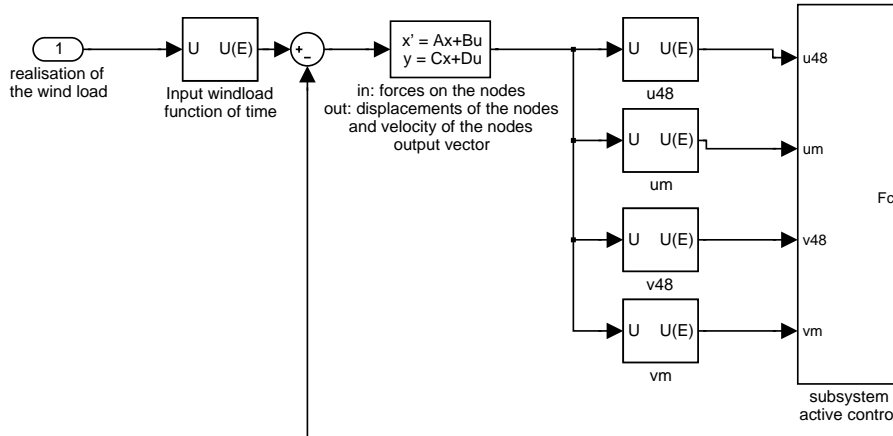


Figure 5.11 Simulink model with displacement and velocity of the mass

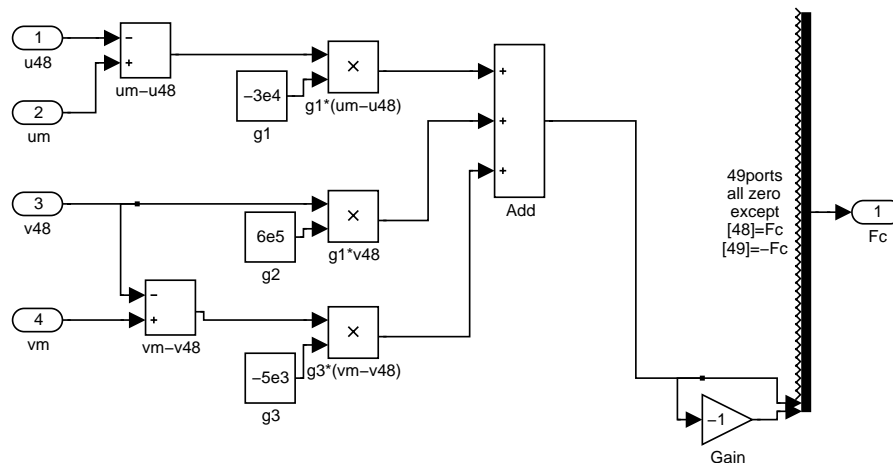


Figure 5.12 Subsystem with as output the control force

As a first estimation the gains and the mass are determined with the trial and error method. The gain for the velocity will be  $g_2 = 6 \cdot 10^5$  Ns/m. The maximum displacement of the mass (about 2 m) multiplied by  $g_1$  may be estimated at about 20 times as large as the maximum velocity of the top of the building (about 0,1 m/s) multiplied by  $g_2$ . Therefore  $g_1 = -3 \cdot 10^4$  N/m which will work as a spring on the mass, is about 20 times as small as  $g_2$ . The weight of the mass will be assumed to be  $m_m = 6 \cdot 10^4$  kg. The velocity of the mass will be limited by  $g_3$  and therefore  $g_3$  can be seen as a damper of the mass. The value will be determined as it is a single mass damper system with a relative damping of about  $\zeta = 5\%$ . This gives

$g_3 = -2\sqrt{g_1 m_m \zeta} = -2\sqrt{3 \cdot 10^4 \cdot 6 \cdot 10^4 \cdot 0,05} \approx -5 \cdot 10^3$  Ns/m. Running this model with the input wind load from section 4.3.1 will give good results: compare Figure 5.13 with Figure 4.8. The accelerations of the top of the building are considerably less and the

displacement of the mass is limited. It can be concluded that this is a good control algorithm.

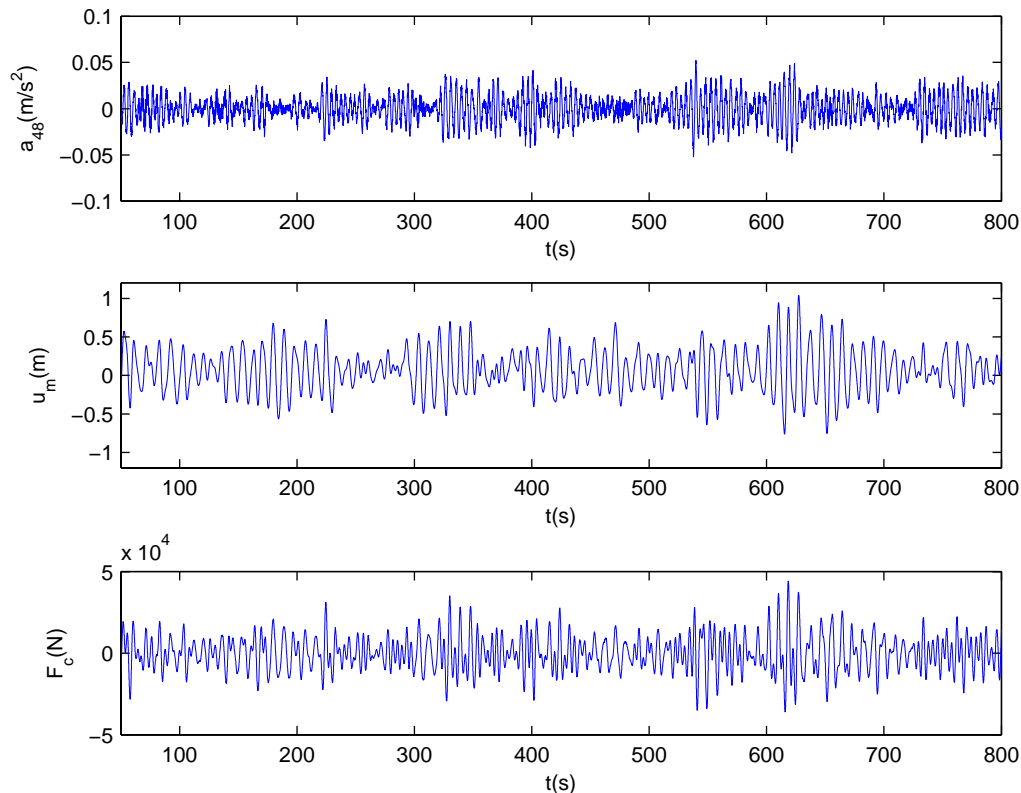


Figure 5.13 Acceleration of the top, global displacement of the mass and active control force

## 5.5. Energy consumption

The acceleration of the mass will be facilitated by a motor. The mechanical power required for accelerating the mass follows from:

$$P = F \cdot v \quad (5.23)$$

The mechanical power can be determined with the output of Simulink, which results in Figure 5.14.

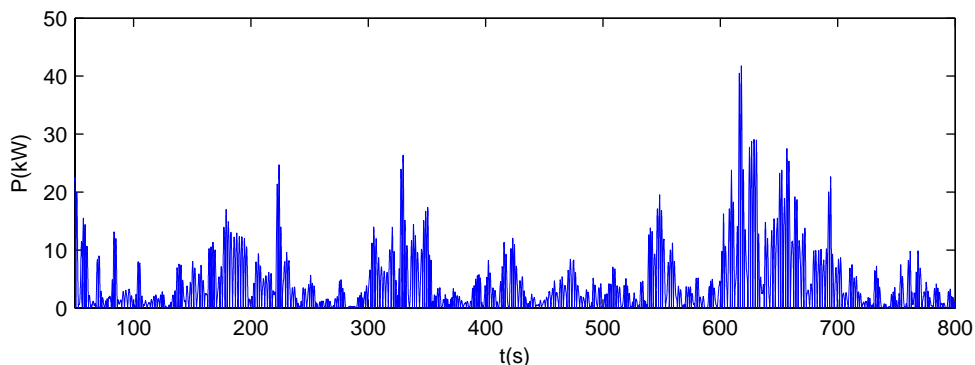
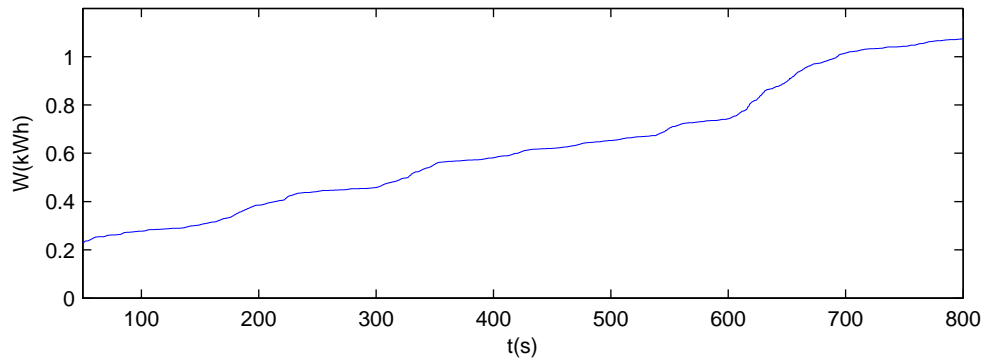


Figure 5.14 Required effective power of the actuator

The work done by the mass equals:

$$W = \int P dt \quad (5.24)$$

This can also be determined with Simulink which results in Figure 5.15.



**Figure 5.15 Work done by the actuator**

The real energy consumption and required power of the jack will be higher due to energy losses. These losses are mainly caused by transformation of electrical to mechanical energy and the friction of the mass on the rail. The amount of these losses should be determined in a mechanical engineering study.



## 6. Implementing an active control system in the Juffertoren

In earlier chapters especially the qualitative aspects of an active control system has been considered. In this chapter, the dimensions of the system will be determined so that the active control system can be implemented in the Juffertoren.

### 6.1. Acceptable comfort level

According to NEN 6702 [5] vibrations are annoying when the acceleration exceeds a value depending on the frequency according to Figure 6.1.

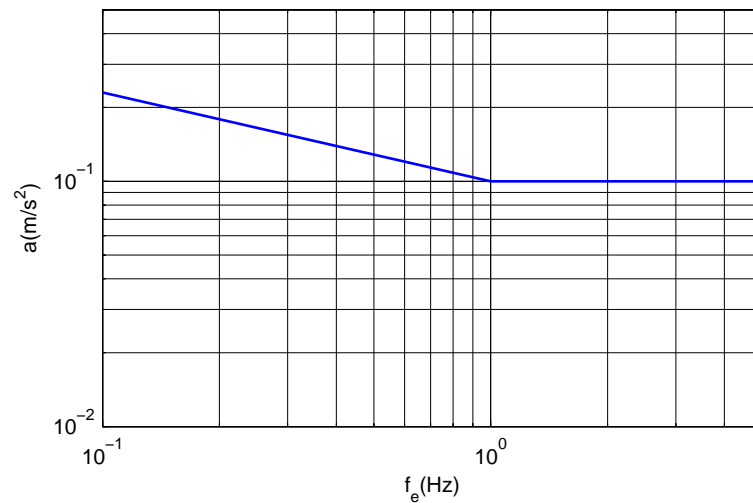


Figure 6.1 limitation demand for the acceleration according to NEN 6702 figure 21

The acceleration of the top of the building without the active control system is shown in Figure 6.2.

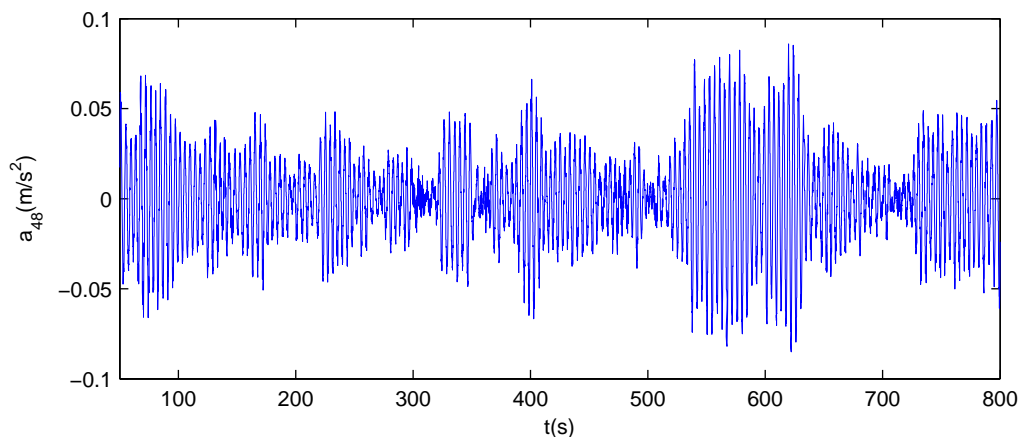


Figure 6.2 Acceleration of the top of the building without active control

The frequency belonging to this acceleration equals the lowest eigenfrequency of the structure. See section 3.1.2:  $f_e = T_e^{-1} = 0,235$  Hz . The peak acceleration of the top of the building equals:  $a_{48;\max} = 0,0821$  m/s<sup>2</sup> which is lower than the maximal acceptable acceleration. We may assume that  $a_{48}$  is a normally distributed signal. The standard deviation of  $a_{48}$  can be determined from:

$$\sigma_{a;48} = \left( \frac{1}{n} \sum_{i=1}^n (a_{48;i} - \mu_{a;48})^2 \right)^{\frac{1}{2}} \quad (6.1)$$

Where:

- $n$  the number of discrete time points for which  $a_{48}$  have been calculated;
- $a_{48;i}$  the acceleration of the top of the building at time point  $i$  ;
- $\mu_{a;48}$  the mean value of  $a_{48}$  .

With  $\sigma_{a;48} = 0,0261 \text{ m/s}^2$  and  $\mu_{a;48} = 1,62 \cdot 10^5 \text{ m/s}^2$  , calculated with Matlab, the expected peak value of the acceleration for a given time range follows from:

$$a_{48;peak} = \mu_{a;48} + \sigma_{a;48} \sqrt{2 \ln(N)} \quad (6.2)$$

Where  $N$  is the number of draws which follows from the number of local peaks in the total time range:

$$N = T_s f_e \quad (6.3)$$

Where:

- $T_s$  time range of the signal;  $T_s = 750 \text{ s}$

Filling in eqn. (6.2) gives:

$$a_{48;peak;750} = 0,0261 \sqrt{2 \ln(750 * 0,235)} = 0,0839 \text{ m/s}^2 \quad (6.4)$$

The difference between the expected peak value and the actual one equals:  
 $(1 - 0,0821 / 0,0839) * 100 = 2,2\%$  which is quite accurate. The expected peak value for a storm of 6 hours 21600 s can be calculated from:

$$a_{48;peak;21600} = 0,0261 \sqrt{2 \ln(21600 * 0,235)} = 0,108 \text{ m/s}^2 \quad (6.5)$$

According to NEN 6702 the limitation demand for the peak value of the acceleration follows from:

$$a_{\max} = 1,6 \frac{\phi_2 \tilde{p}_{w;1} C_t b_m}{\rho_1} < a \quad (6.6)$$

Where:

- $a$  limitation demand of the acceleration according to Figure 6.1  $a = 0,17 \text{ m/s}^2$  ;
- $\rho_1$  mass of the building per meter height, see Appendix I  
 $\rho_1 = 6,3 * 10^5 / 3 = 2,1 * 10^5 \text{ kg/m}$  ;
- $b_m$  average width of the building perpendicular to the wind direction  $b_m = 26,3 \text{ m}$  ;
- $C_t$  summation of the shape factor, See section 4.1  $C_t = 1,2$  ;
- $\tilde{p}_{w;1}$  value for the varying part of the wind pressure  $\tilde{p}_{w;1} = 100 \ln(h/0,2) = 660 \text{ N/m}^2$  ;
- $\phi_2$  value depending on the dimensions, the eigenfrequency and the damping;

$$\phi_2 = \sqrt{\frac{0,0344 f_e^{-2/3}}{\zeta (1 + 0,12 f_e h) (1 + 0,2 f_e b_m)}}$$

Where:

- $f_e$  eigenfrequency  $f_e = T^{-1} = 0,235 \text{ Hz}$  ;
- $\zeta$  damping ratio, see section 2.5  $\zeta = 0,01$  ;

This gives:

$$\phi_2 = \sqrt{\frac{0,0344 * 0,235^{-2/3}}{0,01 (1 + 0,12 * 0,235 * 144) (1 + 0,2 * 0,235 * 26,3)}} = 0,892 \quad (6.7)$$

Filling in eqn. (6.6) gives:

$$1,6 \frac{0,892 * 660 * 1,2 * 26,3}{2,1 * 10^5} = 0,149 \text{ m/s}^2 < 0,17 \text{ m/s}^2 \quad (6.8)$$

The expected peak value for a six hours long storm derived from the Simulink simulation can be validated by comparing it with the maximum acceleration

according to NEN 6702, calculated with eqn. (6.6):  $\frac{a_{\text{max};\text{NEN}}}{a_{48;\text{peak};21600}} = \frac{0,149}{0,108} = 1,38$ .

The calculated maximum acceleration according to eqn. (6.6) can be reduced further by taking into account the aerodynamic admittance factor  $\chi(f_e)$ . So the accelerations of the top of the building found with Simulink and the accelerations found with the rule of thumb of NEN 6702 do not exclude each other.

Now according to eqn. (6.8) no more calculations of the accelerations of the building are required. So it can be concluded that an active control system is not required for the Juffertoren according to NEN 6702. This is not in accordance with the design calculations of DHV. DHV has chosen for a conservative calculation in the preliminary design. In this manner changes later on in the design stage, which will change the stiffness of the structure will not give problems. In this project, my intention is to apply an active control system. For this reason the demand for an acceptable acceleration level is intensified to:  $a_{48;\text{peak};750} < 0,045 \text{ m/s}^2$ .

## 6.2. Parameter study

The active control system parameters are the mass and the control gains, respectively  $m_m$  and  $g_1$ ,  $g_2$  and  $g_3$ . In examining the behaviour of the system when the active control parameters are changed the equation of motion will be rewritten. The active control force, (see eqn. (5.22)), follows from:

$$F_c = g_1 u_m - g_1 u_{48} + g_2 v_{48} + g_3 v_m - g_3 v_{48} \quad (6.9)$$

The displacement of the mass ( $u_m$ ) is about 20 times as large as the displacement of the top of the building ( $u_{48}$ ). Therefore  $g_1 u_{48}$  can be neglected in the active control algorithm. Simulations in Simulink affirm this conclusion. Now substituting eqn. (6.9) without  $g_1 u_{48}$  in eqn. (5.19) leads to:

$$\begin{aligned} & \begin{bmatrix} m_{1,1} & \dots & 0 & 0 \\ \vdots & \ddots & \vdots & \vdots \\ 0 & \dots & m_{48,48} & 0 \\ 0 & \dots & 0 & m_m \end{bmatrix} \begin{bmatrix} \ddot{u}_1 \\ \vdots \\ \ddot{u}_{48} \\ \ddot{u}_m \end{bmatrix} + \begin{bmatrix} c_{1,1} & \dots & 0 & 0 \\ \vdots & \ddots & \vdots & \vdots \\ 0 & \dots & c_{48,48} & 0 \\ 0 & \dots & 0 & 0 \end{bmatrix} \begin{bmatrix} \dot{u}_1 \\ \vdots \\ \dot{u}_{48} \\ \dot{u}_m \end{bmatrix} + \begin{bmatrix} k_{1,1} & \dots & 0 & 0 \\ \vdots & \ddots & \vdots & \vdots \\ 0 & \dots & k_{48,48} & 0 \\ 0 & \dots & 0 & 0 \end{bmatrix} \begin{bmatrix} u_1 \\ \vdots \\ u_{48} \\ u_m \end{bmatrix} \\ & = \begin{bmatrix} F_1 \\ \vdots \\ F_{48} \\ 0 \end{bmatrix} - \begin{bmatrix} 0 \\ \vdots \\ g_1 \\ -g_1 \end{bmatrix} u_m - \begin{bmatrix} 0 \\ \vdots \\ g_2 - g_3 \\ -g_2 + g_3 \end{bmatrix} \dot{u}_{48} - \begin{bmatrix} 0 \\ \vdots \\ g_3 \\ -g_3 \end{bmatrix} \dot{u}_m \end{aligned} \quad (6.10)$$

Substituting the active control force in the damping and stiffness matrix gives:

$$\begin{bmatrix} m_{1,1} & \dots & 0 & 0 \\ \vdots & \ddots & \vdots & \vdots \\ 0 & \dots & m_{48,48} & 0 \\ 0 & \dots & 0 & m_m \end{bmatrix} \begin{bmatrix} \ddot{u}_1 \\ \vdots \\ \ddot{u}_{48} \\ \ddot{u}_m \end{bmatrix} + \begin{bmatrix} c_{1,1} & \dots & 0 & 0 \\ \vdots & \ddots & \vdots & \vdots \\ 0 & \dots & c_{48,48} + g_2 - g_3 & g_3 \\ 0 & \dots & -g_2 + g_3 & -g_3 \end{bmatrix} \begin{bmatrix} \dot{u}_1 \\ \vdots \\ \dot{u}_{48} \\ \dot{u}_m \end{bmatrix} + \begin{bmatrix} k_{1,1} & \dots & 0 & 0 \\ \vdots & \ddots & \vdots & \vdots \\ 0 & \dots & k_{48,48} & g_1 \\ 0 & \dots & 0 & -g_1 \end{bmatrix} \begin{bmatrix} u_1 \\ \vdots \\ u_{48} \\ u_m \end{bmatrix} = \begin{bmatrix} F_1 \\ \vdots \\ F_{48} \\ 0 \end{bmatrix} \quad (6.11)$$

From eqn. (6.11), it can be concluded that, considering the displacement of the mass, the damping of the mass equals  $g_3$ . Taking  $g_3 = 0$  will result in unstable behaviour as can be seen in Figure 6.3. It will be clear that  $g_3$  may not be too small.

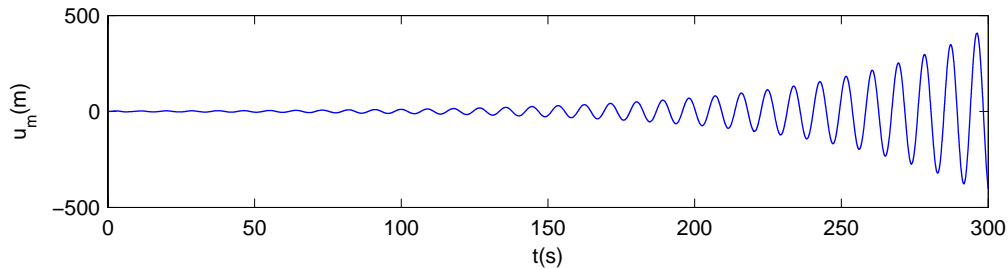


Figure 6.3 With  $g_3 = 0$  the displacement of the mass will be unstable

The control gain  $g_1$  is equivalent to a spring connected to the mass. Taking  $g_1 = 0$  which is equivalent to only a mass with an inertia and friction will result in very large displacements of the mass. See Figure 6.4.

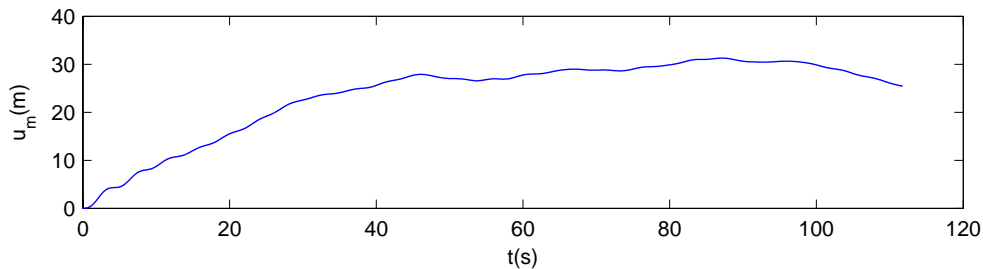


Figure 6.4 With  $g_1 = 0$  the displacement of the mass will become very large

It will be clear that when presuming that  $g_2 = 0$ , the acceleration of the top will not be limited compared to the uncontrolled system.

### 6.2.1. Varying the control gains and the mass of the actuator

When simulations with different control gains and different masses are performed there must be a measure for comparing the qualities of the different systems. While doing this a reference model is taken with:  $m_m = 6 \cdot 10^4$  kg,  $g_1 = -3 \cdot 10^4$  N/m,

$g_2 = 1 \cdot 10^6$  Ns/m and  $g_3 = -5 \cdot 10^3$  Ns/m. These values are chosen by the “trial and error” method. Result of the simulation for the reference model can be seen in Figure 6.5.

Measures for the quality of the system are the peak values of the acceleration of the top of the building, the displacement of the mass and the peak value of the required value for accelerating the mass. Other interesting variables are the peak values of the velocity of the top and the velocity of the mass. These are interesting because these determine together with the displacement of the mass the active control force, see eqn. (6.9).

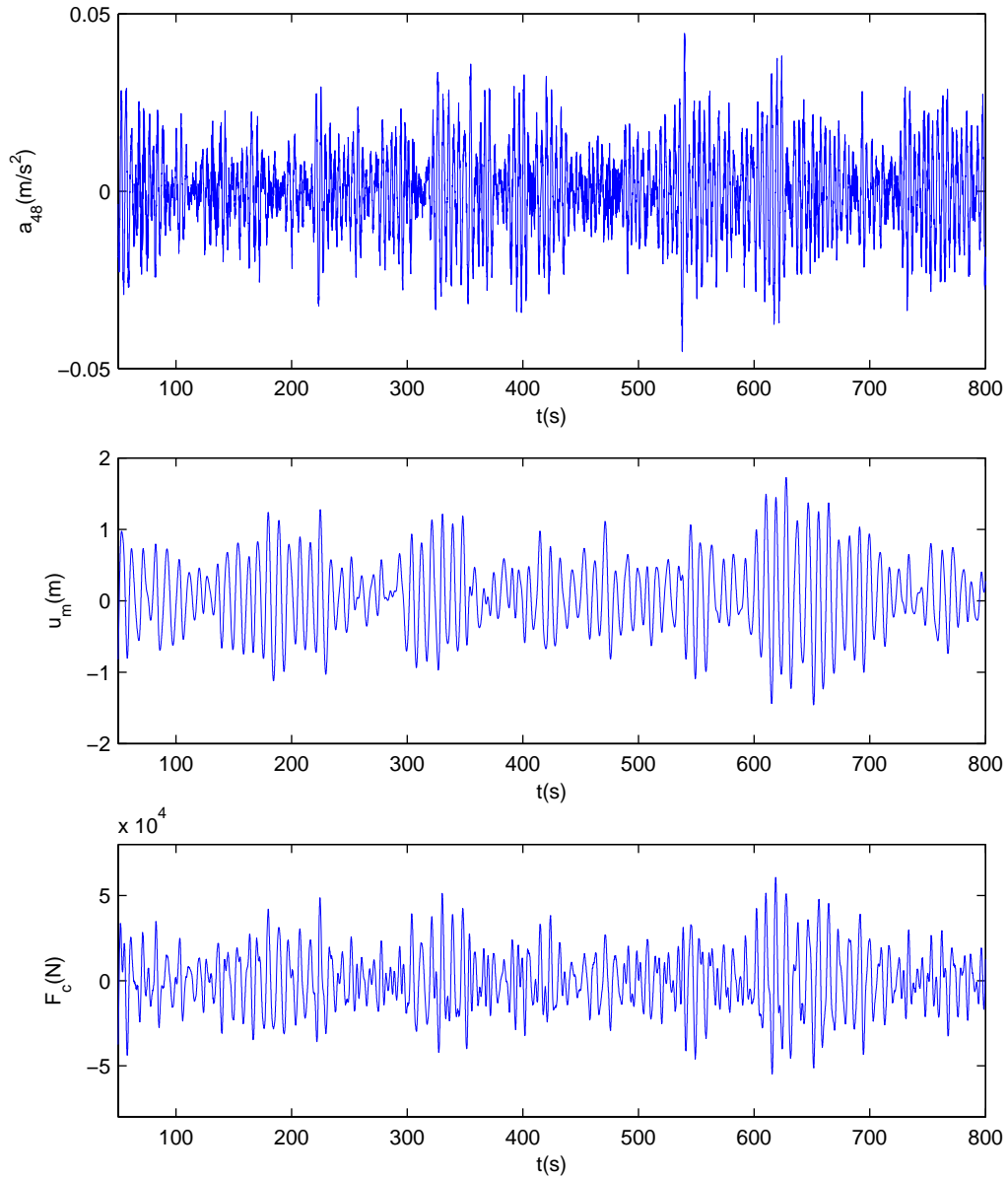


Figure 6.5 a) acceleration of the top, b) global displacement of the mass, c) active control force

The quality measures for the reference model are shown in Table 3.

Reference model: $m_m = 6 \cdot 10^4$ kg, $g_1 = -3 \cdot 10^4$ N/m, $g_2 = 1 \cdot 10^6$ Ns/m and $g_3 = -5 \cdot 10^3$ Ns/m					
$a_{48;peak}$ (m/s <sup>2</sup> )	$u_{m;peak}$ (m)	$F_{c;peak}$ (kN)	$P_{c;peak}$ (kW)	$v_{48;peak}$ (m/s)	$v_{m;peak}$ (m/s)
0,0445	1,79	69,7	30,4	0,0281	1,34

Table 3 Quality measures of the reference model

Six new variables are defined which represent the quality measures normalized to the quality measures of the reference model of Table 3.

$$a_{48;peak}'' = \frac{a_{48;peak}}{0,0445(\text{m/s}^2)} \quad (6.12)$$

$$u_{m;peak}'' = \frac{u_{m;peak}}{1,79(\text{m})} \quad (6.13)$$

$$F_{c;peak}'' = \frac{F_{c;peak}}{69,7(\text{kN})} \quad (6.14)$$

$$P_{c;peak}'' = \frac{P_{c;peak}}{30,4(\text{kW})} \quad (6.15)$$

$$v_{48;peak}'' = \frac{v_{48;peak}}{0,0281(\text{m/s})} \quad (6.16)$$

$$v_{m;peak}'' = \frac{v_{m;peak}}{1,34(\text{m/s})} \quad (6.17)$$

A number of simulations has been made with different control gains and masses. For each simulation only one parameter differs from the reference model. For every simulation the normalized quality measures have been determined. The results of these simulations can be seen in Figure 6.7 - Figure 6.10. Resonance can be expected when the eigenfrequency of the active control mass comes close to one of the eigenfrequencies of the structure. The eigenfrequency of the undamped active control mass can be derived from eqn. (6.9), which leads to:

$$\omega_m = \sqrt{\frac{|g_1|}{m_m}} \quad (6.18)$$

The square of the first and second eigenfrequency of the structure equals respectively  $\omega_{1,2}^2 = 2,19; 88,0 \text{ rad}^2 / \text{s}^2$ . Taking  $m_m = 6 * 10^4 \text{ kg}$  and varying  $g_1$ , will give resonance for:

$$|g_1| = m_m \omega_n^2 = 1,31 * 10^5; 5,28 * 10^6 \text{ N/m} \quad (6.19)$$

Or when  $|g_1| = 3 * 10^4 \text{ N/m}$  and the mass  $m_m$  will be varied, resonance will occur for:

$$m_m = \frac{|g_1|}{\omega_n^2} = 1,37 * 10^4; 341 \text{ kg} \quad (6.20)$$

The values for  $m_m$  and  $|g_1|$  which gives resonance will not be in the domain of Figure 6.7, Figure 6.8 and Figure 6.10. Therefore resonance due to the eigenfrequency of the active control mass which gets close to the one of the structure can not be seen from these figures. The values for the control gains  $g_1 - g_3$  are limited, because at some point instability will occur. For  $g_1$  instability will occur for  $g_1 \leq -1 * 10^5 \text{ (N/m)}$  or  $|g_1| \geq 1 * 10^5 \text{ (N/m)}$ . See Figure 6.6. In this figure the trend of the growing acceleration of the top of the building and the displacement of the mass will continue in time. This behaviour can be explained with the equation of motion of the mass of the active control system which can be derived from eqn. (6.11):

$$m_m \ddot{u}_m - g_3 \dot{u}_m - g_1 u_m = (g_2 - g_3) \dot{u}_{48}(u_m) \quad (6.21)$$

In this equation the velocity of the top of the building is a function of the motion of the mass of the active control system. With eqn. (6.21) the eigenfrequency of the mass of the active control system can be derived:

$$\omega_{0,m} = \sqrt{\frac{-g_1}{m_m}} \quad (6.22)$$

With  $g_1 = -1 \cdot 10^5$  (N/m) and  $m_m = 6 \cdot 10^4$  kg the eigenfrequency of the mass equals

$\omega_{0,m} = 1,29$  rad/s, which gives a period  $T_{0,m} = \frac{2\pi}{\omega} = 4,87$  s. This period can also be seen in

Figure 6.6. So what happens is that the mass of the active control system gets in its eigenmotion. When the mass moves in its eigenmotion the active control force will have a period equal to the period of the mass  $T_{0,m} = 4,87$  s and when the force becomes big enough the structure will also oscillate with this period. As a result of this the active control force will amplify the oscillation of the structure and the other way around. Here we speak about instability. Eqn. (6.21) will make this clear. At the left side we see the equation of motion with mass  $m_m$  damping  $-g_3$  and stiffness  $-g_1$ . On the right side we see the force which is proportional to the velocity of the top of the structure. When the right side has the same frequency as the eigenfrequency of the system on the left side – this is the eigenfrequency of the mass – we get resonance. This behaviour will only occur when the period of the mass is smaller than or equal to the first period of the structure  $T_0 = 4,25$  s. Or in other words, the eigenfrequency of the mass is bigger than the natural frequency of the structure. When this is the case the displacement of the top of the building will be out of phase compared to the control force. But the velocity of the top of the building ( $\dot{u}_{48}$ ) will be in phase with the control force and the control force will be intensified by the motion of the structure. When the natural frequency of the structure is bigger than the natural frequency of the mass, the velocity of the structure will be out of phase compared to the control force. Then the eigenmotion of the mass of the active control system will be attenuated by the motion of the structure. Comparable behaviour occurs for  $g_2 \geq 2 \cdot 10^6$  (Ns/m) and  $g_3 \geq -1,5 \cdot 10^3$  (Ns/m). These values are out of the range of the parameters studies, so further elaboration will not be given here.

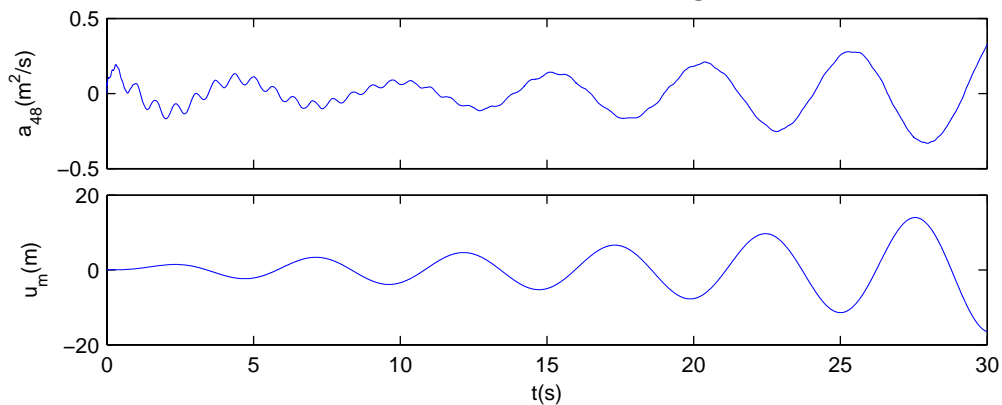


Figure 6.6 Resonance for  $g_1 = -1 \cdot 10^5$  (N/m)

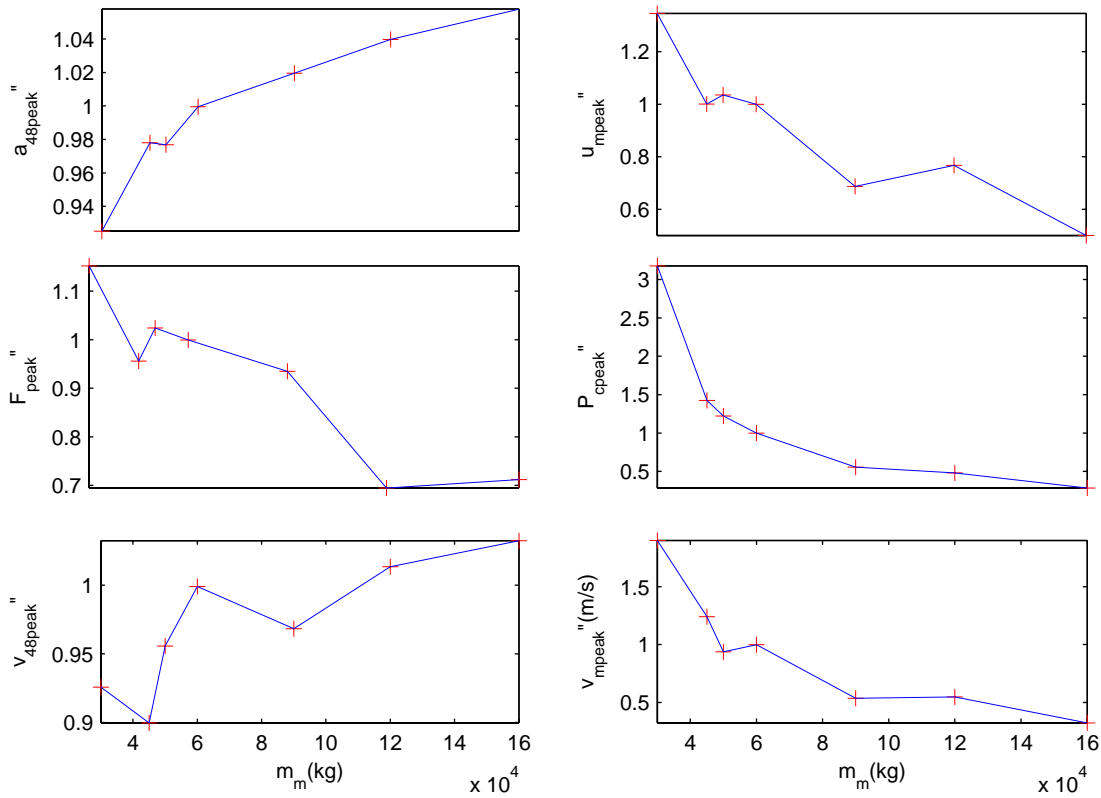


Figure 6.7 Simulation with 7 different masses of the active control system.

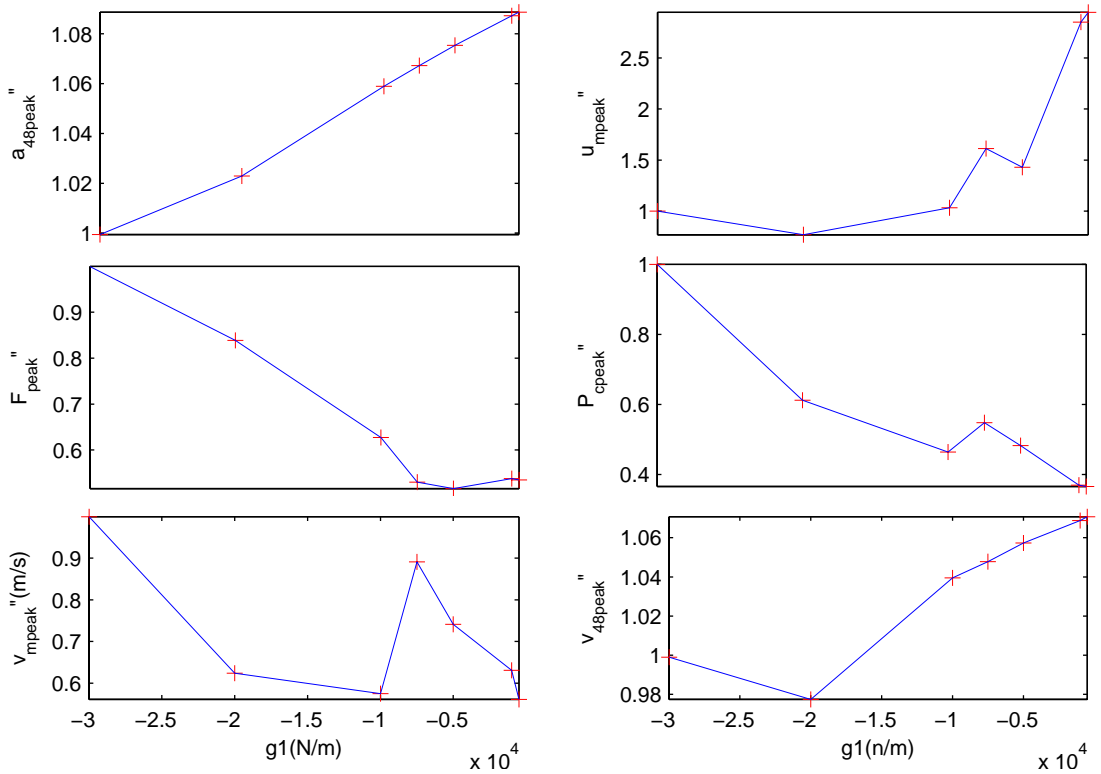


Figure 6.8 Simulation with 7 different values for  $g_1$ . Instability occurs for  $g_1 \leq -1 \times 10^5$  (N/m)

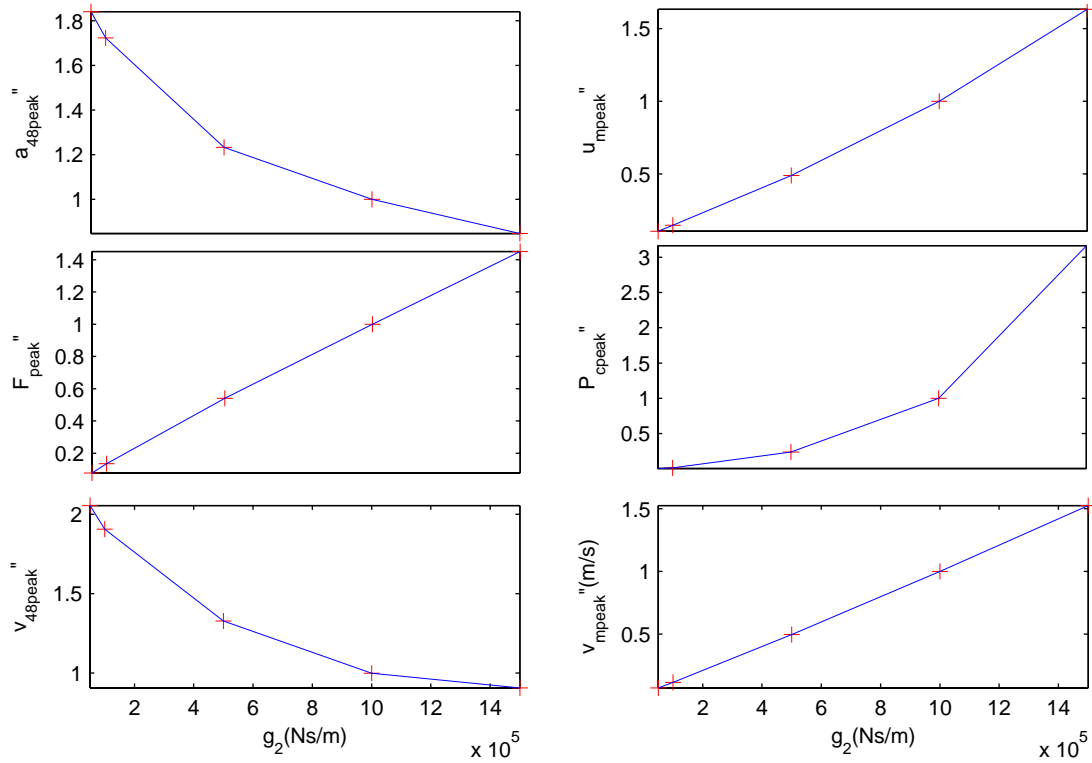


Figure 6.9 Simulation with 5 different values for  $g_2$ . Instability occurs for  $g_2 \geq 2 \cdot 10^6$  (Ns/m)

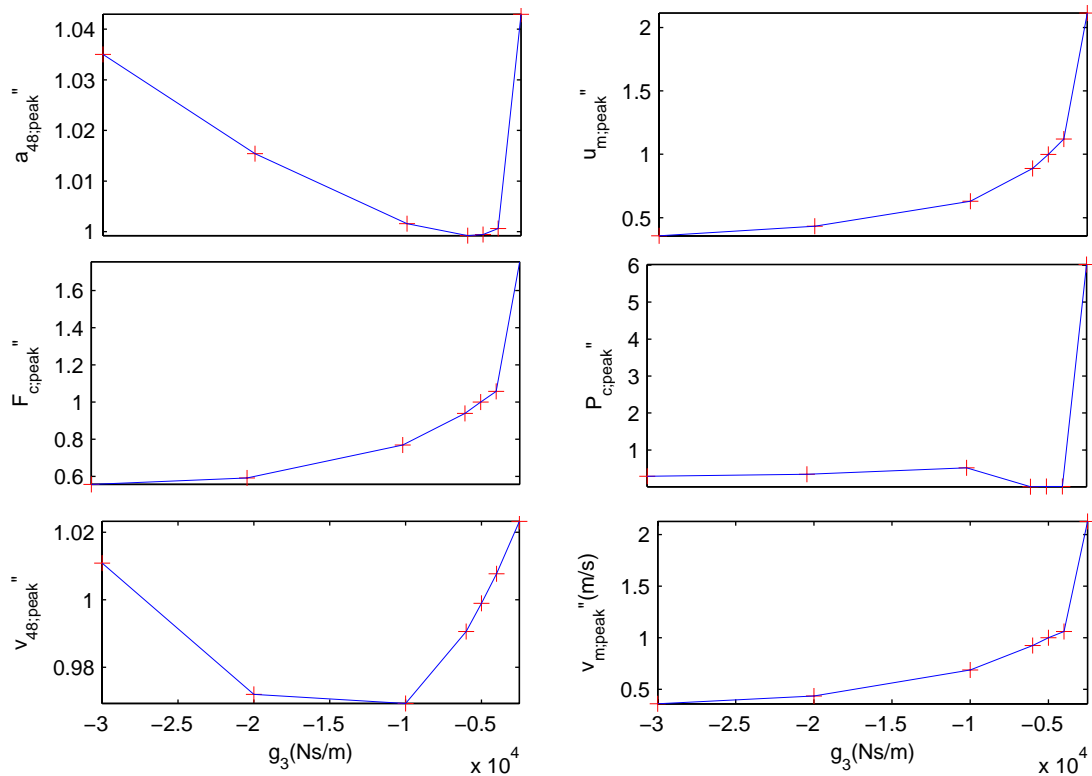


Figure 6.10 Simulation with 7 different values for  $g_3$ . Instability occurs for  $g_3 \geq -1,5 \cdot 10^3$  (Ns/m)

Now by choosing the right control gains and mass we have to fulfil the following requirements:

- The maximal acceptable peak value of the acceleration of the top of the structure is limited by  $a_{48;peak} < 0,045 \text{ m/s}^2$ .

- The width of the building equals 15,44 m so the maximum acceptable displacement of the mass will be assumed to be 8 m from its equilibrium point, what means that the maximal displacement reaches over the top of the building.
- The required power for accelerating the mass and the active control force must be limited because these determine the dimensions of the active control system.
- The dimension of the mass of the active control system itself must be limited.

Looking to the reference system (Table 3) the first requirement is just satisfied, but the displacement of the mass can be a factor 3,5 larger. This is only effective if it decreases the required power, the active control force or the mass of the active control system.

What we first try to do is to decrease the mass of the active control system. Figure 6.7 shows that this gives a considerable decrease of  $a_{48;peak}$  but it also gives a considerable unwanted increase of the required power of the active control system. An attempt has been made to compensate for this increase of power by decreasing  $g_1$ , (see Figure 6.8), which will give a little increase of  $a_{48;peak}$ . In this way different systems, (see Table 4), have been tested and the results are compared to the reference system, see Figure 6.11. The aim of this is tuning the system so that it will work with a lighter mass, with the same peak value for the acceleration of the top of the building and an acceptable value for the peak of the required power.

system	$m_m$ (*10 <sup>3</sup> kg)	$g_1$ (*10 <sup>3</sup> N/m)	$g_2$ (*10 <sup>6</sup> Ns/m)	$g_3$ (*10 <sup>3</sup> Ns/m)
1 (reference system)	60	-30	1	-5
2	30	-5	1	-5
3	10	-5	1	-5
4	10	-2	1	-5
5	10	-2	2	-5
6	10	-10	1	-5
7	10	-2	1,5	-5
8	10	-2	1,25	-5
9	10	-1,5	1,5	-5
10	5	-1,5	1,5	-5

**Table 4** Different systems have been tested in search of the optimal system

Comparing the results of system 5 with the reference system, it can be concluded that with a 6 times smaller mass the accelerations at the top are smaller, but the peak value of the displacement of the mass and the required power is somewhat too high. The latter can be reduced by a lower value for  $g_2$  - see system 7 and 8. Increasing  $g_1$  will also give an improvement considering the peak value of the required power - see system 6. In general, it holds that, when the mass decreases, the active control force remains equal, so the acceleration of the mass increases. This results in increasing velocities, displacements and required power for the active control system. The choice is made to apply a light mass on a rail with a maximum displacement that reaches just over the top of the building. So finally system 10 is chosen as the best system to apply to the Juffertoren. The configuration of this system will be worked out in section 6.4. The results of the simulation for system 10 can be seen in Figure 6.12.

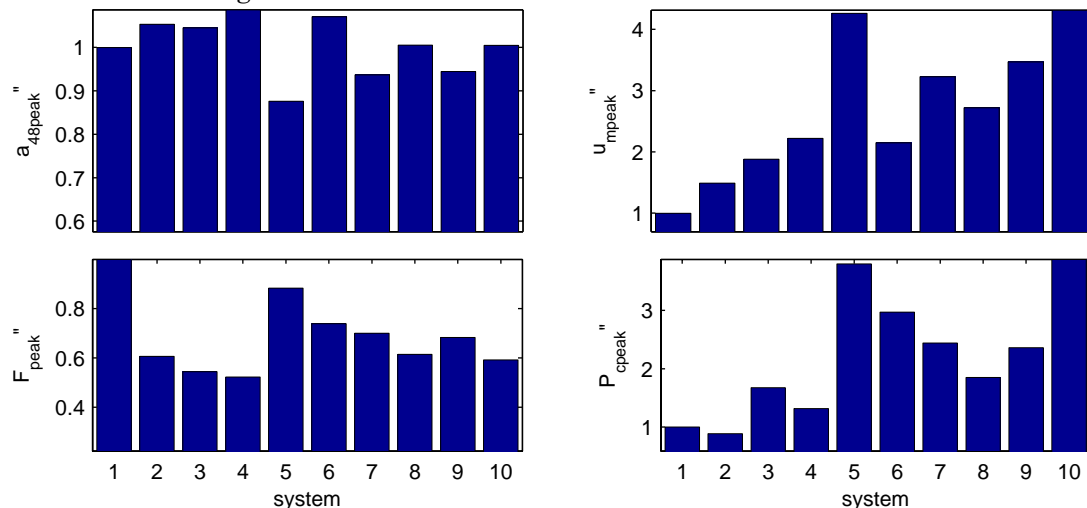


**Figure 6.11** Normalized outputs of the peak values of the different systems

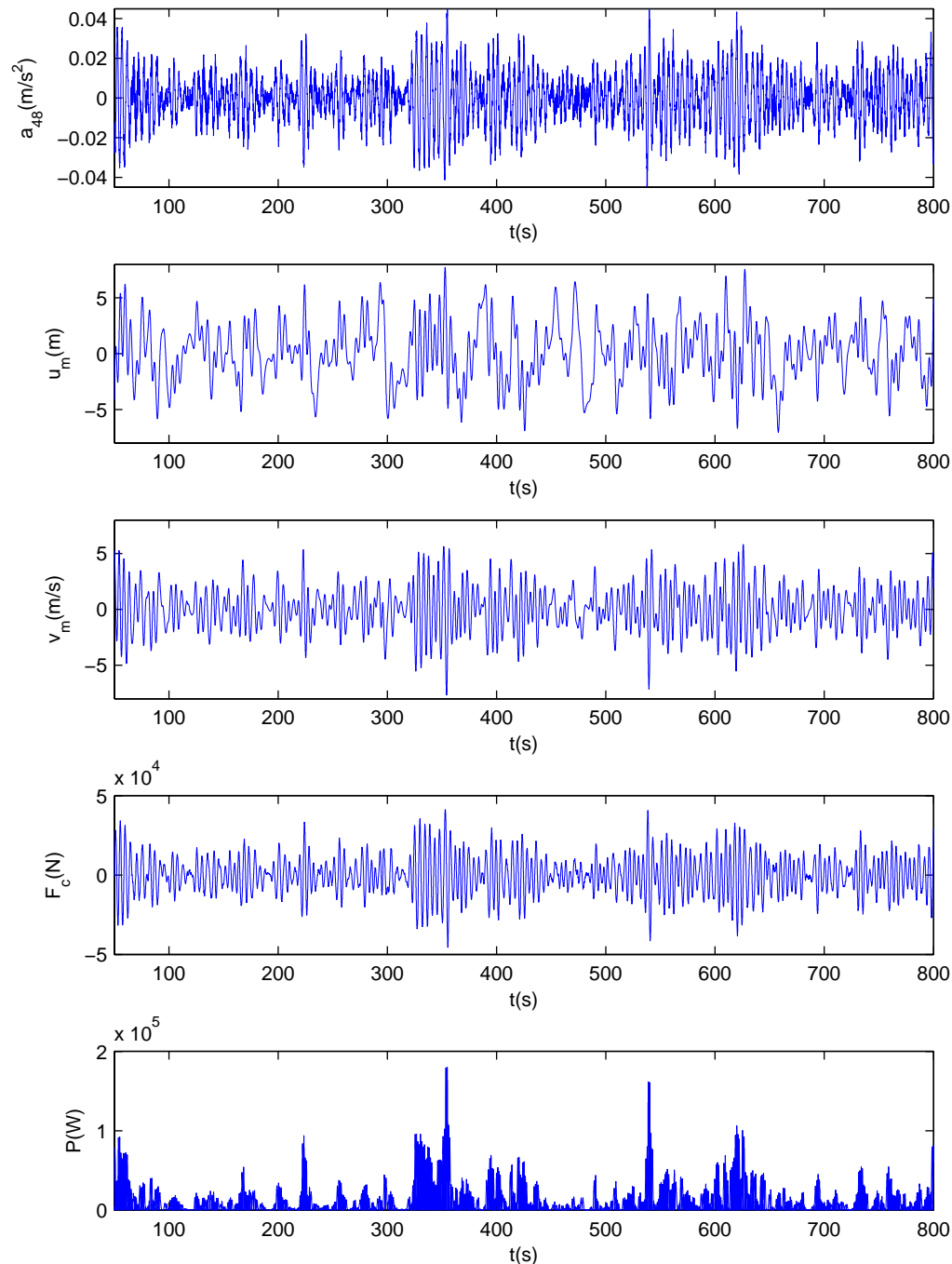


Figure 6.12 Results for system 10

### 6.2.2. Varying the mass, stiffness and damping of the structure

In chapter 2, the mass, stiffness and damping of the structure have been determined but in fact these parameters possess some uncertainty. In this section, I will examine what the influence is on the structural behaviour of some deviation in these structural parameters. It will be most transparent when all the values (the system parameters as well as the quality measures) will be normalized to the values of the system chosen in previous section (system 10). Here system 10 of previous section is called the reference system, so as not to confuse it with the reference system in previous section.

Reference model: $m_m = 5 \cdot 10^3 \text{ kg}$ , $g_1 = -1,5 \cdot 10^3 \text{ N/m}$ , $g_2 = 1,5 \cdot 10^6 \text{ Ns/m}$ and $g_3 = -5 \cdot 10^3 \text{ Ns/m}$			
$a_{48;peak} \text{ (m/s}^2\text{)}$	$u_{m;peak} \text{ (m)}$	$F_{c;peak} \text{ (kN)}$	$P_{c;peak} \text{ (kW)}$
0,0447	7,72	41,3	180

**Table 5 Quality measures of the reference model**

Four new variables are defined which represent the quality measures normalized to the quality measures of the reference model of Table 5.

$$a_{48;peak}^{''''} = \frac{a_{48;peak}}{0,0447 \text{ (m/s}^2\text{)}} \quad (6.23)$$

$$u_{m;peak}^{''''} = \frac{u_{m;peak}}{7,72 \text{ (m)}} \quad (6.24)$$

$$F_{c;peak}^{''''} = \frac{F_{c;peak}}{41,3 \text{ (kN)}} \quad (6.25)$$

$$P_{c;peak}^{''''} = \frac{P_{c;peak}}{180 \text{ (kW)}} \quad (6.26)$$

Now 6 systems will be tested, each with one parameter different from the reference system as shown in Table 6.

system	difference from reference system
1	
2	25% more mass of the structure
3	25% less mass of the structure
4	25% more stiffness of the structure
5	25% less stiffness of the structure
6	10% more damping of the structure
7	25% less damping of the structure

**Table 6 Varying mass, stiffness and damping of the structure**

The results for the normalized peak values of the acceleration of the top, the displacement of the mass, the active control force and the required power can be seen in Figure 6.13. It can be seen that more or less damping has hardly any influence on the structural behaviour. The influence of more or less mass or stiffness on the acceleration of the top of the building is considerably more, but this difference will also be expected for the uncontrolled system. Figure 6.13 makes once more clear that adding stiffness (equivalent to velocity control) to the structure is the best way of reducing the accelerations of the top of the structure.

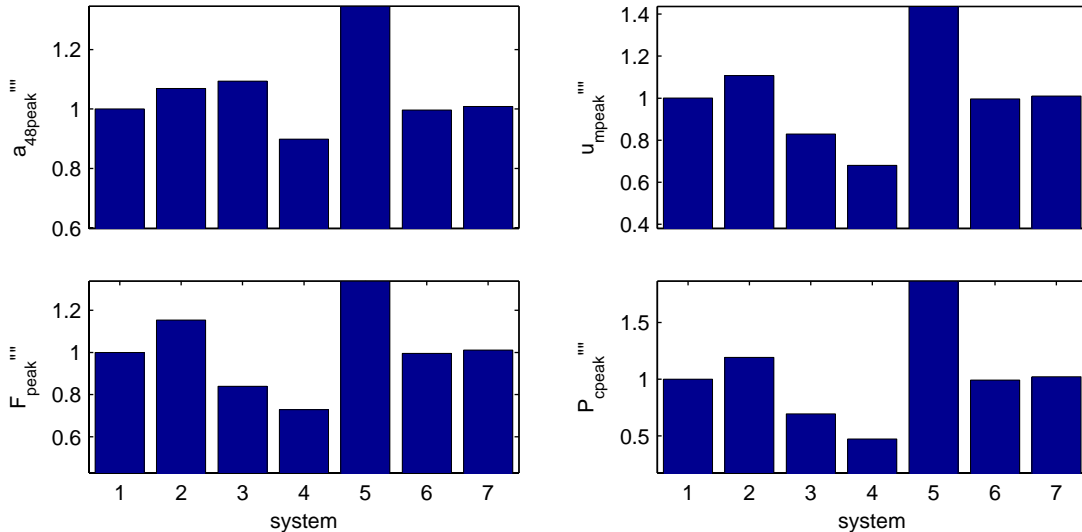


Figure 6.13 The result of an inaccurate determination of the system parameters

### 6.2.3. Time delay

When the top of the building has a specific velocity, the magnitude of the control force can be determined. When this control force is applied, the velocity of the building is just changed, so that the control force is somewhat later than desired. In other words, there will be some time delay which is the sum of the time required to carry out the following actions:

- acquiring the data from the sensor
- calculating the desired control force
- transmitting the control force signal to the actuator
- ramping up the actuator to the desired force level

The peak values of the quality measures, scaled to unity for no time delay, are determined with Simulink for different time delay  $t_d$  as can be seen in Figure 6.14.

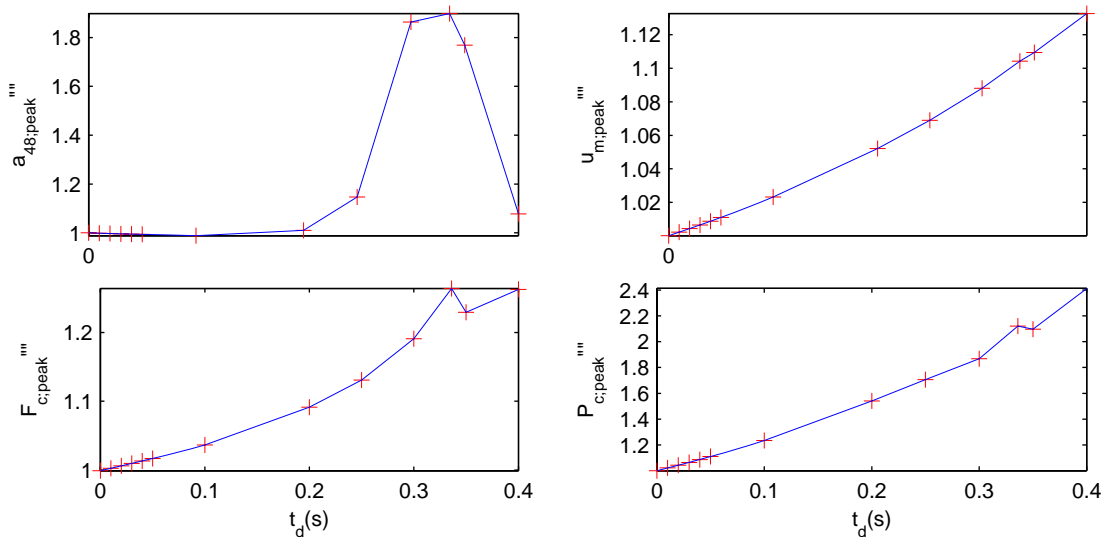


Figure 6.14 The effect of time delay

The value for time delay in practice will depend on the system characteristics and will be in the order of magnitude of 0,01 s [7]. For small time delay the quality measures will hardly differ from the system without time delay.

The big disturbance around  $t_d = 0,336$  s can be explained with the second eigenfrequency. The second eigenfrequency  $\omega_2 = 9,38$  rad/s has been determined with Matlab; see also section 7.2. The oscillation time belonging to this frequency equals  $T_2 = \frac{2\pi}{\omega_2} = 0,670$  s. This equals twice the time delay  $t_d = 0,336$  s. This means that

the control force for the second eigenmotion is just applied half a period later than desired, which causes resonance.

#### 6.2.4. Disturbances of the active control force

The magnitude of the active control force is a function of the displacement of the mass and the velocity of the mass and the top of the building. In the measurements of these variables disturbances will occur. Also in the driving gear disturbances can be expected. To gain some insight into the consequences of disturbances in the active control force, simulations with a disturbed active control force have been carried out:

$$F_{c, \text{disturbed}}(t) = F_c(t) * [1 + y(t)] \quad (6.27)$$

Where  $y$  is a normally distributed random signal, with a mean  $\mu = 0$  and a standard deviation  $\sigma_y$ . A number of simulations have been carried out with different values for the standard deviation. There seems to be a linear relation between the quality measures of the system, judging from eqn.(6.23), up to eqn. (6.26), and the standard deviation of the signal  $y$  as can be seen in Figure 6.15. Note that a standard deviation of  $\sigma_y = 0,1$ , means very large disturbances in the control force, which in reality would not be expected.

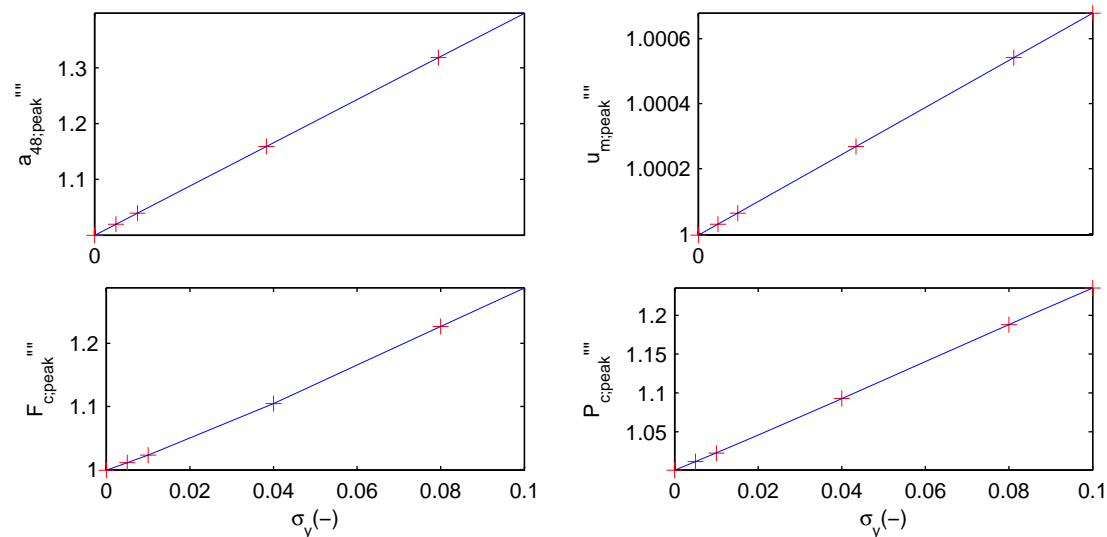


Figure 6.15 Disturbance in the active control force

### 6.3. Check of the accelerations at lower stories

When there is no control force, the vibration of the building will be dominated by its first eigenmode. Then the accelerations of the building will be maximal at the top. When there is a very strong active control force it could be possible that the accelerations of the top goes to zero whereas the maximal accelerations occurs somewhere between the top and the bottom of the building. Plotting the accelerations of some stories makes clear that the accelerations are maximal at the top. See Figure 6.16. Simulations with larger gains for the velocity of the top  $g_2$  have also been carried out but this does not change the conclusion.

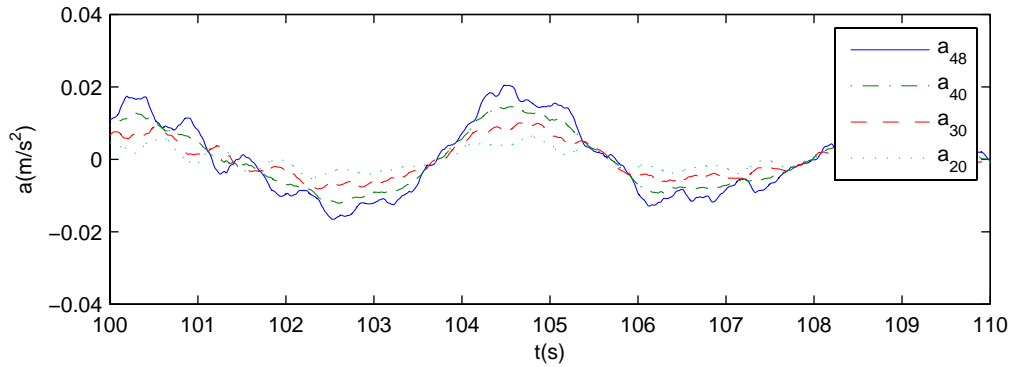
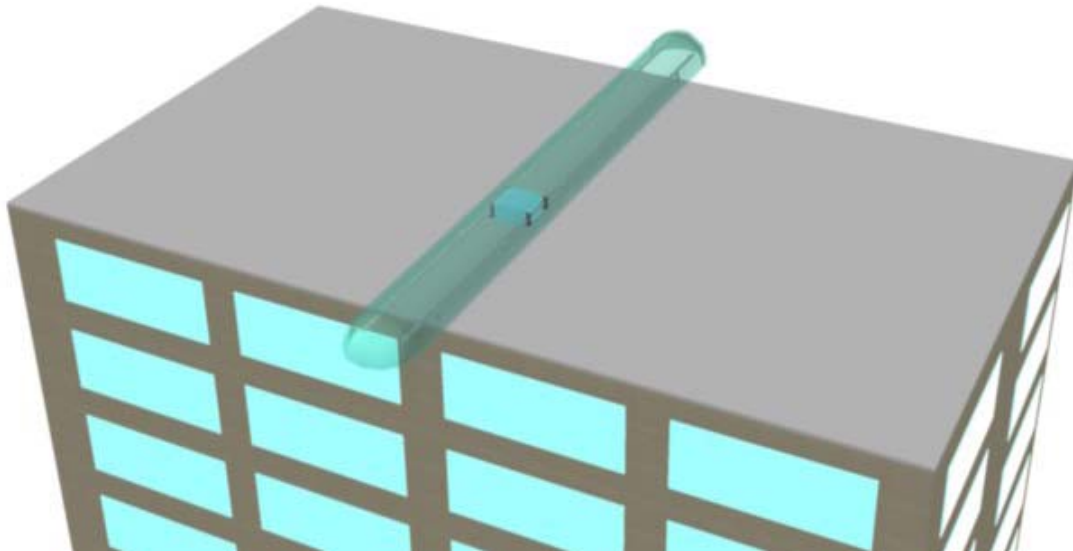


Figure 6.16 The accelerations will be maximal at the top

#### 6.4. Configuration of the system

On the roof of the building, a rail will be installed with, on top of that, a mass of 5 tons which is about the mass of 5 small cars. See Figure 6.17. The mass will be self driven by an electric motor and to prevent slipping of the wheels the transmission can be applied with cogwheels connected to the mass and a chain connected to the structure. See Figure 6.18 b). The mass will move with a maximum velocity of about 30 km/h and a maximum acceleration of about 8 m/s<sup>2</sup>. Comparing this with a normal car we can imagine that the required motor must be very strong. Therefore I asked for advice from a company – called “Lenze” – specialised in driving techniques. They told me this motion can be made possible with a heavy electric motor. The motor with a weight of about 2500 kg will be placed upon the cart. This reduces the required adding mass. The electric motor must be provided with a reducer. This is a device that ensures that the cart can still be accelerated at higher velocities. The cost of this motor including reducer and gear case will be about €50.000. If further investigations leads to the conclusion that these high accelerations at high speeds are not possible with a normal electric motor, a solution can be found in the linear induction motor. This is a motor where the stator is “unrolled” to a strip connected with the top of the building between the rails. At the bottom of the cart a big magnet is connected. By changing the electrical magnetic field of the stator, forces are applied to the magnet connected to the cart. Both solutions have been discussed with a consultant of Lenze. The advantage of the linear induction motor compared to the electric motor is the high acceleration which can be reached. Disadvantages are the expensiveness and the large amount of energy required. Linear induction motors are often applied in roller coaster trains and elevators. Independent of the applied motor, the friction between the moving mass and rail must be minimized.



**Figure 6.17** Roof of the building with on top of it a rail with the mass

The accelerations of the top of the building will continuously be measured by one or more accelerometers at the top of the building. The system will only be turned on when the peak value of the acceleration exceeds a specific level. The system will therefore mostly be in the standby mode, which increases the life-span and decreases the maintenance and energy consumption. A glass envelope around the rail and the mass could be aesthetically interesting and it provides a good environment for the mechanical system. If it adds to the design of the tower it could add a new dimension to the Juffertoren.

To prevent that the mass will reach over the end of the rails, some kind of hard stop has to be added, which in practice would not be reached. This hard stop serves only for safety in extreme situations which normally will not appear during the lifespan of the structure. Nevertheless, there is a probability that the hard stop will be reached. The probability that this hard stop will be reached once within for example a hundred years can be calculated. In consultation with the principal the acceptable probability has to be chosen. It will be obvious taking this acceptable probability equal to the probability of exceeding the acceptable accelerations of an uncontrolled building according to the code NEN 6702. When the acceptable probability is determined, the system can be tuned – by a longer rail or other control gains  $g_1 - g_3$  – such that this probability will not be exceeded. If the hard stop will be reached during a very heavy storm uncomfortable situations will become acceptable on condition that this will not cause any damage on the construction.

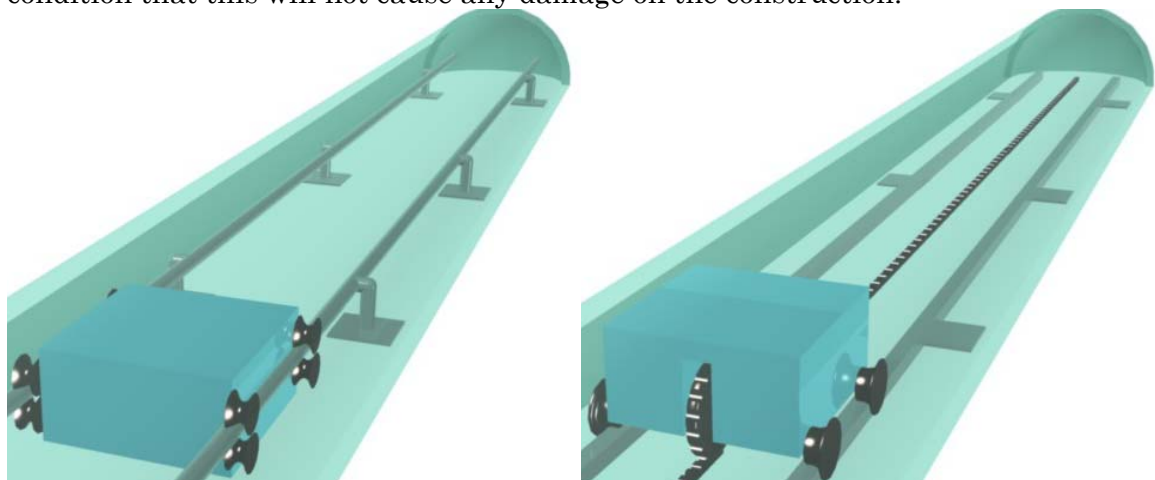


**Figure 6.18** a) Cart without cogwheel b) Cart with cogwheel



## 7. Frequency-domain response analysis

With the frequency-domain response analysis, the amplitude of the steady-state output of a system as a function of the input frequency can be determined. In section 6.2 the forces of the active control system have been added to the equation of motion of the total system, see eqn. (7.1). As a result of this the damping matrix is not proportional to the mass- and stiffness matrix anymore, as this was derived in section 2.5. Therefore the well-known method of modal analysis<sup>2</sup> [2] will not result in a diagonal modal damping matrix; so the system will not be uncoupled.

$$\begin{bmatrix} m_{1,1} & \dots & 0 & 0 \\ \vdots & \ddots & \vdots & \vdots \\ 0 & \dots & m_{48,48} & 0 \\ 0 & \dots & 0 & m_m \end{bmatrix} \begin{bmatrix} \ddot{u}_1 \\ \vdots \\ \ddot{u}_{48} \\ \ddot{u}_m \end{bmatrix} + \begin{bmatrix} c_{1,1} & \dots & 0 & 0 \\ \vdots & \ddots & \vdots & \vdots \\ 0 & \dots & c_{48,48} + g_2 - g_3 & g_3 \\ 0 & \dots & -g_2 + g_3 & -g_3 \end{bmatrix} \begin{bmatrix} \dot{u}_1 \\ \vdots \\ \dot{u}_{48} \\ \dot{u}_m \end{bmatrix} + \begin{bmatrix} k_{1,1} & \dots & 0 & 0 \\ \vdots & \ddots & \vdots & \vdots \\ 0 & \dots & k_{48,48} & g_1 \\ 0 & \dots & 0 & -g_1 \end{bmatrix} \begin{bmatrix} u_1 \\ \vdots \\ u_{48} \\ u_m \end{bmatrix} = \begin{bmatrix} F_1 \\ \vdots \\ F_{48} \\ 0 \end{bmatrix} \quad (7.1)$$

Another method for analysing the frequency domain response is making use of complex quantities.

### 7.1. Single degree of freedom system

First a single degree of freedom system with a harmonic excitation is discussed

$$m\ddot{u} + c\dot{u} + ku = \hat{F} \cos(\omega t) \quad (7.2)$$

The harmonic force can also be written as the real part of a complex function, with complex amplitude:

$$|F(\omega)| \cos(\omega t) = \text{Re}[F(\omega) e^{i\omega t}] \quad (7.3)$$

The particular solution to eqn. (7.2) equals:

$$u(t) = |u(\omega)| \cos(\omega t + \varphi(\omega)) \quad (7.4)$$

Or in the form of the real part of a complex function with complex amplitude:

$$u(t) = \text{Re}[u(\omega) e^{i\omega t}] \quad (7.5)$$

To simplify the nomenclature the symbol  $\text{Re}$  will be omitted and at the end of the operation the imaginary part is disregarded. Expanding eqn. (7.4) and eqn. (7.5) will establish the relationship between the constants. Expanding eqn. (7.4) gives:

$$u(t) = |u(\omega)| \{ \cos \varphi(\omega) \cos \omega t - \sin \varphi(\omega) \sin \omega t \} \quad (7.6)$$

Expanding eqn. (7.5) gives:

$$u(t) = \text{Re} \{ \text{Re} u(\omega) + i \text{Im} u(\omega) \} \{ \cos(\omega t) + i \sin(\omega t) \} = \text{Re} u(\omega) \cos(\omega t) - \text{Im} u(\omega) \sin(\omega t) \quad (7.7)$$

<sup>2</sup> The idea behind modal analysis is that the modal mass matrix as well as the modal damping matrix and the modal stiffness matrix will be diagonal. When this is the case, the modal equation of motion is fully decoupled which results in  $n$  second order differential equations. These can be solved easily.

Setting the coefficients of  $\cos(\omega t)$  and  $\sin(\omega t)$  equal in eqn. (7.6) and eqn. (7.7) leads to:

$$\operatorname{Re} u(\omega) = |u(\omega)| \cos \varphi(\omega) \quad (7.8)$$

$$\operatorname{Im} u(\omega) = |u(\omega)| \sin \varphi(\omega) \quad (7.9)$$

This leads to the amplitude of the actual particular solution of eqn. (7.4):

$$|u(\omega)| = \sqrt{\operatorname{Re} u(\omega)^2 + \operatorname{Im} u(\omega)^2} \quad (7.10)$$

And the phase angle:

$$|\varphi(\omega)| = \arctan \frac{\operatorname{Im} u(\omega)}{\operatorname{Re} u(\omega)} \quad (7.11)$$

Above mentioned method also applies for a harmonic force according to eqn. (7.3), which leads to:

$$|F(\omega)| = \sqrt{\operatorname{Re} F(\omega)^2 + \operatorname{Im} F(\omega)^2} \quad (7.12)$$

$$|\varphi_F(\omega)| = \arctan \frac{\operatorname{Im} F(\omega)}{\operatorname{Re} F(\omega)} \quad (7.13)$$

Substituting eqn. (7.3) and eqn. (7.5) in eqn. (7.2) leads, after cancelling out  $e^{i\omega t}$ , to:

$$-\omega^2 m u(\omega) + i\omega c u(\omega) + k u(\omega) = F(\omega) \quad (7.14)$$

Which is the force displacement relationship expressed in complex amplitudes. With the dynamic-stiffness coefficient  $S_{uF}(\omega)$  this can be written as:

$$F(\omega) = (-\omega^2 m + i\omega c + k) u(\omega) = S_{uF}(\omega) u(\omega) \quad (7.15)$$

With the dynamic-flexibility coefficient or transfer function  $H_{uF}(\omega) = S_{uF}(\omega)^{-1}$ , the complex amplitude follows from:

$$u(\omega) = H_{uF}(\omega) F(\omega) \quad (7.16)$$

By applying a harmonic force with phase angle  $\varphi_F = 0$ , (see eqn. (7.2)) the amplitude of the response can be determined as follows. With  $\varphi = 0$  and eqn. (7.13) it follows that  $\operatorname{Im} F(\omega) = 0$ . With eqn. (7.4) and eqn. (7.16), the maximum amplitude of the response will be:

$$|u(\omega)| = |H_{uF}(\omega)| |F(\omega)| \quad (7.17)$$

## 7.2. Multi degree of freedom system

The above method can also be applied to the multi degree of freedom system. The equation of motion now gives:

$$\mathbf{M}\ddot{\mathbf{u}} + \mathbf{C}\dot{\mathbf{u}} + \mathbf{K}\mathbf{u} = \mathbf{F}(t) \quad (7.18)$$

Where  $\mathbf{M}$ ,  $\mathbf{C}$  and  $\mathbf{K}$  are  $(n \times n)$  matrices and  $\mathbf{u}$  and  $\mathbf{F}$  are  $(n \times 1)$  vectors. By writing:

$$\mathbf{F}(t) = \mathbf{F}(\omega) e^{i\omega t} \quad (7.19)$$

$$\mathbf{u}(t) = \mathbf{u}(\omega) e^{i\omega t} \quad (7.20)$$

The frequency dependent dynamic-stiffness matrix follows from:

$$\mathbf{S}_{uF}(\omega) = \mathbf{K} - \omega^2 \mathbf{M} + i\omega \mathbf{C} \quad (7.21)$$

With  $\mathbf{K}$ ,  $\mathbf{M}$  and  $\mathbf{C}$  from eqn. (3.1) for the uncontrolled system and from eqn. (7.1) for the controlled system. With the dynamic-flexibility coefficient or transfer function  $\mathbf{H}_{uF}(\omega) = \mathbf{S}_{uF}(\omega)^{-1}$ , the maximum real amplitude follows from:

$$|\mathbf{u}(\omega)| = |\mathbf{H}_{uF}(\omega)| |\mathbf{F}(\omega)| \quad (7.22)$$

Actually we are not interested in the displacements of the structure, but in the accelerations of the structure. The relation between the amplitudes of the accelerations  $|\mathbf{a}(\omega)|$  and the amplitude of the displacement follows from the second derivative of eqn. (7.20).

$$\ddot{\mathbf{u}}(t) = \frac{d^2}{dt^2} \mathbf{u}(\omega) e^{i\omega t} = -\omega^2 \mathbf{u}(\omega) e^{i\omega t} \quad (7.23)$$

Now the amplitudes of the accelerations can be determined from:

$$|\mathbf{a}(\omega)| = \omega^2 |\mathbf{u}(\omega)| = \omega^2 |\mathbf{H}_{uF}(\omega)| |\mathbf{F}(\omega)| = |\mathbf{H}_{aF}(\omega)| |\mathbf{F}(\omega)| \quad (7.24)$$

Where the frequency-response function for the acceleration is:

$$|\mathbf{H}_{aF}(\omega)| = \omega^2 |\mathbf{H}_{uF}(\omega)| \quad (7.25)$$

This is a (48\*48) matrix for the uncontrolled system and a (49\*49) matrix for the controlled system. The transfer function for the acceleration  $a_{48}$  for a synchronic load  $F = \hat{F} \cos \omega t$  on all nodes can be found by:

$$|H_{a_{48}F}(\omega)| = \sum_{i=1}^{48} H_{a_{48}F_i}(\omega) \quad (7.26)$$

This transfer function is determined with the Matlab code of Appendix I. The results can be seen in Figure 7.1. The eigenfrequencies can be seen at  $\omega_{1,2,3,4,5} = 1,5; 9,4; 26; 52; 87$  rad/s, which agrees with formerly found eigenfrequencies with Matlab, according to the code of Appendix I. The mode shapes belonging to this eigenfrequencies are represented in Figure 7.3. In Figure 7.2 the transfer function for the controlled system can be seen. It is striking that the reduction of the amplitude of the accelerations of the controlled system compared to the uncontrolled system will mainly be seen in the lower eigenmodes. This can be explained by the following. Considering the first and second eigenmode, both moving in their sinusoidal eigenmotion with unit amplitude for the acceleration at the top. See respectively eqn. (7.27) and eqn. (7.28).

$$v_{48} = \frac{1}{\omega_1} \sin(\omega_1 t) \rightarrow a_{48} = \cos(\omega_1 t) \rightarrow |a_{48}| = 1 \quad (7.27)$$

$$v_{48} = \frac{1}{\omega_2} \sin(\omega_2 t) \rightarrow a_{48} = \cos(\omega_2 t) \rightarrow |a_{48}| = 1 \quad (7.28)$$

From these equations it follows that the amplitude of the velocity of the first eigenmotion is a factor  $\omega_2 / \omega_1 = 6,3$  times the amplitude of the velocity of the second eigenmotion. The magnitude of the active control force is proportional to the velocity of the top of the building and therefore the active control force for the first eigenmotion will be about 6,3 times as large as the active control force for the second

eigenmotion. Therefore the active control system will mainly damp the accelerations of the natural mode.

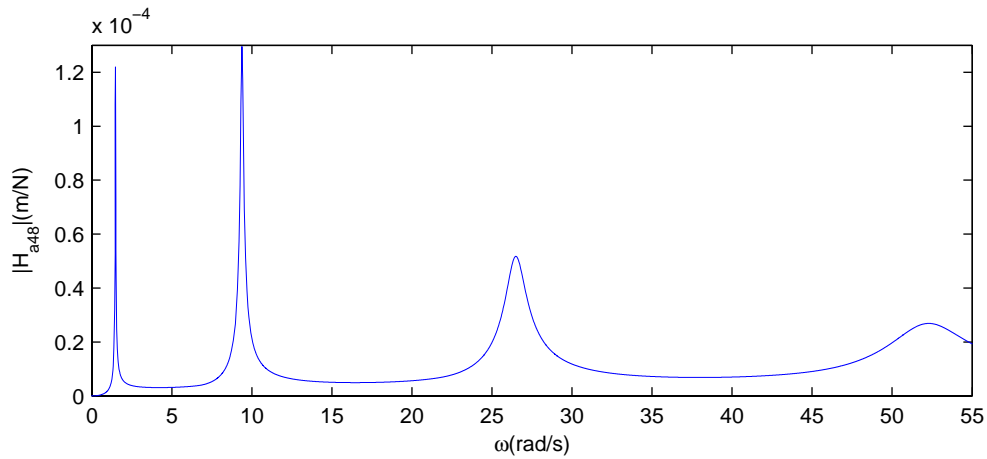


Figure 7.1 Transfer function of the uncontrolled system of the acceleration of the top of the building for a synchronic load on all nodes.

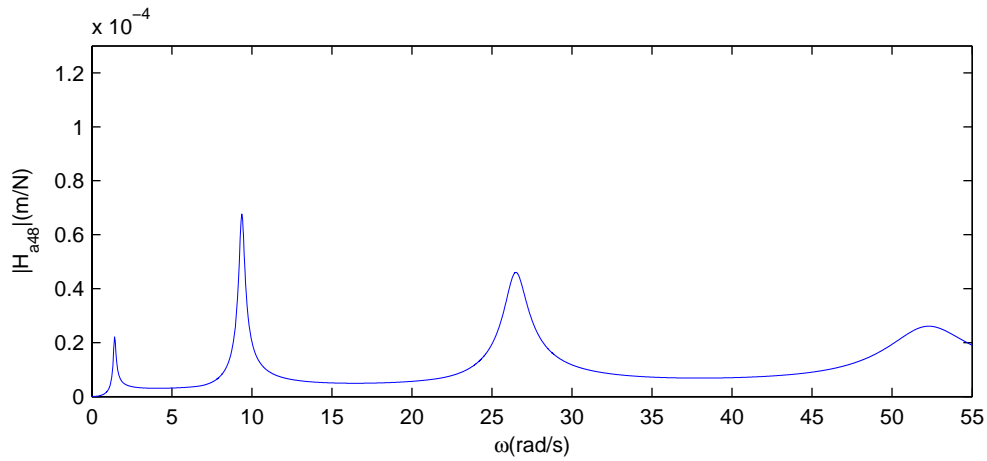


Figure 7.2 Transfer function of the controlled system of the acceleration of the top of the building for a synchronic load on all nodes.

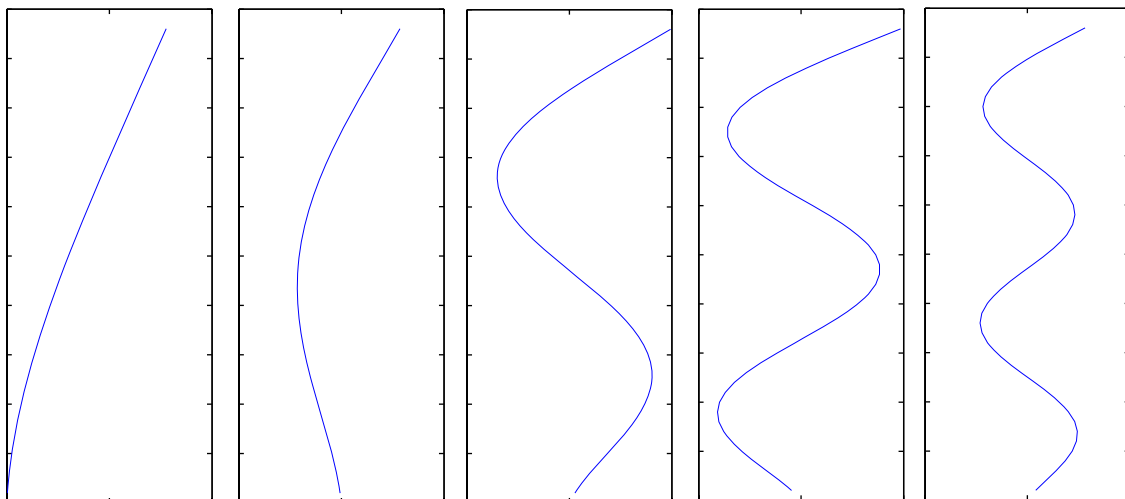


Figure 7.3 The first to the fifth mode shape

### 7.3. Spectrum of the accelerations

In the previous section it has been shown that the active control system mainly damps the accelerations of the natural frequency. Therefore it is important to examine if the accelerations of the structure due to the wind load are caused by the natural frequency or by the higher eigenfrequencies. Looking to the spectrum of the wind speed, (see Figure 4.3) it can be seen that the standard deviation at  $\omega_1 = 1,48$  rad/s is somewhat larger than the standard deviation at the second eigenfrequency  $\omega_2 = 9,38$  rad/s. On the other hand the controlled system is much more sensitive for the accelerations of the second eigenmode. See Figure 7.2. Therefore it is advisable to examine at which excitation frequency the accelerations of the top of the building are maximal. This can be made clear by the variance spectrum of the acceleration. From eqn. (4.1) and eqn. (4.2) it follows:

$$F_w = \frac{1}{2} AC_h \rho (\bar{v} + \tilde{v})^2 = AC_h \rho \left( \frac{1}{2} \bar{v}^2 + \frac{1}{2} \tilde{v}^2 + \bar{v}\tilde{v} \right) \quad (7.29)$$

Where the static part  $\bar{v}^2$  gives no contribution to the accelerations and the higher order term  $\tilde{v}^2$  can be neglected this leads to:

$$F_w = AC_h \rho \bar{v} \tilde{v} \quad (7.30)$$

It is known that the fluctuating part of the wind speed  $\tilde{v}$  with the Fourier method can be split up in a finite number of sine functions. The spectrum of  $\tilde{v}$  follows from the Davenport spectrum, as derived in eqn. (4.9). Now the spectrum of the forces on the nodes  $S_{FF}(\omega)$ , follows with the theory of Appendix VI from:

$$S_{FF}(\omega) = (\bar{v} \rho AC_h)^2 S_{vv}(\omega) \quad (7.31)$$

As derived in eqn. (7.24) the acceleration follows from:

$$|\mathbf{a}(\omega)| = |\mathbf{H}_{aF}(\omega)| |\mathbf{F}(\omega)| \quad (7.32)$$

It is a very sizable calculation to determine the spectrum of the accelerations of the top of the building when at all 48 nodes a force is placed with a spectrum according to eqn. (7.31). This calculation includes the correlation between the forces on the different nodes, which has to be taken into account with the cross-spectra. These cross-spectra are determined with the coherence factor which is a function of the distance between the points and the frequency. The formulae for the spectrum of the acceleration of the top of the building will be given here; the derivation can be found in [1]:

$$S_{a_{48}a_{48}}(\omega) = \sum_{i=1}^{48} \sum_{j=1}^{48} H_{a_{48}F_i}(\omega) H_{a_{48}F_j}^*(\omega) S_{F_i F_j}(\omega) \quad (7.33)$$

Where  $H_{a_{48}F_i}$  is the complex transfer function of the acceleration of the 48<sup>th</sup> node for a harmonic force on node  $i$  and  $H_{a_{48}F_j}^*$  is the complex conjugate of  $H_{a_{48}F_j}$ . For  $i = j$ ,  $S_{F_i F_j}(\omega)$  is the auto-spectrum of the force and for  $i \neq j$ ,  $S_{F_i F_j}(\omega)$  is the cross-spectrum of the force. It will be clear that this calculation will be very large and therefore the correlation – which can be taken into account by the coherence factor – will not be taken into account. To determine nevertheless if the first or the second frequency causes the biggest accelerations at the top of the building, the spectrum of the acceleration of the top of the building will be calculated for a totally correlated wind load on the façade of the building. The calculation from eqn. (7.33) with total

correlation can be seen in Appendix VIII. Where the autospectrum from the wind load follows from eqn. (7.31) with  $\bar{v}$  depending on the height above the surface according to Figure 4.2

The spectrum of the wind load and the spectrum of the acceleration of the top of the building for a totally correlated wind load have been determined for the uncontrolled and controlled system. The result can be seen in Figure 7.4 up to Figure 7.6. It is clear that the acceleration of the top of the building of the controlled system is still dominated by the natural frequency but the accelerations of the second eigenfrequency are becoming relatively more important for the damped system. Taking into account the correlation, this will make the natural frequency relatively more important compared to the second eigenfrequency. This is because lower frequencies mean less fluctuations and larger wind gusts with more correlation. Increasing the control gains more and more will give more and more damping on the natural frequency but this makes the second eigenfrequency more and more important. At some point the second eigenfrequency will dominate the acceleration of the top of the building. From this point increasing the control gains further will have no effect.

The conclusion from this is that the reduction of the acceleration with an active control system is limited. In practice this would give no problems because when accelerations due to the second eigenmotion are higher then the acceptable comfort level, the structure is so slender that other problems will become normative e.g. the distortions. In this project a reduction of about 50% of the accelerations have been achieved. Judging from Figure 7.6, it can be assumed that this is about the maximum reduction which can be achieved with an active control system in the Juffertoren.

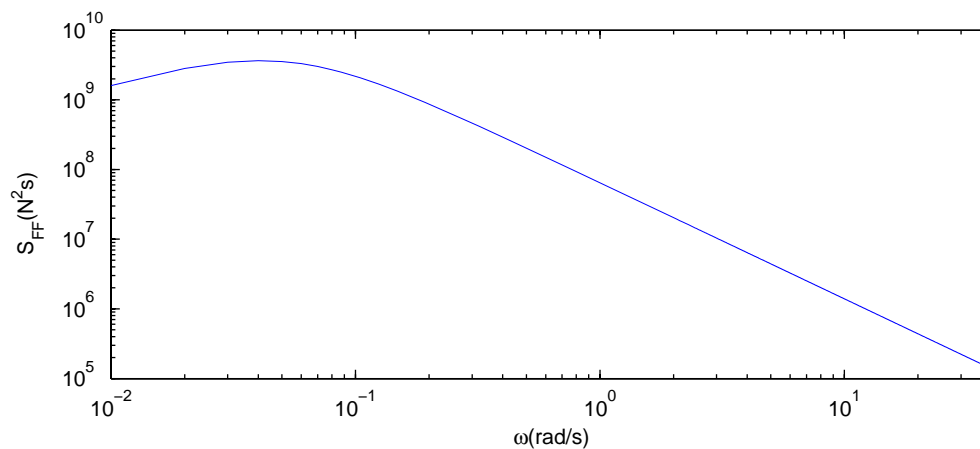


Figure 7.4 Spectrum of the forces on the nodes

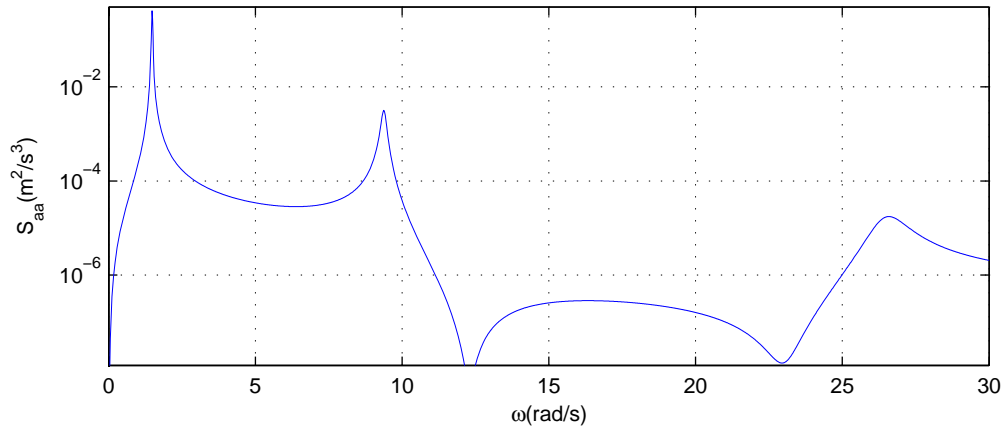


Figure 7.5 Spectrum of the accelerations of the uncontrolled system

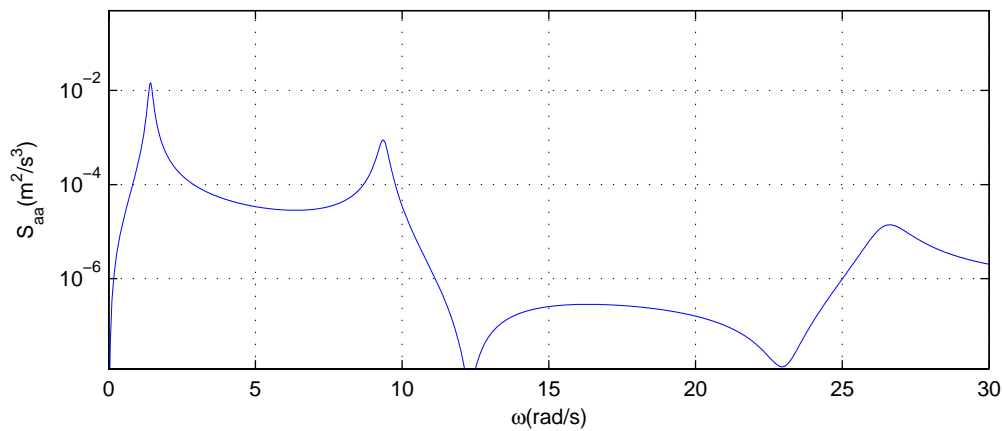


Figure 7.6 Spectrum of the accelerations of the controlled system

A realisation of the acceleration of the top of the building can be generated with:

$$a_{48} = \sum_{k=1}^N a_k \sin(\omega_k t + \varphi_k) \quad (7.34)$$

with:

$$a_k = \sqrt{2S_{aa} \Delta\omega_k}$$

$\varphi_k$  Random number between 0 and  $2\pi$

The results of these realisations can be seen in Figure 7.7 for the uncontrolled system and Figure 7.8 for the controlled system. Comparing Figure 7.7 – which is a realisation following from the spectral analysis – with Figure 4.5 – which is a simulations in the time-domain – both for a totally correlated wind load, makes clear that the spectral analysis agrees with the simulations in the time-domain. From the spectra of the accelerations the variance of the acceleration can be determined by:

$$\sigma_{a;48}^2 = \int_0^{\infty} S_{aa}(\omega) d\omega \quad (7.35)$$

And the standard deviation follows from:

$$\sigma_{a;48} = \sqrt{\sigma_{a;48}^2} \quad (7.36)$$

The standard deviation for the uncontrolled and controlled system equals respectively:  $\sigma_{a;48;uncontrolled} = 0,143 \text{ m/s}^2$  and  $\sigma_{a;48;controlled} = 0,064 \text{ m/s}^2$ . The expected peak value can be calculated from:

$$a_{48;peak;expected} = \sigma_{a;48} \sqrt{2 \ln(T_s f_e)} \quad (7.37)$$

With  $T_s = 300 \text{ s}$  and  $f_e = 0,235 \text{ Hz}$  the expected peak values for respectively the uncontrolled and controlled system equals:  $a_{48;peak;uncontrolled} = 0,417 \text{ m/s}^2$  and  $a_{48;peak;controlled} = 0,187 \text{ m/s}^2$ , which come close to the peak values of the realisation in Figure 7.7 and Figure 7.8.

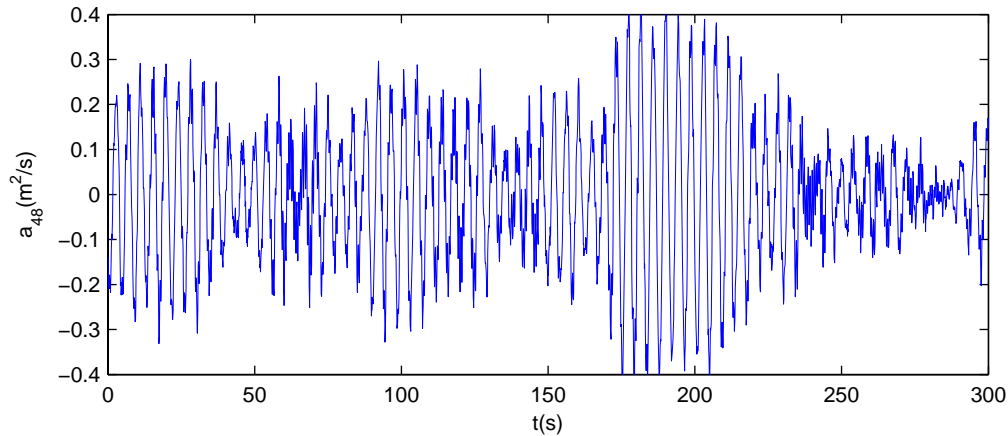


Figure 7.7 A realisation out of the spectrum of Figure 7.5 for the uncontrolled system

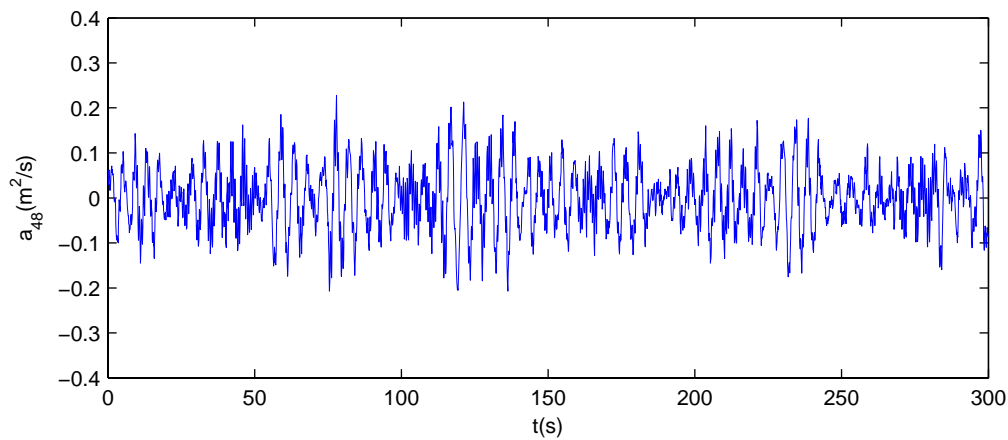


Figure 7.8 A realisation out of the spectrum of Figure 7.6 for the uncontrolled system

## 8. Conclusions and recommendations

### 8.1. Conclusions

- The deformation of the Juffertoren is dominated by bending and shear deformation is negligible. Simulink is suitable for modelling the wind load, structure and control system. It is important to take into account the spatial correlation within the wind field.
- The natural mode is most important but the second mode cannot be neglected considering the accelerations.
- The active control force needs to be coupled to the velocity of the top of the building. Coupling of the active control force to the displacement or acceleration of the building gives no improvement of the system. Because the displacement of the mass must be limited, the active control force should also be coupled to the dynamic state of the mass.
- The active control system mainly damps the natural mode. A practical active damping system can reduce the maximum accelerations with more than 50% compared to the uncontrolled system.
- Surprisingly an active control system is not necessary if the Juffertoren will be constructed as assumed in this thesis.
- The spectral analysis and the simulations in the time-domain will give almost the same results.

### 8.2. Recommendations

- Further elaboration of the spectral analysis with the right cross-spectra for the wind load will give a better insight into the total system. For the undamped system it will become clear at what values for the control gains the second eigenmode becomes normative. From this it will become clear what the maximum damping with an active control system will be.
- Detailed design of the control system should involve mechanical engineers. Different masses and different driving mechanisms can be chosen. Which of these systems provides the best solution cannot only be based on structural properties of the building. The engine and required power are also important in the design.
- It should be examined if torsion oscillations will be of consequence

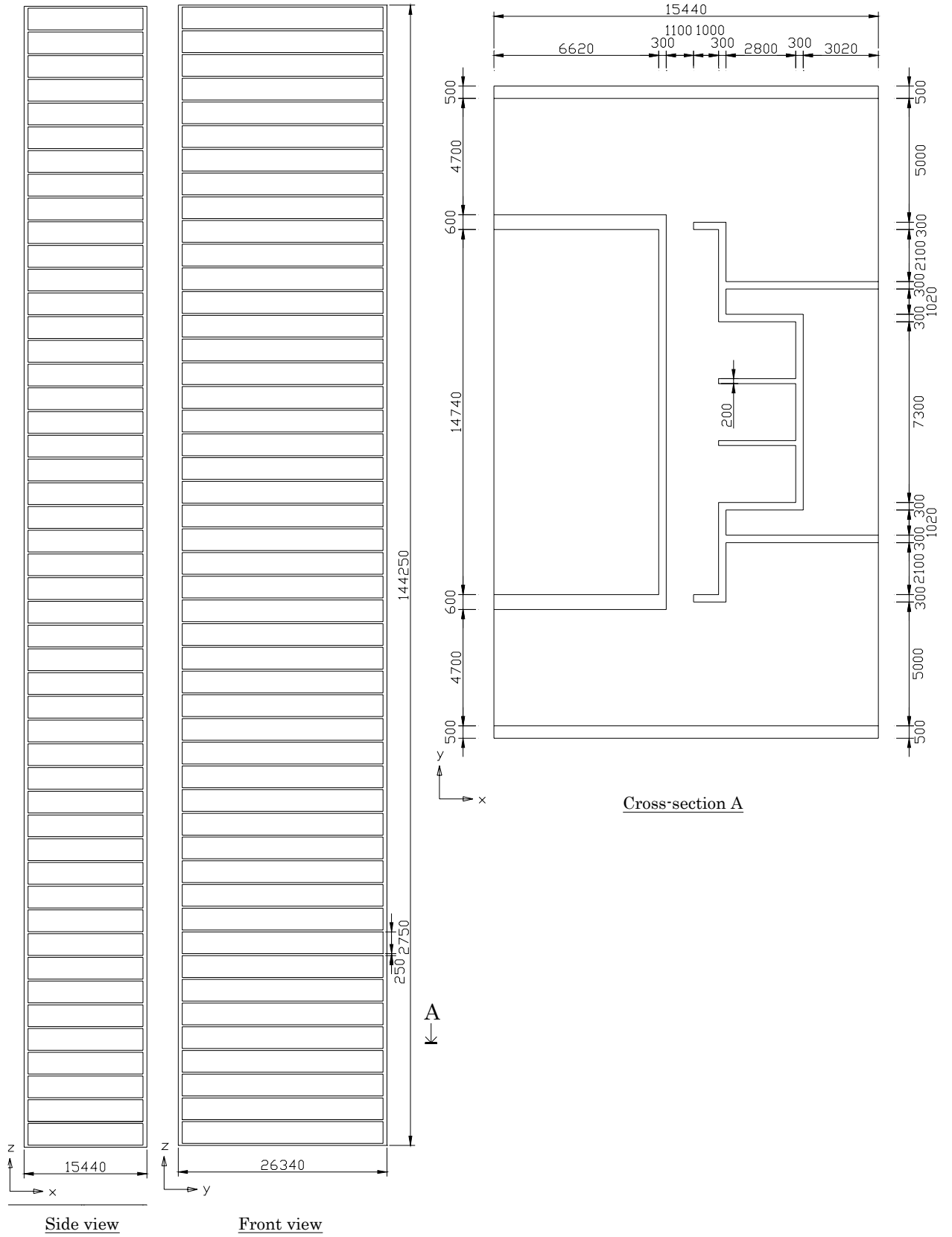


## References

- [1] A.C.W.M. Vrouwenvelder, “Lecture notes Ct5145: Random vibrations”, Technical University Delft, 2004.
- [2] J.M.J. Spijkers, A.W.C.M. Vrouwenvelder, E.C. Klaver, “Lecture notes Structural Ct4140: Structural dynamics part1”, Technical University Delft, 2005.
- [3] Anil K. Chopra, “Dynamics of structures” University of California at Berkeley, 1995.
- [4] G.P.C. van Oosterhout, “Thesis: Wind-induced Dynamic Behaviour of Tall Buildings”, Technical University Delft, 1996.
- [5] Nederlands Normalisatie Instituut, “NEN 6702”, Delft, 2001.
- [6] Madelon Burgmeijer “Afstudeerverslag: Actieve demping van hoge gebouwen, ontwikkeling van een demonstratieopstelling” Technical University Delft, 1996.
- [7] S. Y. Chu, T. T. Soong, A.M. Reinhorn, “Active, Hybrid and semi-active structural control”, The State University of New York at Buffalo, 2005
- [8] Ifke Brunings “High-rise buildings: Discomfort at the top a study on active structural control”, Technical University Delft, 1993.
- [9] Wim Bierbooms, “Simulation of stochastic wind fields which encompass measured wind speed series enabling time domain comparison of simulated and measured wind turbine loads”, European Wind Energy Conference '04, London, 2005

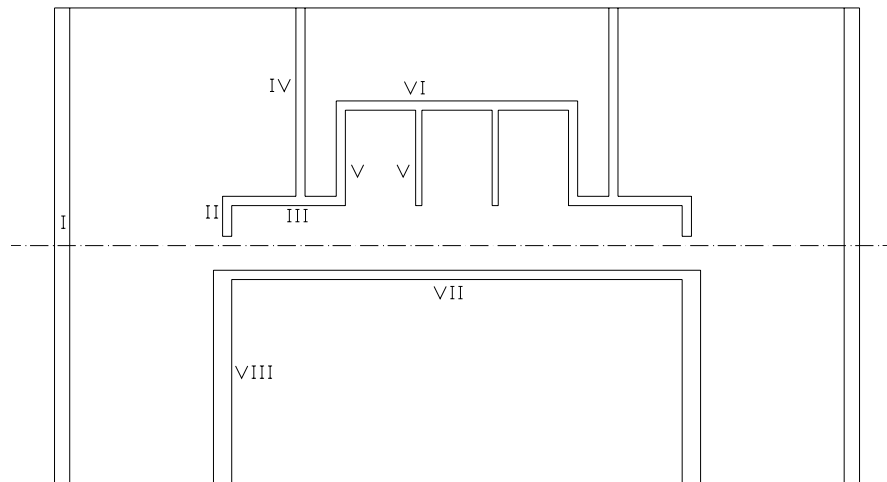


# Appendix I Drawing of the building





## Appendix II Matlab code: mechanical characteristics of the structure



The cross-section is divided into 8 walls numbered from I to VIII for the ease of the calculation

### Matlab input

```
% The cross-section is divided into 8 walls. See figure above

% Location of the neutral-axis, the centre line is taken as the
reference line
% Area of the walls
A(1)=2*0.5*15.44;
A(2)=2*0.3*1;
A(3)=2*0.3*3.72;
A(4)=2*0.3*6.12;
A(5)=2*(0.3+0.2)*3.1;
A(6)=0.3*7.9;
A(7)=0.3*14.74;
A(8)=2*6.92*0.6;
% Perpendicular distance between centre of mass and reference line
s(1)=0;
s(2)=0.8;
s(3)=1.3+0.15;
s(4)=6.12/2+1.6;
s(5)=3.1/2+1.3;
s(6)=0.3/2+3.1+1.3;
s(7)=-(0.15+0.8);
s(8)=-(6.92/2+0.8);
% Distance between the reference line and the neutral axis
na=dot(A,s)/(sum(A))

% The second moment of inertia
Ieig(1)=2*1/12*.5*15.44^3;
Ieig(2)=2*1/12*.3*1^3;
Ieig(3)=2*1/12*.3*3.72^3;
Ieig(4)=2*1/12*.3*6.12^3;
Ieig(5)=2*1/12*.5*3.1^3;
Ieig(6)=1/12*7.9*.3^3;
Ieig(7)=1*1/12*14.74*.3^3;
Ieig(8)=2*1/12*.6*6.92^3;
```

```
% Rule of Steiner
Isteiner=sum(s.^2.*A);
% Total second moment of inertia
I=sum(Ieig)+Isteiner;
E=3e10;
EI=E*I

% The mass of one storey existing of walls, floor and loading on the
floor
mass=sum(A)*2.75*2500+15.44*26.34*.25*2500+15.44*26.34*250
```

### Matlab output

```
na = 0.0217           % [m]
EI = 2.0030e+013     % [Nm^2]
mass = 6.3182e+005   % [kg/storey]
```

## Appendix III Derivation of the element stiffness matrix

### Field element

The aim is to find a relation between the nodal displacements and the nodal forces. By putting a constant moment on a bending element the rotation at each end is:

$$e' = \frac{l M}{2 EI} \quad (III.1)$$

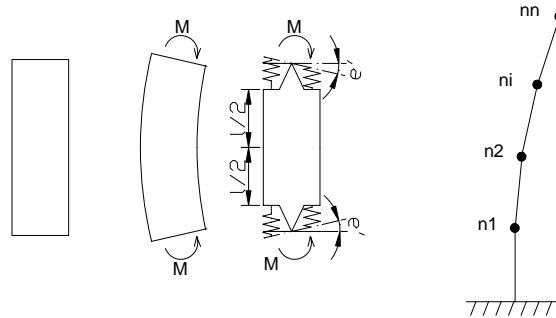


**Figure III. 1** The building will be modelled as a bending beam with lumped deformations  
The rotation stiffness  $K$  can be calculated with:

$$M = Ke' \quad (III.2)$$

$$K = 2 \frac{EI}{l} \quad (III.3)$$

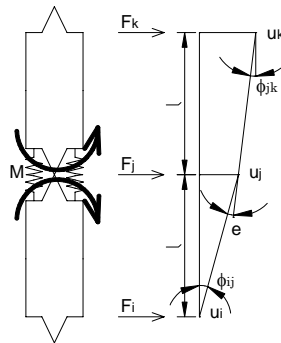


**Figure III. 2** Bending element

When two nodes are connected the rotation is:

$$e = 2e' \quad (III.4)$$

The relation between the rotation and nodal displacements can be found with

$$\left. \begin{aligned} \phi_{ij} &= \frac{1}{l}(u_j - u_i) \\ \phi_{jk} &= \frac{1}{l}(u_k - u_j) \end{aligned} \right\} \rightarrow e = \phi_{ij} - \phi_{jk} = \frac{1}{l}(-u_i + 2u_j - u_k) \quad (III.5)$$

Hence:

$$M = K \frac{e}{2} = \frac{1}{2} \frac{K}{l} (-u_i + 2u_j - u_k) \quad (III.6)$$

Moment equilibrium gives:

$$F_i = -\frac{M}{l} = \frac{K}{2l^2}(u_i - 2u_j + u_k) \quad (III.7)$$

$$F_k = -\frac{M}{l} = \frac{K}{2l^2}(u_i - 2u_j + u_k)$$

Horizontal equilibrium gives:

$$F_i + F_j + F_k = 0 \rightarrow F_j = -F_i - F_k = 2\frac{M}{l} = \frac{K}{l^2}(-u_i + 2u_j - u_k) \quad (III.8)$$

This provides the stiffness matrix of a bending element:

$$\begin{Bmatrix} F_i \\ F_j \\ F_k \end{Bmatrix} = \frac{EI}{l^3} \begin{bmatrix} 1 & -2 & 1 \\ -2 & 4 & -2 \\ 1 & -2 & 1 \end{bmatrix} \begin{Bmatrix} u_i \\ u_j \\ u_k \end{Bmatrix} \quad (III.9)$$

### Bottom element

The rotation of the foundation is, see Figure III. 3:

$$e_f = \frac{M}{C_r} \quad (III.10)$$

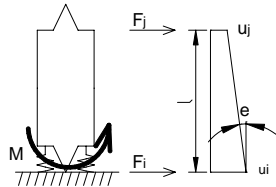


Figure III. 3 Bottom element

So the total rotation of node  $i$  is equal to:

$$e = e' + e_f \quad (III.11)$$

Combining eqn. (III.1) eqn. (III.10) and eqn. (III.11) gives:

$$e = \frac{l}{2EI} \frac{M}{l} + \frac{M}{C_r} \rightarrow M = \left( \frac{1}{\frac{l}{2EI} + \frac{1}{C_r}} \right) e \quad (III.12)$$

From Figure III. 3 it can be seen that:

$$e = \frac{1}{l}(u_j - u_i) \quad (III.13)$$

Combining eqn. (III.12) and eqn. (III.13) gives:

$$M = Ke = \frac{1}{l} \left( \frac{1}{\frac{l}{2EI} + \frac{1}{C_r}} \right) (u_j - u_i) \quad (III.14)$$

Moment equilibrium gives:

$$F_j = \frac{M}{l} = \frac{1}{l^2} \left( \frac{1}{\frac{2EI}{l} + \frac{1}{C_r}} \right) (u_j - u_i) \quad (\text{III.15})$$

Horizontal equilibrium gives:

$$F_i = -F_j = -\frac{1}{l^2} \left( \frac{1}{\frac{2EI}{l} + \frac{1}{C_r}} \right) (u_j - u_i) \quad (\text{III.16})$$

This leads to the stiffness matrix of the bottom element:

$$\begin{Bmatrix} F_i \\ F_j \end{Bmatrix} = \frac{1}{l^2} \frac{1}{\frac{2EI}{l} + \frac{1}{C_r}} \begin{bmatrix} 1 & -1 \\ -1 & 1 \end{bmatrix} \begin{Bmatrix} u_i \\ u_j \end{Bmatrix} \quad (\text{III.17})$$



## Appendix IV Matlab code: Stiffness-, mass- and damping matrix and eigenfrequencies

```

%{
input
v = degrees of freedom
EI = bending stiffness
L = height of the structure
l = length of element
zeta1 = damping ratio of first eigenmode
zeta2 = damping ratio of second eigenmode
%}
Cr=20*EI/L; % rotational stiffness of the foundation

% stiffness matrix
% Field elements
k=EI/l^3*[1 -2 1;
         -2 4 -2;
         1 -2 1];% bending element stiffness matrix
K=zeros(v+1,v+1); % Total system matrix bending
for o=0:1:46
    for n=1:1:3
        for m=1:1:3
            K(o+n,o+m)=K(o+n,o+m)+k(n,m);
        end
    end
end
% Edge element (including rotation of the foundation)
K(2,2)=K(2,2)+l/l^2*(1/(1/(2*EI)+1/Cr));
K(2,1)=K(2,1)-l/l^2*(1/(1/(2*EI)+1/Cr));
K(1,2)=K(1,2)-l/l^2*(1/(1/(2*EI)+1/Cr));
K(1,1)=K(1,1)+l/l^2*(1/(1/(2*EI)+1/Cr));
K(:,1)=[]; % restrained displacement of node 0 = 0
K(1,:)=[]; % restrained displacement of node 0 = 0
% end stiffness matrix

% mass matrix
M=zeros(v,v);
for n=1:1:v;
    M(n,n)=mass;
end
% end mass matrix

% eigenfrequency
[E,omegakw] = eig(K,M);
for n=1:1:v
    omega_eig(n)=sqrt(omegakw(n,n));
end
% end eigenfrequency

% damping matrix
a=2*inv([1/(omega_eig(1)) (omega_eig(1)); 1/omega_eig(2)
omega_eig(2)])*[zeta1;zeta2];
Cd=a(1,1)*M+a(2,1)*K;
% end damping matrix

```



## Appendix V Matlab code: correlation wind

### Coher.m

```
function Coh=coher(f,r,v_10)
% syntax: function Coh=coher(f,r,v_10)
% Coherency function
% of longitudinal wind velocity fluctuations
% Input:
%   f: frequency (Hz)
%   r: mutual distance coordinates
%   V_10: the 10 minute average wind speed at hub height (m/s)
% Output:
%   Coh: coherency (-)

C=10; % coherence constant
x=f.*C.*r./v_10
Coh=exp(-1.*x);
```

### Autopow.m

```
function S=autopow(f,v_10,sigma)
% syntax: function S=autopow(f,v_10,sigma)
% Autopower spectral density function of turbulence
% Input:
%   f: frequency (Hz)
%   v_10: the mean wind speed at 10 m above (m/s)
%   sigma: standard deviation (m/s)
% Output:
%   S: autopower spectral density (m^2/s)

sigma_v=6.345; % standard deviation of the wind speed
L=1200; % characteristic length Davenport
v_10=10; % mean wind speed at 10 m height

% spectrum of the wind speed as a function of the frequency
S=2/3*(f.*L/v_10).^2 ./ ((1+(f.*L/(v_10)).^2).^(4/3)).*sigma_v^2./(f);
% end spectrum of the wind speed as a function of the frequency
```

### Wind.m

```
function [UC]=wind0(yr,zr,v_10,sigma,N,deltat,fmax);
% simulation of a turbulent wind field

% INPUT:
%   yr, zr: specification of coordinates on the facade of the structure
%   v_10: mean wind velocity at 10 m above the surface of the earth (m/s)
%   N: number of time points (including zero); N must be a power of 2
%   deltat: time step (s)
%   fmax: maximum frequency spectrum (Hz)
% OUTPUT:
%   UC: constrained turbulent wind velocities (m/s)
yr=1.3:2.6:24.7;
zr=9:1.5:144;
v_10=10;
N=8192;
deltat=.1;
fmax=10;
% number of points in rotor plane
Ny=length(yr);
Nz=length(zr);
Np=Ny*Nz;
```

```

% y and z coordinates of all rotor points in one column vector
Yr=reshape(yr'*ones(1,Nz),Np,1);
Zr=reshape(ones(Ny,1)*zr,Np,1);

r=zeros(Np,Np);
for i=1:Np
    for j=i+1:Np
        % distances between points
        r(i,j)=sqrt((Yr(i)-Yr(j))^2+(Zr(i)-Zr(j))^2);
        r(j,i)=r(i,j);
    end
end
% time vector
t=[0:N-1]'*deltat;
% period
T=N*deltat;
% frequency step
deltaf=1/T;
% discretised frequencies
k=[1:N/2-1]';
f=k.*deltaf;
% autopower spectral density (one-sided)
Sa=autopow(f,v_10,sigma);
% spectrum is cut-off above fmax by application of window
Index=find(f>fmax);
if ~isempty(Index)
    Nw=Index(1);
    w=zeros(N/2-1,1);
    W=window('hann',2*Nw+1);w(1:Nw+1)=W(Nw+1:2*Nw+1);
    Sa=w.*Sa;
end
% renormalize Sa to variance
Sa=sigma^2/(sum(Sa)/T)*Sa;

% Fourier coefficients points in rotor plane
ak=zeros(Np,N/2-1);
bk=zeros(Np,N/2-1);
for k=1:N/2-1
    Coh=coher(f(k),r,v_10);
    % Choleski decomposition
    L=sqrt(Sa(k)/T)*chol(Coh)';
    % vector of unit variance normal random numbers
    ran=randn(Np,1);
    ak(:,k)=L*ran;
    ran=randn(Np,1);
    bk(:,k)=L*ran;
end

% complex notation
i=sqrt(-1);
UC=zeros(N,Np);
for j=1:Np
    C=ak(j,:)-i*bk(j,:);
    C=1/2*[0;C;0;rot90(C')];
    % inverse FFT
    uc=N*iFFT(C);
    if any(abs(imag(uc)) >= 1e-7*abs(uc) & abs(imag(uc)) >= 1e-12)
        max(abs(uc))
        max(imag(uc))
    end
end

```

```

        error('imag too large uc')
    end
    UC(:,j)=real(uc);
end
% reshape UC: separate indices for y and z
UC=reshape(UC,N,Ny,Nz);

save ('UC1','UC')

```

### Force.m

```

% Calculating the forces on the 48 nodes
rho=1.25;
Area=3*26.34/20; % dimension of the area of the mesh [m^2]
Ch=1.2;
u_star=2.82;
kappa=0.4;
d=3.5;
z_0=2;
z=(9:1.5:144); % points on the façade of the building in z-direction
load UC1
Uf(:,:,3:1:93)=UC;
Uf(:,:,1)=Uf(:,:,3);
Uf(:,:,2)=Uf(:,:,3);
% average part
v_mean(1,1,3:1:93)=u_star/kappa*log(z-d/z_0);
speed at reference height
v_mean(1,1,1:1:2)=v_mean(1,1,3);
v_mean(:,1,:)=v_mean(1,1,:);
v_mean(:,2,:)=v_mean(1,1,:);
v_mean(:,3,:)=v_mean(1,1,:);
v_mean(:,4,:)=v_mean(1,1,:);
v_mean(:,5,:)=v_mean(1,1,:);
v_mean(:,6,:)=v_mean(1,1,:);
v_mean(:,7,:)=v_mean(1,1,:);
v_mean(:,8,:)=v_mean(1,1,:);
v_mean(:,9,:)=v_mean(1,1,:);
v_mean(:,10,:)=v_mean(1,1,:);
v_mean= repmat(v_mean,[8192 1 1]);

U=Uf+v_mean;
U(:,:,94)=0;

F=1/2*Area*Ch*rho*(U).^2;
F=sum(F,2);
F=squeeze(F);

f(1:1:8192,1:1:2)=2*F(1:1:8192,1:1:2);
for n=3:1:48
    f(:,n)=F(:,2*n-3)+F(:,2*n-2); % nodes below z=9 m
end
F=f;
F(:,49)=0;
t=[.1:.1:819.2]';
save ('F','F','t')

```



## Appendix VI Unsuccessful control algorithms

### Switching on/off the active control system

As stated in section 1.1, the displacement of the mass will have an unacceptable growth in time. To avoid this, a hard stop can be built into the system. This is a device that decelerates the mass to a velocity of zero, when the displacement of the mass becomes too large. In the moving mass a large amount of kinetic energy has been stored. In decelerating the mass a part of this energy will get lost through a damping device and a part will be taken by the dynamics of the building. This results in an undesired force on the building in the direction it is already moving. Without a hard stop the kinetic energy will be released when the velocity of the building is in the opposite direction. Then the energy is used in a desired way. For this reason a hard stop is not a good solution.

Another solution could entail turning off the system when the acceleration at the top of the building is at an acceptable level. When the system is turned off the mass can move back to its initial position. Turning off the system means decelerating the mass slowly so that the forces on the structure are negligible. This is a more promising solution which will be elaborated.

In turning on the active control system, two systems can be chosen, see Figure VI. 1. The first system turns on when a specific acceleration of the top is exceeded. This system will turn off when the acceleration crosses the specific level again. The second system will turn on, under the same condition as the first system. This system turns off when the next peak of the acceleration of the top of the building lies within the specific area.

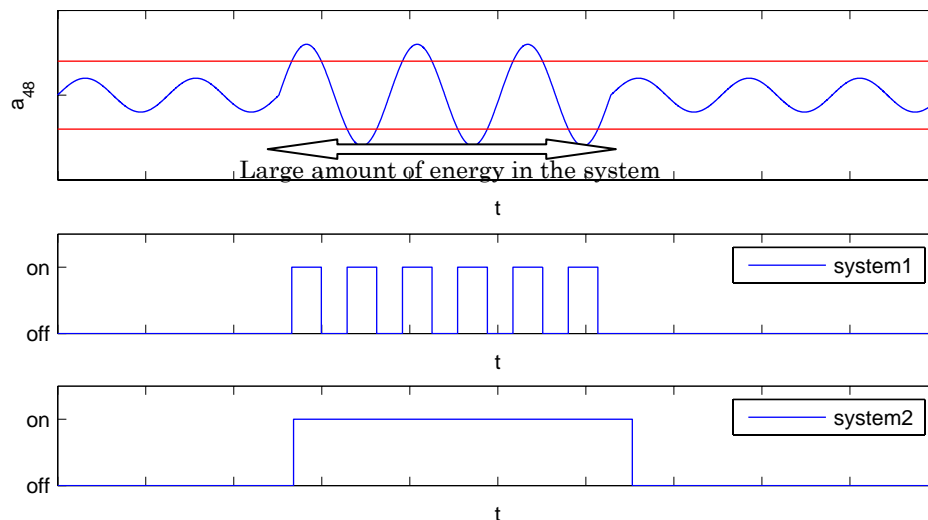


**Figure VI. 1** two on/off systems of active control for exceeding a specific acceleration

It is known that the building will oscillate in its natural frequency as can be seen in Figure 4.8. Under certain conditions the oscillation will get heavier and heavier. The acceleration of the top of the building is an oscillation around zero, but when the acceleration crosses zero the “problem” has not been solved. A quarter of a period later the acceleration will have a new peak. The “problem” is actually the large amount of kinetic and distortion energy in the system which causes the heavy oscillations as indicated in Figure VI. 1. The aim of the active control system is getting energy out of the total system. Bearing this in mind, it would be foolish to turn off the system when the acceleration is small for a short period as this has been done for system1. For this reason system2 is applied and from here on this is called

the on/off system.

Figure VI. 2 illustrates how the displacement of the mass can be derived. The third graph above left, shows that at  $t_0$  the active control system is turned on because  $a_{48}$  exceeds the specific acceleration. So from  $t_0$  the mass will accelerate. Integrating the acceleration of the mass gives the velocity and integrating once more gives the displacement of the mass. As can be seen in Figure VI. 2 again the displacement of the mass is growing in time. It can also be seen that the velocity of the mass  $v_m$  is not an oscillation around zero, as we would like to have it, but it has shifted. This shift equals the integration constant as derived in eqn. (5.13). The magnitude of this integration constant depends on the phase of  $a_m$  at the moment that the system is turned on. In the on/off system as it now stands the system is turned on at an “arbitrary” moment. See the third graph from above left in Figure VI. 2. To limit the displacement of the mass, the on/off system will be improved by starting the system at  $t_1$  in stead of  $t_0$ , see the graphs in the right column of Figure VI. 2. The starting moment  $t_1$  will be determined as a function of the phase. The starting phase  $\varphi$  will be determined in such a way that the integration constant  $c_1$  equals zero. The integration constant can be determined with:

$$v_m = \int a_m dt = \int \hat{a}_m \sin(\omega t + \varphi) dt = \frac{\hat{a}_m}{\omega} \cos(\omega t + \varphi) + c_1 \quad (\text{VI.1})$$

With the condition  $c_1 = 0$  and the initial condition  $v_m(t_1) = 0$  with  $t_1 = 0$  the starting phase can be determined with:

$$v_m(0) = \frac{\hat{a}_m}{\omega} \cos(\varphi) = 0 \rightarrow \varphi = k \frac{\pi}{2} \text{ with } k = 1, 3, 5, \dots \quad (\text{VI.2})$$

So the system should only be turned on when:

$$a_m = \hat{a}_m \sin(k\pi/2) \text{ with } k = 1, 3, 5, \dots \quad (\text{VI.3})$$

Because the acceleration of the mass is coupled to the velocity of the top of the building this constraint can also be written as:

$$v_{48} = \hat{v}_{48} \sin(\omega t) = \hat{v}_{48} \sin(k\pi/2) \text{ with } k = 1, 3, 5, \dots \quad (\text{VI.4})$$

This means that the system can only be turned on when the velocity of the top of the building  $v_{48}$  has a peak value. When the velocity has a peak value, the acceleration which is the derivative of the velocity equals zero. So adding the constraint  $a_{48} = 0 \text{ m/s}^2$  for turning on the active control system will improve the system considering the displacement of the mass.

The system has to be turned off when the velocity of the mass is zero. This will give the same constraint as defined in eqn. (VI.2), for the turn on moment. And this will also result in the constraint  $a_{48} = 0 \text{ m/s}^2$  for turning off the active control system.

Before the turn off algorithm is built in, in Simulink, the system will be tested on a “real” signal

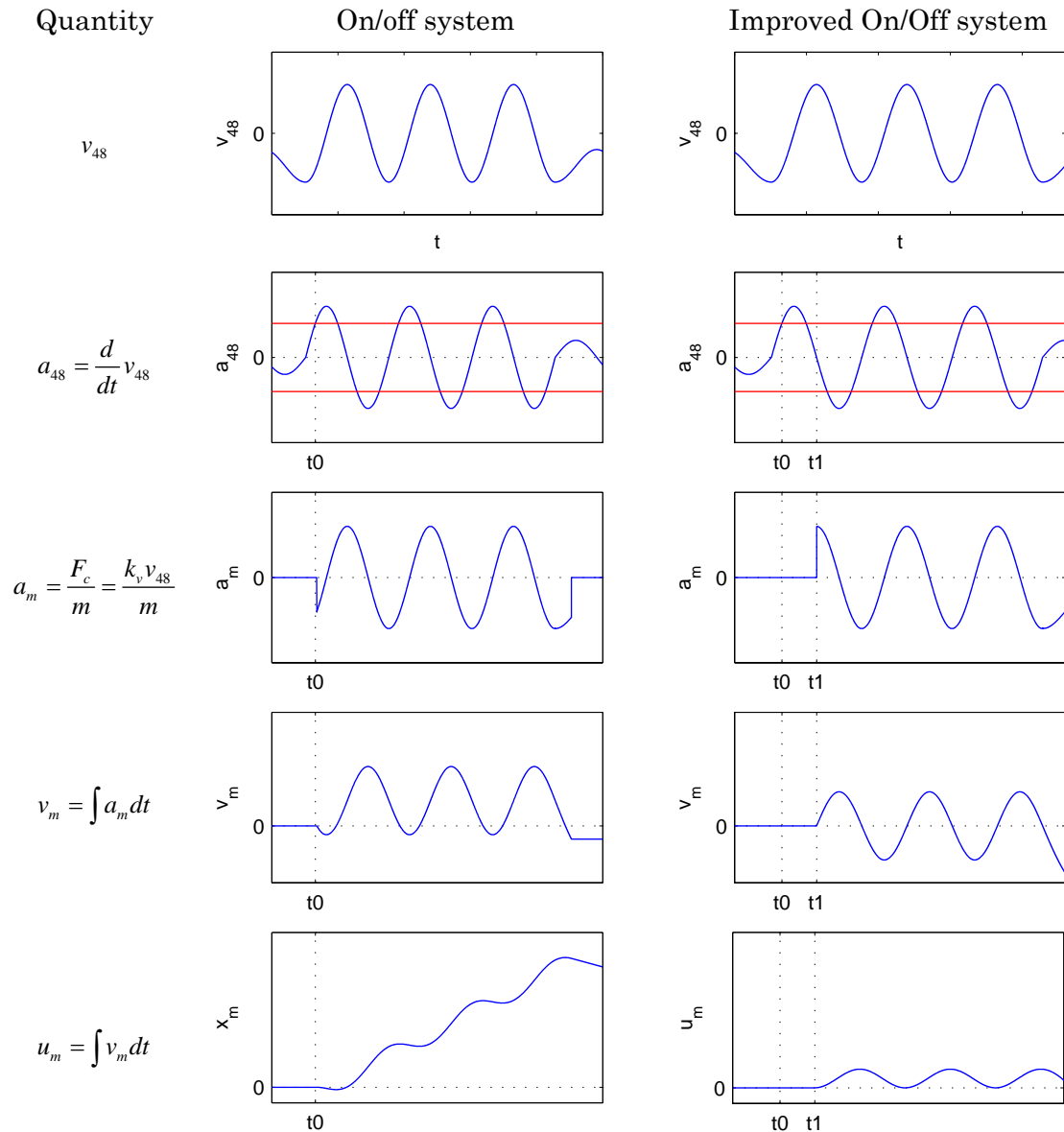


**Figure VI. 2** The displacement of the mass will be limited when the system is turned on at  $t_1$  instead of  $t_0$

The real displacement and acceleration consists of a lot of sines signals together. The mass has been presumed equal to  $k_v$ , the results of this simulation are shown in Figure VI. 3. Even with the improved system the displacement will increase in time. This can be explained as follows. The starting point when the system is turned on must be at a moment when  $a_{48} = 0 \text{ m/s}^2$ . When the acceleration of the top equals zero the velocity has a local peak, but this is not necessarily the peak of the oscillation of the first mode. And that was precisely the condition for the right starting moment. Another cause has already been illustrated in Figure 5.9, which illustrates that a ramp in the displacement of the top of the building means a growth of the displacement of the mass in time.

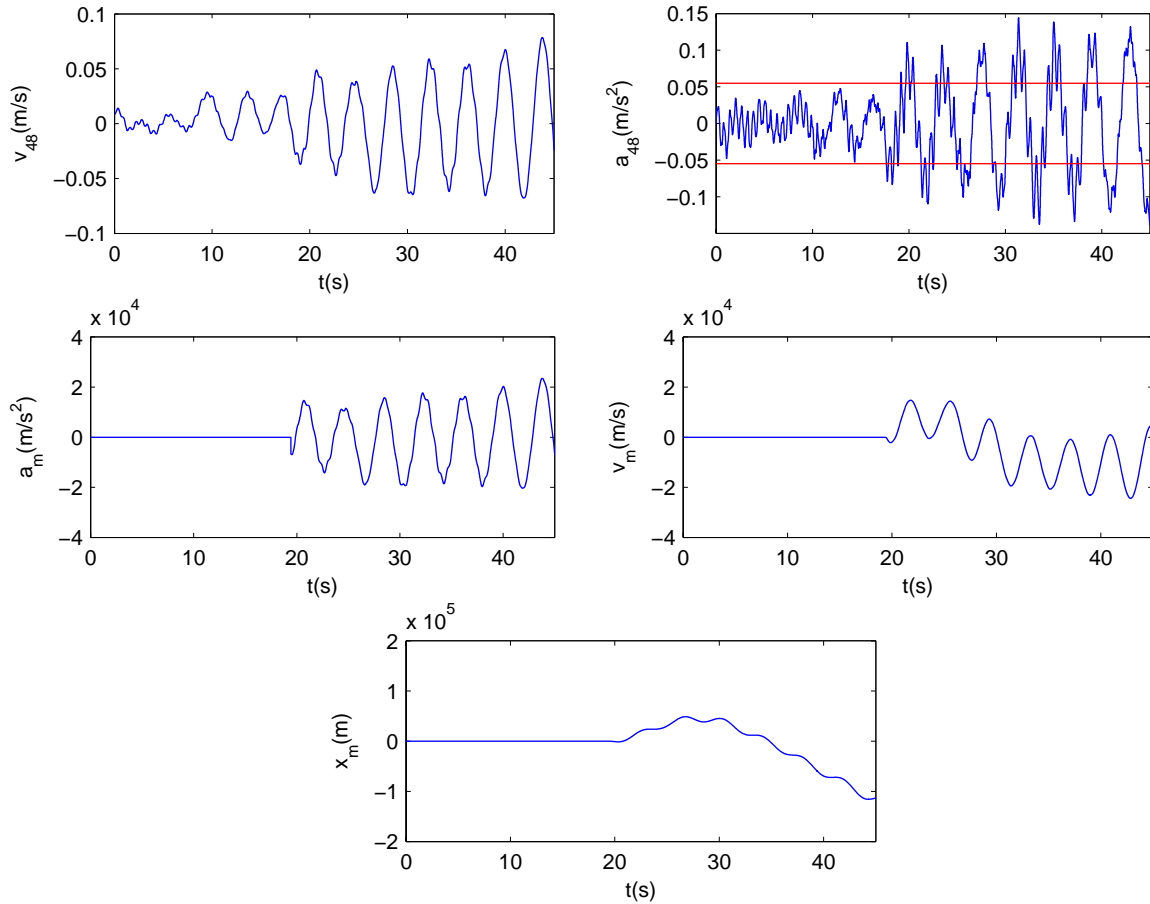


**Figure VI. 3** The displacement of the mass will also increase with the improved on/off system

### Adapting the gain of the active control force

When a hard stop and an on/off system are not the solution for limiting the displacement of the mass, there is one other conceivable solution left. This involves adapting the gain of the active control system to the state of the system. This means that, when the mass has a large displacement in the positive direction, the acceleration of the mass in the positive direction must be limited and the acceleration of the mass in the negative direction can be enlarged. The acceleration of the mass is coupled to the velocity of the top of the building. So the acceleration of the mass will be a function of the displacement of the mass  $u_m$  and the velocity of the top of the building  $v_{48}$ . The acceleration of the mass follows from:

$$a_m = F_c / m \quad (\text{VI.5})$$

Because the mass is constant the active control force has to be a function of  $u_m$  and  $v_{48}$ :

$$F_c(t) = k_v(u_m, v_{48})v_{48} \quad (\text{VI.6})$$

Now  $k_v$  is a coefficient that makes the control force and therefore also the acceleration of the mass dependent on  $u_m$  and  $v_{48}$ . The coefficient must be limited by  $k_v > 0$ , because otherwise the control force eqn. (VI.6) can become negative where it should be positive and the other way around as well. For  $k_v$  the following rules will apply:

When the displacement of the mass is positive, the acceleration of the mass in the positive direction must be reduced, and the acceleration in the negative direction must be enlarged:

$$u_m > 0 \text{ and } a_m > 0 \rightarrow \text{reduce } k_v \quad (\text{VI.7})$$

$$u_m > 0 \text{ and } a_m < 0 \rightarrow \text{enlarge } k_v \quad (\text{VI.8})$$

When the displacement of the mass is negative, the acceleration of the mass in the positive direction must be enlarged, and the acceleration in negative direction must be reduced:

$$u_m < 0 \text{ en } a_m < 0 \rightarrow \text{enlarge } k_v \quad (\text{VI.9})$$

$$u_m < 0 \text{ en } a_m > 0 \rightarrow \text{reduce } k_v \quad (\text{VI.10})$$

With  $k_v \geq 0$  and eqn. (VI.5) and (VI.6) it can be seen that  $a_m$  has the same sign (positive or negative) as  $v_{48}$ . So eqn. (VI.7) till (VI.10) can also be written as:

$$u_m > 0 \text{ and } v_{48} > 0 \rightarrow \text{reduce } k_v \quad (\text{VI.11})$$

$$u_m > 0 \text{ and } v_{48} < 0 \rightarrow \text{enlarge } k_v \quad (\text{VI.12})$$

$$u_m < 0 \text{ en } v_{48} < 0 \rightarrow \text{reduce } k_v \quad (\text{VI.13})$$

$$u_m < 0 \text{ en } v_{48} > 0 \rightarrow \text{enlarge } k_v \quad (\text{VI.14})$$

Assuming a linear relation between  $k_v$  and  $u_m$ ,  $k_v$  can be defined by:

$$\begin{aligned} k_v &= a(1+bu_m) \not\leq 0 \text{ for } v_{48} < 0 \\ k_v &= a(1-bu_m) \not\leq 0 \text{ for } v_{48} > 0 \end{aligned} \quad (\text{VI.15})$$

By taking the same input signal as is done in Figure VI. 3, the system is tested and the displacement of the mass will be limited. The results can be seen in Figure VI. 4. In this simulation, the constants from eqn. (VI.15) are  $a=1$  and  $b=3$ . The active control force will be very small with these values, but here we will only test if adapting of the gain will limit the displacement of the mass. It has been shown that the displacement of the mass will be limited. The optimal values for  $a$  and  $b$  will be determined later.

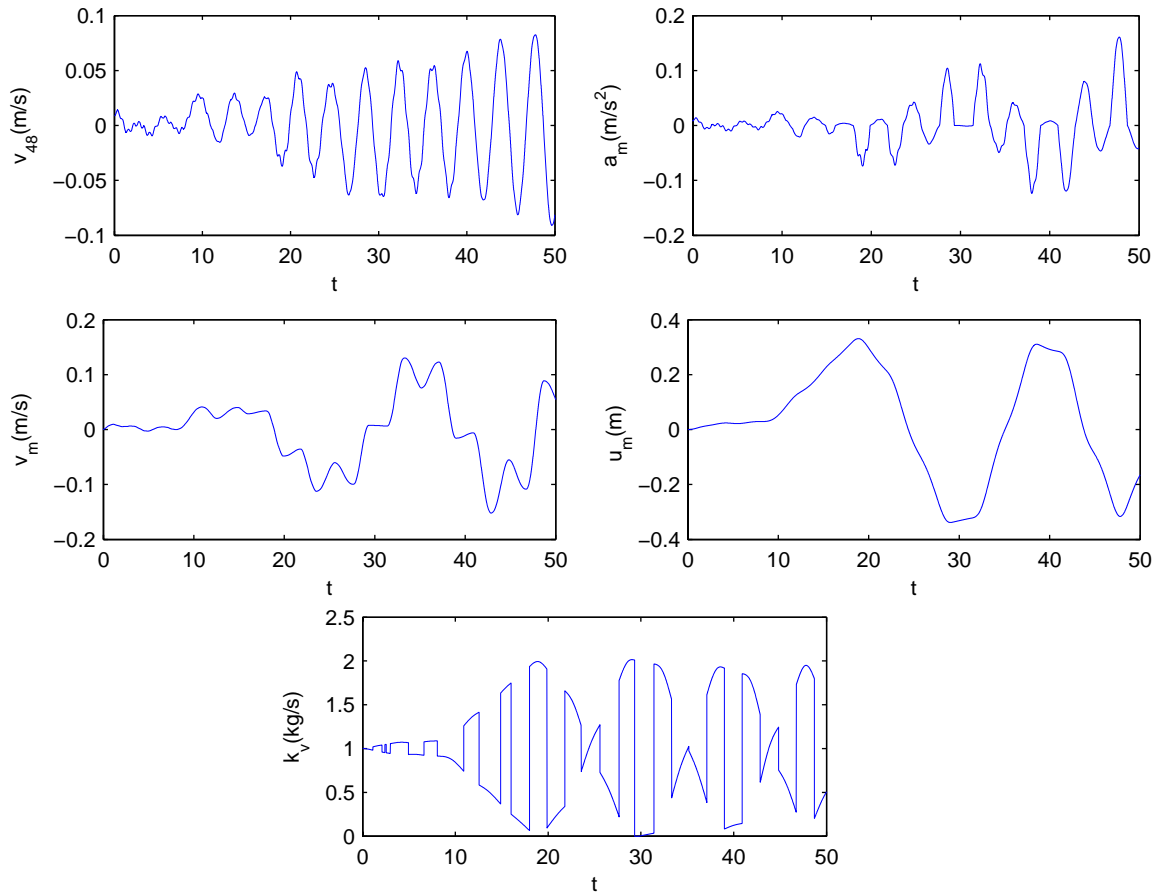


**Figure VI. 4** The displacement of the mass  $x_m$  will be limited when  $k_v$  is a function of  $x_m$  and  $v_{48}$

Up to now only the limiting of the displacement of the mass has been considered in this appendix. By doing this, the active control force has been redefined, eqn. (VI.6), but does this have effect on limiting the dynamic behaviour of the building? The idea of limiting the dynamic behaviour of the building is about getting energy out of the moving structure. This is done by placing a force on the structure which has a direction opposite to the direction of the velocity of the structure. The kinetic energy subtracted from the moving structure, when the top of the building displaces a distance  $dx$ , equals:

$$E = \int F_c dx = \int F_c v_{48} dt \quad (\text{VI.16})$$

With eqn. (VI.6) this gives:

$$E = \int k_v v_{48}^2 dt \quad (\text{VI.17})$$

With the condition  $k_v \geq 0$  the energy subtracted from the moving structure eqn. (VI.17) will never get negative  $E \geq 0$ . In other words, the active control system will only subtract energy from the moving structure and it will never add energy to it. It seems that by defining  $k_v$  as is done in eqn. (VI.15), the displacement of the mass is limited and the active control system will do its work. Unfortunately on a larger timescale, instability will occur as can be seen in Figure VI. 5.

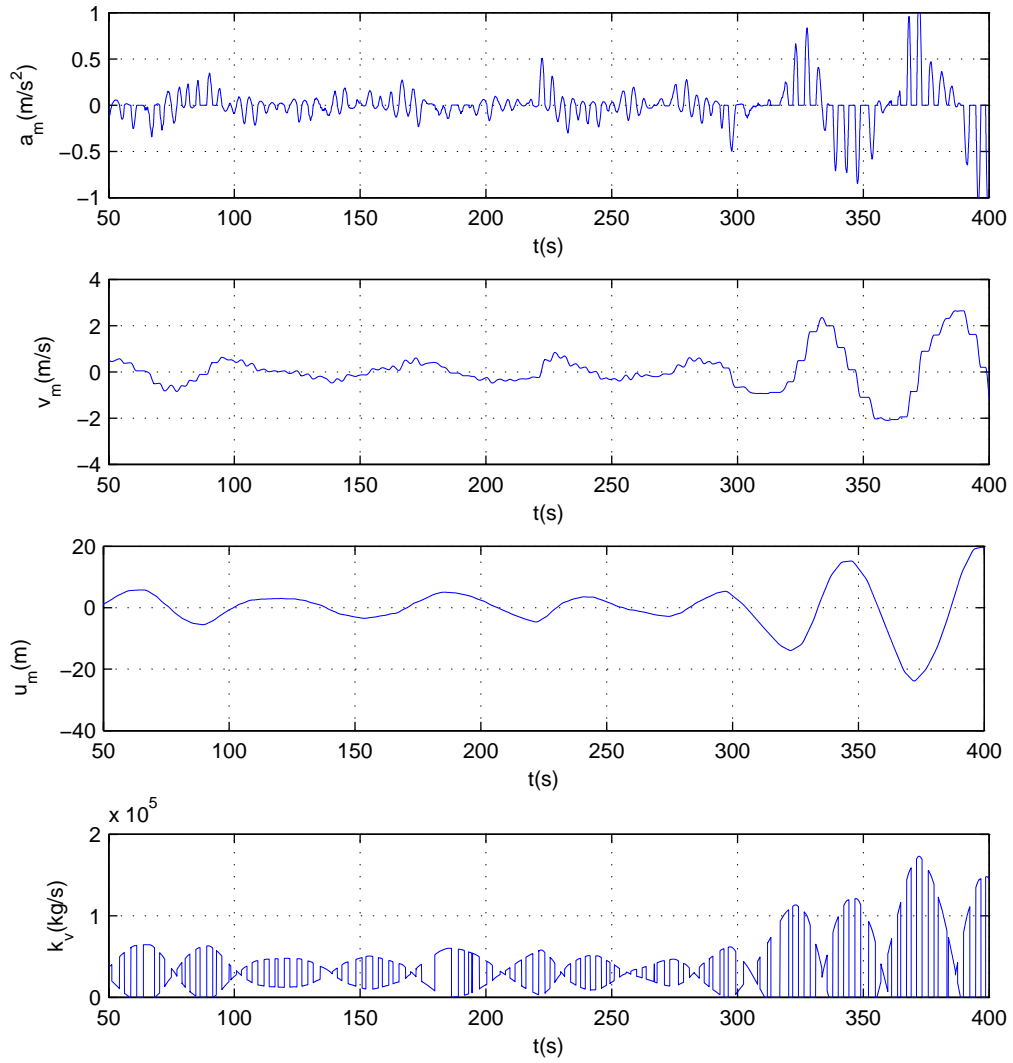


Figure VI. 5  $k_v$  will grow in time which will cause instability



## Appendix VII Deriving the spectrum from a linear relation

Assuming the signal

$$x(t) = \hat{x} \sin(\omega t + \phi) \quad (\text{VII.1})$$

from which the spectrum is known. And assuming a linear related signal

$$y(t) = C * x(t) \quad (\text{VII.2})$$

from which the spectrum has to be determined. The standard deviation of both signals is defined by:

$$\sigma_x^2 = \int_0^{2\pi} x^2(t) f(\phi) d\phi \quad (\text{VII.3})$$

$$\sigma_y^2 = \int_0^{2\pi} y^2(t) f(\phi) d\phi \quad (\text{VII.4})$$

Where  $f(\phi)$  is the probability density function which is by definition, See Figure VII 1:

$$\int_0^{2\pi} f(\phi) d\phi = 1 \quad (\text{VII.5})$$



Figure VII 1 probability density function  $f(\phi)$

The spectrum of both signals is defined by:

$$S_{xx} = \frac{d\sigma_x^2}{d\omega} \quad (\text{VII.6})$$

$$S_{yy} = \frac{d\sigma_y^2}{d\omega} \quad (\text{VII.7})$$

Substituting eqn. (VII.2) in eqn. (VII.4) gives:

$$\sigma_y^2 = \int_0^{2\pi} (C * x(t))^2 f(\phi) d\phi = C^2 \int_0^{2\pi} (x(t))^2 f(\phi) d\phi \quad (\text{VII.8})$$

With eqn. (VII.3) this leads to:

$$\sigma_y^2 = C^2 \sigma_x^2 \quad (\text{VII.9})$$

Combining eqn. (VII.6), eqn. (VII.7) and eqn. (VII.9) gives the spectrum of  $y(t)$ :

$$S_{yy} = C^2 S_{xx} \quad (\text{VII.10})$$



## Appendix VIII Matlab code: Transfer function, spectrum forces, spectrum of the acceleration

### Transfer function acceleration of the top

```
% This file calculates the transfer function of the acceleration of the
top.

%K:      Stiffness matrix
%M:      Mass matrix
%Cd:     Damping matrix
%output
%S:      Flexibility matrix
%H:      Matrix containing the transfer functions of the accelerations.
%H_u:    Absolute values of H
%H_a48:  Damping matrix

load matrices % file containing among other things K,M and Cd
for n=1:1:1000;
    omega(n)=n/10; % Divides the omega domain in discrete intervals
    S=K-omega(n)^2*M+i*omega(n)*Cd;
    H=S^-1;
    H_u=abs(H);
    H_a48(n)=sum(H_u(48,:))*omega(n)^2;% H_a48 for every discrete omega
end
plot(omega,H_a48)% see Figure 7.1 and Figure 7.2
```

### Autospectrum of the forces on the nodes and spectrum of the accelerations

```
load matrices K M Cd
sigma_v=6.345; % standard deviation of the wind speed
L=1200; % characteristic length Davenport
v_10=10; % mean wind speed at 10 m height
rho=1.25; % mean wind speed at 10 m height
A=3*26.34; % Wind affected area
Ch=1.2; % mean wind speed at 10 m height
ve=3000;
deltaom=.01;
v_gem=35;
u_star=2.82;
kappa=0.4;
d=3.5;
z_0=.7;
z(3:48)=(9:3:144)';
v_mean=u_star/kappa*log(z-d/z_0); % mean wind speed at reference height
v_mean(1:1:2)=v_mean(3);

for n=1:1:ve;
    omega(n)=n*deltaom;
    S_vv(n)=(L/v_10)^2/(1+(omega(n)*L/(2*pi*v_10))^2)^(4/3)
    *omega(n)*sigma_v^2/(6*pi^2);
    for a=1:1:48 % every node has its own spectrum depending on the mean
        windspeed (v_mean) at that height
        S_FF(a,n)=(rho*A*Ch*v_mean(a))^2*S_vv(n);
    end
end

for n=1:1:ve;
    S_u=K-omega(n)^2*M+i*omega(n)*Cd;
    H_u=S_u^-1; % complex according to eqn. (7.43)
```

```
H_u=H_u(1:1:48,1:1:48); % wipes out the 49th degree of freedom,  
                        which is the moving mass on top of the building  
H_a=H_u*omega(n)^2; % see eqn. (7.25)  
S_aa(n)=0;  
for k=1:1:48;  
    for j=1:1:48;  
        S_aa(n)=S_aa(n)+H_a(48,j)*conj(H_a(48,k))  
                *sqrt(S_FF(k,n)*S_FF(j,n));  
    end  
end  
end  
% See Figure 7.5 and Figure 7.6
```